NAVAL BIODYNAMICS LABORATORY
NBDL-89R006

(2)

A STATISTICAL ANALYSIS OF -X RHESUS HEAD KINEMATICS

SALVADORE J. GUCCIONE, JR.

Research Report

October 1990

NAVAL BIODYNAMICS LABORATORY
Box 29407
New Orleans, LA 70189-0407

Approved for public release; distribution is unlimited.

Prepared for

Naval Medical Research and Development Command
Bethesda, MD 20889-5044

Approved by

Thomas G. Dobie, M.D.
Chairman, Scientific Review Committee

Released by

CAPT Douglas W. Call, MSC, USN
Commanding Officer

Naval Biodynamics Laboratory
P. O. Box 29407
New Orleans, LA 70189-0407

The animals used in this work were handled in accordance with the principles outlined in "Guide for the Care and Use of Laboratory Animals" (National Institutes of Health Document No. NIH 80-23), established by the Institute of Laboratory Animal Resources, National Research Council.

In the interest of precision, trade names of products are cited. These citations do not constitute endorsements of the products.

REPORT DOCUMENTATION PAGE

Form Approved
OMB No. 0704-0188

1. AGENCY USE ONLY *(Leave blank)*

2. REPORT DATE
1 Oct 1990

3. REPORT TYPE AND DATES COVERED
Final: 1985 - 1987

4. TITLE AND SUBTITLE
A Statistical Analysis of -X Rhesus Head Kinematics

5. FUNDING NUMBERS
63216N M0097 .001

6. AUTHOR(S)
Salvadore J. Guccione, Jr., Ph.D.

7. PERFORMING ORGANIZATION NAME(S) AND ADDRESS(ES)
Naval Biodynamics Laboratory
P. O. Box 29407
New Orleans, LA 70189-0407

8. PERFORMING ORGANIZATION REPORT NUMBER
NBDL-89R006

9. SPONSORING/MONITORING AGENCY NAME(S) AND ADDRESS(ES)
Naval Medical Research and Development Command
National Naval Medical Center
Building 1, Tower 12
Bethesda, MD 20889-5044

10. SPONSORING/MONITORING AGENCY REPORT NUMBER

11. SUPPLEMENTARY NOTES

12a. DISTRIBUTION/AVAILABILITY STATEMENT
Approved for public release; distribution is unlimited.

12b. DISTRIBUTION CODE

13. ABSTRACT *(Maximum 200 words)*

The use of the rhesus as a human surrogate in studying head-neck injury due to impact acceleration depends on the similarity of human and rhesus head-neck kinematic and dynamic responses. This report addresses the question of -X rhesus head-neck kinematics. The dependence of the first major peaks of head linear and angular accelerations, velocities and displacements on sled acceleration parameters and initial head position is statistically analyzed. The effects of anesthetic state, repeated exposures and out-of-plane response on these key kinematic outputs are assessed. Various graphical and statistical comparisons indicate that: (1) human and rhesus -X head kinematics are not only similar in shape but, more importantly, depend on the same sled and head initial position parameters; (2) anesthetic state has no significant statistical effect on rhesus kinematic output; and (3) the effects of repeated tests and out-of-plane response can be reasonably explained. These results justify a full scale attempt to fit key human and rhesus kinematic and dynamic responses and develop appropriate scaling procedures. Recommendations concerning the structuring of future human and rhesus experiments to facilitate the necessary statistical comparisons are also given.

14. SUBJECT TERMS
Rhesus -G_x head-neck kinematics; statistical modeling.

15. NUMBER OF PAGES
113

16. PRICE CODE

17. SECURITY CLASSIFICATION OF REPORT	18. SECURITY CLASSIFICATION OF THIS PAGE	19. SECURITY CLASSIFICATION OF ABSTRACT	20. LIMITATION OF ABSTRACT
Unclassified	Unclassified	Unclassified	

NSN 7540-01-280-5500

Standard Form 298 (Rev 2-89)
Prescribed by ANSI Std Z39-18
298-102

SUMMARY

THE PROBLEM

While human head-neck kinematics for the −X vector direction have been successfully predicted utilizing a deterministic head-neck linkage computer model driven by first thoracic vertebral body (T-1) acceleration data, the lack of rhesus T-1 data has precluded the development of a similar animal model. Therefore, an alternate method of relating human and rhesus head kinematic responses is required to fully utilize the large database of rhesus kinematic, injury, and pre-injury data collected at the Naval Biodynamics Laboratory (NAVBIODYNLAB).

Since key human and rhesus head kinematic response curves are remarkably similar, except for scale, and since various sled acceleration and head initial position parameters are common to both the human and rhesus databases, a statistical modeling procedure can be used to relate these responses to sled acceleration and head initial position parameters.

FINDINGS

(1) The first major peaks of key rhesus head kinematic response curves regress excellently on sled acceleration and head initial position parameters.

(2) The effect of anesthesia on the rhesus head kinematic response is not statistically significant.

(3) The effect of repeated exposures and out-of-plane kinematic behavior can be explained.

(4) The −X rhesus data are not well distributed among the various levels of sled acceleration and head initial position parameters.

(5) Inconsistencies between sensor acceleration variables and photo displacement variables, and gaps in the photo displacement variables in high-g runs, prevented key velocity and displacement variables from being modeled.

RECOMMENDATIONS

(1) Parametric methods for curve fitting the entire time histories of key kinematic variables should be developed.

(2) Future human and rhesus run protocols should be designed to facilitate the necessary statistical comparisons.

(3) Data reduction methods (e.g., EZFLOW) should be modified to eliminate photo gaps in high-g runs.

(4) Rhesus biomechanical data (e.g., mass, center of gravity, moments) should be collected to allow the comparison of human and rhesus head dynamics.

ACKNOWLEDGEMENT

The author wishes to thank Mr. Ronnie Wilson of the Mathematics Division for his tireless efforts in executing the myriad software, plotting, and data-handling tasks related to this report. Mr. Bill Muzzy of the Technology Department provided invaluable assistance in the use of the Sigma Plot™ graphics system. Dr. David Matson of the Research Department, and LCDR Steven Mawn and Capt. Shanna Nesby of the Biomedical Department, provided expert advice regarding the interpretation of rhesus injury and somatosensory evoked potential data. Dr. Terry Watkins of the Mathematics Department, University of New Orleans, gave generously of his time and thoughts relating to the statistical analysis aspects of this report. Finally, Ms. Pat Hinson and Ms. Connie Dummitt, both of the Research Department, contributed many hours of word processing support in completing this report.

CONTENTS

A STATISTICAL ANALYSIS OF -X RHESUS HEAD KINEMATICS

INTRODUCTION

This report addresses the question of rhesus head kinematic behavior.* From a database of 53 $-G_x$ rhesus tests from the 1984, 1985, and 1987 series (see Appendix A), statistical relationships are developed, linking key head kinematic variables to anesthetic state, sled acceleration, and initial head orientation. In addition, qualitative and quantitative comparisons are made between human and rhesus kinematic response and anesthetized and unanesthetized rhesus kinematic response. Assessments of the effect of repeated exposures and out-of-plane response are also made.

EXPERIMENTAL METHODOLOGY

The reference and bibliography sections list technical information detailing the various methodological issues involved in the acquisition, editing, and analysis of the rhesus database. Various aspects of the medical, engineering/technical, data quality, and analytical concerns are addressed in this literature.

DEFINITIONS

This section provides basic definitions and abbreviations for various input and output variables analyzed in this report. Further details may be found in the work of Becker, Ewing, Frisch, Lustick, Majewski, Muzzy, Seemann, Thomas, and Willems [2–6].

The dependent and independent variables used in the various regressions are defined with respect to either the laboratory coordinate system or the head anatomical coordinate system.

The laboratory coordinate system is a non-translating, non-rotating orthogonal right hand triad. The origin of the laboratory system is defined as the top center of a 3-in high, 2.5-in diameter aluminum cylinder located at the northwest corner of the west rail. Positive X (+X) is north and opposite to the thrust vector. Positive Z (+Z) is up and anti-parallel to the local gravity vector at the Naval Biodynamics Laboratory in New Orleans. Positive Y (+Y) is west and the cross product of Z x X.

The sled coordinate system is parallel to the laboratory one and its origin is defined by a marker located on its longitudinal midline near the safety pin attachment point.

The head anatomical coordinate system is an orthogonal right hand triad defined as follows: Points on the skin over the left and right infraorbital notches and at the superior edge of the left and right external auditory meatus are labeled with radiopaque markers. A plane is established as the best least squares fit to these four markers. This is approximately the Frankfort plane. The origin of the head anatomical coordinate system is at the midpoint of the

---

*A quantitative statistical model for human kinematic response for the -X vector direction has been developed by Watkins and the author [1].

line connecting the left and right external auditory meatus markers in the plane. The +X axis is from the origin to a point between the infraorbital notches. The Z axis is from the origin to a cephalad direction perpendicular to the plane formed by the +X axis and the line between the auditory meatus markers. The Y axis is from the origin toward the left ear perpendicular to the XZ plane. The XZ plane is considered the mid-sagittal plane. The head anatomical co-ordinate system is initially aligned with the laboratory co-ordinate system.

The dependent variables used in the various regressions are values of the first significant peaks of the head kinematic variables defined in Table 1. These variables are all sensor-derived (i.e., acquired by accelerometers or derived from accelerometer data).

The independent regression variables are the various sled acceleration and initial head orientation parameters defined in Tables 2 and 3, plus a grouping variable included to assess the effect of anesthesia.

The sled acceleration parameters are the classic characteristics of the sled acceleration profile, namely peak sled acceleration, endstroke sled velocity, rate of onset, and duration of the peak.

The initial head orientation parameters are photo-derived initial Euler angles with respect to the head anatomical coordinate system. The initial photo linear displacements of the head anatomical origin with respect to the X, Y, and Z axes of the sled coordinate system were not included as independent regression variables since they are subject to large between-animal variation. Since rhesus kinematic data are not *margorized* [7], linear and angular velocities were also not considered. Finally, the peak linear and angular photo displacements were not included among the dependent variables because of photographic lapses occurring during many high-g rhesus impact tests. A final independent variable was used to account for the possible effect of the anesthetic state on kinematic response. This grouping variable was denoted IGP where IGP = 0 for an unanesthetized test and IGP = 1 for an anesthetized test.

TABLE 1. Definition of Head Kinematic Variables.

NAME	DESCRIPTION	UNITS	CO-ORDINATE SYSTEM
QHB	Angular acceleration about Y-axis	rad/sec^2	Head Anatomical
RHB	Angular velocity about Y-axis	rad/sec^2	Head Anatomical
AAX	X-component of linear acceleration	m/sec^2	Laboratory
AAZ	Z-component of linear acceleration	m/sec^2	Laboratory
AAR	X-Z plane component of linear acceleration	m/sec^2	Laboratory

TABLE 2. Definition of Sled Acceleration Parameters.

NAME	DESCRIPTION	UNITS
PSA	Unsmoothed peak of the sled acceleration profile	m/sec^2
ESV	Endstroke sled velocity; velocity acquired between time of first motion and end of sled acceleration profile	m/sec^2
ROO	Slope of least squares line fit to that portion of the sled acceleration profile occurring in the range [.2 PSA, .5 PSA] and before the time of PSA	m/sec^3 or g/sec
DOP	The total amount of time both pre- and post-PSA spent above 75% of PSA	ms

TABLE 3. Definition of Head Angular Initial Position Parameters.

NAME	DESCRIPTION	UNITS	CO-ORDINATE SYSTEM
PHA	The initial angle of rotation about the X-axis ("roll")	rad	Head Anatomical
PHB	The initial angle of rotation about the carried Y-axis ("pitch")	rad	Head Anatomical
PHC	The initial angle of rotation about the carried Z-axis ("yaw")	rad	Head Anatomical

DATABASE PARTITIONING

This section details the steps taken in partitioning the rhesus kinematic database. Appendix B contains all relevant tables and plots referred to here. The tests in the 1984, 1985, and 1987 rhesus -X series were first screened for data quality. For each test, a folder was prepared containing plots of all head kinematic quantities, information on anesthetic state, sled parameters, head initial condition parameters, and other relevant data.

All plots were checked for artifacts and other abnormal values. Descriptive statistics, including means, standard deviations, maximum and minimum values and coefficients of variation were computed. Histograms were generated to study the distribution of the independent and dependent variables. All available medical information on the rhesus subjects was gathered, including data on pre-test preparation, both long-term and routine, between-test symptomatology, post-test medical status, and necropsy findings. Various preliminary graphical analyses of the data were performed. Plots comparing unanesthetized and anesthetized tests in the 1985 series were generated and analyzed.

Since human $-G_x$ tests are almost invariably conducted in-plane and with the neck-up/chin-up initial head orientation, various subsets of rhesus tests differing in planarity and initial head orientation were identified. The subset of rhesus tests comparable to the in-plane -X neck-up/chin-up human tests was too small to derive any reliable statistical inferences, so new criteria were developed for comparing the key midsagittal in-plane kinematic responses of human and rhesus subjects.

Employing a four-stage procedure, the rhesus kinematic database was partitioned into two basic subsets:

Dataset A: a set of 29 runs termed NUCU (neck-up/chin-up), but in reality encompassing the type of head kinematic behavior observed in the human NUCU, NUCD (neck-up/chin-down), and NFCU (neck-forward/ chin-up) initial head orientations.

Dataset B: a set of 24 runs denoted by NFCD (neck-forward/chin-down) exhibiting the head kinematic behavior observed in human NFCD runs.

As noted in "The Effects of the Initial Position of the Head and Neck on the Dynamic Response of the Human Head and Neck to $-G_x$ Impact Acceleration" [6], the response curves for head angular acceleration (QHB) and velocity (RHB) in the NUCU, NUCD, and NFCU orientations are very similar. The predominant first peak of both QHB and RHB is positive, with the largest values being attained in the NUCU condition, followed by NUCD and NFCU respectively. For human NFCD runs, however, the maximum positive peak for head angular acceleration and velocity is preceded by a comparable, often larger, negative peak. The magnitude of the predominant NFCD positive or negative peaks are severely reduced with respect to the corresponding peaks for the other three conditions.

As the first stage in the partitioning process, the rhesus NUCU, NUCD, NFCU, and NFCD tests were identified by comparing the shapes of human and rhesus kinematic plots. Any test with a significant first negative peak for head angular acceleration (QHB) and velocity (RHB) was deemed NFCD (see Appendix B, pp. B-1 through B-6). Although direct measurement of the rhesus head/neck relative angle was not available, tests with a large negative first peak of head angular acceleration and velocity almost invariably corresponded to large positive initial values of PHB_0, while those with a predominant positive first peak usually corresponded to the smaller positive or to negative values of PHB_0.

The second stage of the partitioning process involved assessing the effect of large out-of-plane kinematic response components on mid-sagittal kinematic response. Since twenty-nine of the fifty-three tests used unanesthetized subjects, with head initial conditions uncontrolled, the initial head roll (PHA_0) and yaw (PHC_0) components were frequently large. In the typical human -X test, the out-of-plane head angular initial conditions (PHA_0 and PHC_0) are negligible and the primary peaks of the out-of-plane kinematic quantities (QHA, QHC, RHA, RHC, AAY) are small in comparison to their midsagittal plane counterparts (QHB, RHB, AAX, and AAZ). Fortunately, there were sufficient numbers of in-plane rhesus tests (13) to allow for comparison with various types of human -X in-plane tests, and with the out-of-plane portion of the rhesus data set (see Appendix B, pp. B-7 through B-40).

The third stage in test partitioning was to determine the effect of anesthetic state. In the 1984 series, all animals were unanesthetized. In the 1985 series, devoted to determining the effects of anesthesia on head kinematic output, the head initial conditions for the anesthetized test for a given animal were matched to those for a comparable unanesthetized test of the same animal. In the 1987 series all animals were anesthetized, resulting in enhanced control of head

initial conditions and test planarity. All twelve tests from the 1987 series are in the NUCU dataset; nine are in-plane.

The effect of the anesthetic state on kinematic output was assessed in three different ways. The first method involved various graphical comparisons of key kinematic outputs to determine within-subject repeatability in the anesthetized and unanesthetized states, and the differences between unanesthetized and anesthetized responses (see Appendix B, pp. B-41 through B-58). Due to the small number of animals available for comparison and the unbalanced distribution of the tests among the various g levels and anesthetic states, no formal analysis of a variance (ANOVA) procedure was attempted.

However, with the pooling of the 1984, 1985, and 1987 series and the subsequent partitioning into datasets A and B, a sufficient number of anesthetized and unanesthetized tests existed in dataset A (NUCU) for a second assessment of the effect of anesthesia on kinematic response. This assessment involved including a grouping variable (IGP) among the independent variables in the various head kinematic regressions. As a third and final assessment, the regression equations obtained for the 18 anesthetized NUCU tests in dataset A were used to predict the kinematics of the other 11 unanesthetized NUCU tests. Since dataset B (NFCD) contained only six anesthetized tests, no similar validation was attempted.

The final stage in the partitioning was to evaluate the effect of repeated exposures on kinematic output, since the full dataset of 53 tests utilized a total of 26 animals. To evaluate the effect of repeated exposures on kinematic output, the following assumptions were made:

(1) High g-level exposures in the NFCD position are less hazardous than comparable NUCU exposures.

(2) Tests at the 40 g level are not injurious.

(3) If a set of tests for a given animal with approximately the same inputs yield approximately the same outputs, regardless of the number of intervening tests, no injury adversely affecting head kinematics will have occurred.

Evidence to support the above assumptions is provided by plots on pp. B-53 through B-58 in Appendix B.

MATHEMATICAL METHODOLOGY

The following steps were taken in the statistical analysis of datasets A and B.*

(1) Descriptive statistics for all variables were generated using P1D and P9R.

(2) Univariate regressions of each dependent variable QHB, RHB, AAX, AAZ, and AAR on the independent variable vector (IGP, PSA, ESV,ROO, DOP, PHA, PHB, and PHC) were performed using P9R (best subsets regression). In most cases regression on the whole independent variable vector containing sled, head, and grouping parameters using the R^2 or adjusted R^2 criteria provided an over-fitted model, yielding a good estimate of the minimal residual sum of squares (RSS). Since no true replications were available, this estimate was compared with the RSS of models with fewer variables to check goodness of fit.

By analyzing the correlation structure of the independent variables, various candidates for minimal subsets of independent variables were determined. These candidates were then processed with P9R, using both the adjusted R^2 and the CP criteria to identify unbiased minimal models for each dependent variable.

(3) The minimal fits obtained in step 2 (above) were assessed by checking standard

*All statistical regression programs referred to are from the BMDP statistical software package [8].

residual plots, by analyzing the t-statistics for the significance of the regression coefficients, and by noting the F-statistic for significance of the overall regression.

(4) Careful study of the Mahalanobis [9] and Cook [10] statistics, and additional analyses of various residual plots and histograms were made to check for and evaluate outlier, influential points, and clusters in the data and to assess the need for higher order terms in the model.

(5) Using the results of steps 1 through 4, a maximal subset of outlier-free tests and a minimal subset of independent variables was determined for each of the 5 dependent variables (QHB, RHB, AAX, AAZ, and AAR) for datasets A and B.

Appendix C contains the tabulated and plotted results of these final regressions.

In order to test the models produced by P9R and to check on the effects of possible outlier and the high correlation between the independent variables, the data in sets A and B were regressed using stepwise regression (P2R), principal components regression (P4R), and rank regression (P9R). These results corroborated the original models. Various cross-validations were attempted using P9R. Regression equations based on data from anesthetized tests were used to predict the results of unanesthetized tests in dataset A. Similarly, in-plane data were used to predict out-of-plane results, single exposure data to predict the results of later subjects exposed to multiple runs. However, due to the uneven distribution of tests among the various categories—anesthetized, unanesthetized, in-plane, out-of-plane, single or multiple exposures — no conclusive results were obtained.

The results of these model tests and cross-validations are *not* included in this report. However, all these results, as well as those addressed in Appendix C and various other statistical data, may be found in file 7933/USERS/SAL/ANIMALTECH1 on the NAVBIODYNLAB in-house HP9000/550 system.

DISCUSSION

The following observations are made concerning the results of this study:

(1) The similarity of human and rhesus mid-sagittal head kinematic responses in both the NUCU and NFCD head orientations is undeniable (Appendix B, pp. B-1 through B-6).

(2) In dataset A, the grouping variable (IGP) was not statistically significant. This, combined with the various anesthetized and unanesthetized plots (Appendix B, pp. B-41 through B-58) strongly suggest that anesthesia has no appreciable effect on rhesus head kinematics.

(3) The extremely high correlation among the sled parameters (PSA, ESV, ROO, DOP), the small coefficients of variation of ESV, ROO, DOP, and the controllability of PSA led to the choice of PSA as the representative sled parameter.

(4) No viable assessment of the effect of varying PSA, ESV, ROO, and DOP on kinematic output was possible with the given data.

(5) PHB was found to be the most significant parameter in 23 in-plane animal tests. Also, PHA and PHC correspond to an out-of-plane response not observed in human $-G_x$ tests. Therefore, PHB was chosen as the representative head angular parameter.

(6) The effect of the observed out-of-plane kinematic responses is to decrease the primary peak values of OHB and RHB. The underlying shape characteristics are left intact. AAX, AAZ, and AAR are much less affected by out-of-plane behavior (Appendix B, pp. B-39 and B-40).

(7) For multiple exposures, a rhesus subject may be tested at higher g levels (70^+g) in the NFCD position without apparent degradation of kinematic output (Appendix B, pp. B-53

through B-58). No comparable statement can be made about repeated high-g NUCU exposures.

Observations (1) through (7) imply that models based on PSA and PHB, while ignoring the effects of anesthesia, lack of planarity, and repeated exposures, are justifiable. Such models are desirable for comparison with human $-G_x$ results. Such comparisons should be made only with sets of human $-G_x$ tests having small coefficients of variation for ESV, ROO, and DOP.

The primary peaks of the five key kinematic variables (QHB, RHB, AAX, AAZ, and AAR) regressed excellently on PSA, PHB, and PHB^2 in almost all cases, with R^2 values ranging from .84 to .94. Though obtained using best subsets regression (P9R), essentially the same models resulted when, stepwise, rank and principal components regression techniques were applied. The regressions for the linear accelerations AAX, AAZ, and AXZ were the best. The relatively poor regression of AAZ in the NFCD case (R^2=.65) may be due to restraint interaction or anatomical constraints in the rhesus head-neck area. Fourteen of the twenty-four runs in dataset B have initial head pitches (PHB) ranging from 28° to 70° forward.

The 95% confidence intervals about the predicted mean responses contained the observed responses in almost all cases. These intervals were usually fairly wide, sometimes allowing a change in the sign of the response. This may be attributed to the larger variation in rhesus head responses and to the imperfect classification of tests as either NUCU or NFCD.

CONCLUSIONS AND RECOMMENDATIONS

The following conclusions may be made:

(1) Rhesus mid-sagittal head-kinematic responses are repeatable and are not appreciably affected by the anesthetic state.

(2) Rhesus head-kinematic responses regress well on the same input parameters (PSA, PHB), as do human responses. Therefore, the similarity of human and rhesus response curves is not coincidental.

(3) Head angular acceleration and velocity are most sensitive to out-of-plane kinematic response while linear accelerations are extremely robust.

(4) Tests under extreme NUCU or NFCD conditions (i.e., large forward or backward pitch) may require the addition of anatomical and/or restraint variables for improved modeling.

(5) Unbalanced data distribution prevented adequate assessment of model stability and determination of the effects of the sled parameters ESV, ROO, and DOP.

(6) Photo gaps in high-g tests prevented modeling of the photo displacements DAX, DAZ, and PHB.

In light of the above conclusions, it is recommended that:

(1) All kinematic response curves in dataset A be fitted to the same parametric models as human responses. If this proves successful, methods for scaling human and rhesus head-kinematic response should be developed.

(2) Attempts should be made to remove the photo gaps in future high-g rhesus runs, so that displacement data may also be modeled.

(3) Future human and animal experimental series should be jointly planned to facilitate statistical modeling.

(4) A set of –X rhesus experiments to determine the effects of sled parameters ESV, ROO, and DOP should be conducted.

REFERENCES

1. Watkins, T. A. and Guccione, S. J., Jr., "A Statistical Approach to Human Kinematic Response to Impact Acceleration," *Sixteenth Annual International Workshop,* Human Subjects for Biomechanical Research, Atlanta, GA, 1988, pp. 209-225.
2. Seemann, M. R., Lustick, L. S., and Frisch, G. D., "Mechanism for Control of Head and Neck Dynamic Response," *Transactions of the Society of Automotive Engineers,* Warrendale, PA, 1984, pp. 213-219.
3. Becker, E., "Stereoradiographic Measurements for Anatomically Mounted Instruments," *Proceedings of the Twenty-First Stapp Car Crash Conference*, Society of Automotive Engineers, Inc., Warrendale, PA. 1977, pp. 478-480.
4. Ewing, C. L., Thomas, D. J., Lustick, L. S., Muzzy, W. H., III, Willems, G. C., and Majewski, P. J., "Dynamic Response of Human Head and Neck to $+G_y$ Impact Acceleration," *Proceedings of the Twenty-First Stapp Car Crash Conference*, Society of Automotive Engineers, Inc., Warrendale, PA, 1975, p. 554.
5. Ewing, C. L., Thomas, D. J., Lustick, L. S., Muzzy, W. H., III, Willems, G. C., and Majewski, P. J., "The Effects of Duration, Rate of Onset, and Peak Sled Acceleration on the Dynamic Response of the Human Head and Neck," *Proceedings of the Twentieth Stapp Car Crash Conference*, Society of Automotive Engineers, Inc., Warrendale, PA, 1976, pp. 4-5.
6. Ewing, C. L., Thomas, D. J., Lustick, L. S., Muzzy, W. H., III, Willems, G. C., and Becker, E. B., "The Effects of the Initial Position of the Head and Neck on the Dynamic Response of Human Head and Neck to $-G_x$ Impact Acceleration," *Proceedings of the Nineteenth Stapp Car Crash Conference*, Society of Automotive Engineers, Inc., Warrendale, PA, 1975, pp. 489-490.
7. Seemann, M. R. and Lustick, L. S., "Combination of Accelerometer and Photographically Derived Kinematic Variables Defining Three-Dimensional Rigid Body Motion," *Proceedings of the Second International Symposium of Biomechanics Cinematography and High Speed Photography*, Society of Photo-Optical Instrumentation Engineers, Bellingham, WA, 1981, Vol. 291, pp. 133-140.
8. Dixon, W. J., Brown, M. B., Engelman, L, Frane, J. W., Hill, M. A., Jennrich, R. I., and Toporek, J. D., *BMDP Statistical Software 1985 Printing*, University of California Press, Berkley, CA, 1988.
9. Roy, S. N., *Some Aspects of Multivariate Analysis*, Wiley, NY, 1957.
10. Draper, N. and Smith, H., *Applied Regression Analysis* (2nd Edition), John Wiley & Sons, New York, NY, 1966, pp. 170-175.

BIBLIOGRAPHY

Bartholomew, J. M., "Data Reduction for –X Rhesus Experiments," Memorandum, NAVBIODYNLAB, New Orleans, LA, 1 March 1985.

Bartholomew, J. M., "Data Summary for –X Rhesus Experiments (Lightweight Sled)," Memorandum, NAVBIODYNLAB, New Orleans, LA, 5 September 1984.

Bartholomew, J. M., "Data Summary for –X Rhesus Experiments (Unanesthetized vs, Anesthetized)," Memorandum, NAVBIODYNLAB, New Orleans, LA, 7 May 1985.

Bartholomew, J. M., "Data Summary for –X Rhesus Experiments (Anesthetized and Cadavers)," Memorandum, NAVBIODYNLAB, New Orleans, LA, 8 April 1987.

Lustick, L., "Initial Head and Neck Position for –X Vector Direction Animal Runs," Memorandum, NAVBIODYNLAB, New Orleans, LA, 1985.

Lustick, L., "Estimation of Severity of –X Rhesus Runs," Memorandum, NAVBIODYNLAB, New Orleans, LA, 22 March 1985.

Lustick, L., "Processing of Inertial Data from $-G_x$ Rhesus Runs," Memorandum, NAVBIODYNLAB, New Orleans, LA, 10 February 1981.

Unterharnscheidt, F. J., "Neuropathology of Rhesus Monkeys Subjected to $-G_x$ Impact Acceleration." In: Ewing, C. L. Thomas, D. J. Sances, A., and Larson, J. (Eds.), *Impact Injury of the Head and Spine*, Charles C. Thomas, Publishers, Springfield, IL, 1983, pp. 94–176.

Watkins, T. A. and Guccione, S. J., "A Consistent Statistical Model for Human Kinematic Response to Impact Acceleration." *Seventeenth Annual International Workshop on Human Subjects for Biomechanical Research*, Society of Automotive Engineers, Warrendale, PA, pp. 117–132, 1989.

Weiss, M. S., Guccione, S. J., and Watkins, T. A., "A Kinematic/Dynamic Model for Prediction of Neck Injury During Impact Acceleration." *AGARD Conference Proceedings No. 471*, North Atlantic Treaty Organization Advisory Group for Aerospace Research and Development, Neuilly-sur-Seine, France, pp. 11:1-6, 1990.

Willems, G. L., "Quality Check of Impact Database," Memorandum, NAVBIODYNLAB, New Orleans, LA, 8 December 1987.

APPENDIX A

1984, 1985, 1987 RHESUS -X EXPERIMENTAL SERIES

TABLE A1. 1984 Animal -X Experimental Series: Summary.					
TEST	ID	G LEVEL	HEAD POSITION	CONSCIOUSNESS	EVOKED POTENTIAL
LX4783	AR660B	57	NFCD	U	
LX4784	AR660B	64	NFCD	U	
LX4785	AR660B	79	NFCD	U	
LX4786	AR660B	96	NFCD	U	
LX4788	ARNR16	56	NFCD	U	
LX4789	ARNR16	71	NFCD	U	
LX4790	ARNR16	85	NUCU	U	
LX4791	ARNR16	101	NUCU	U	
LX4795	ARNR21	101	NFCD	U	YES
LX4799	ARNR18	106	NUCU	U	YES
LX4801*	ARNR34	102	NUCU	U	
LX4803*	ARNR24	86	NUCU	U	YES
LX4806	ARNR11	86	NFCD	U	
LX4808	AR8739	56	NFCD	U	
LX4810	ARNR23	56	NUCU	U	YES
LX4812	AR8696	86	NFCD	U	YES
LX4814	ARNR36	71	NUCU	U	
LX4818	AR8789	71	NFCD	U	YES
LX4820	AR8739	56	NUCU	U	YES
LX4822	ARNR39	86	NUCU	U	

* Fatal run.

Number of runs: 20
Number of NUCU: 9
Number of NFCD: 11
Number of anesthetized: 0
Number of unanesthetized: 20
Number of evoked potentials: 7
Number of fatal runs: 2

TABLE A2. 1985 Animal -X Experimental Series: Summary.

TEST	ID	G LEVEL	HEAD POSITION	CONSCIOUSNESS
LX5123	AR0016	41	NFCD	U
LX5125	AR0016	74	NFCD	U
LX5128	AR0016	42	NFCD	U
LX5129	AR0016	74	NFCD	A
LX5132	AR8858	42	NFCD	U
LX5135	AR8845	42	NUCU	U
LX5138	ARNR16	42	NFCD	U
LX5141	ARNR16	75	NFCD	U
LX5144	AR8858	75	NFCD	U
LX5147	AR8845	74	NUCU	U
LX5150	ARNR16	42	NUCU	A
LX5151	ARNR16	42	NFCD	A
LX5152	ARNR16	42	NFCD	A
LX5155	AR0016	42	NUCU	A
LX5156	AR0016	42	NUCU	A
LX5157	AR0016	42	NUCU	A
LX5160	AR0016	74	NFCD	A
LX5161	AR0016	75	NFCD	A
LX5162	AR0016	75	NFCD	A
LX5164	AR0016	75	NUCU	A
LX5165	AR0016	76	NUCU	A

Number of NUCU: 8
Number of NFCD: 13
Number of anesthetized: 12
Number of unanesthetized: 9
Number of evoked potentials: 0
Number of fatal runs: 0

TABLE A3. 1986 Animal -X Experimental Series: Summary.

TEST	ID	G LEVEL	HEAD POSITION	CONSCIOUSNESS	EVOKED POTENTIAL
LX5768	AR5855	58	NUCU	A	
LX5770	AR5852	57	NUCU	A	
LX5772	AR986B	57	NUCU	A	YES
LX5774	AR5855	57	NUCU	A	
LX5777	AR8776	75	NUCU	A	YES
LX5779	AR0019	57	NUCU	A	YES
LX5782	AR5851	75	NUCU	A	YES
LX5784	AR5852	75	NUCU	A	
LX5786	AR894C	89	NUCU	A	YES
LX5793	AR5853	90	NUCU	A	
LX5795	AR798B	92	NUCU	A	
LX5797	ARNR20	91	NUCU	A	

Number of runs: 12
Number of NUCU: 12
Number of NFCD: 0
Number of anesthetized: 12
Number of unanesthetized: 0
Number of evoked potentials: 5
Number of fatal runs: 0

APPENDIX B

KINEMATIC PLOTS AND TABLES

CONTENTS

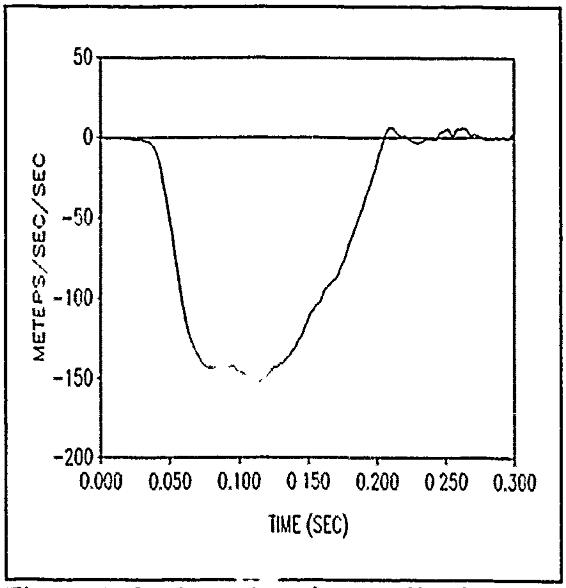

Figure 1. Sled acceleration profile for 15 g, -X human NUCU run.

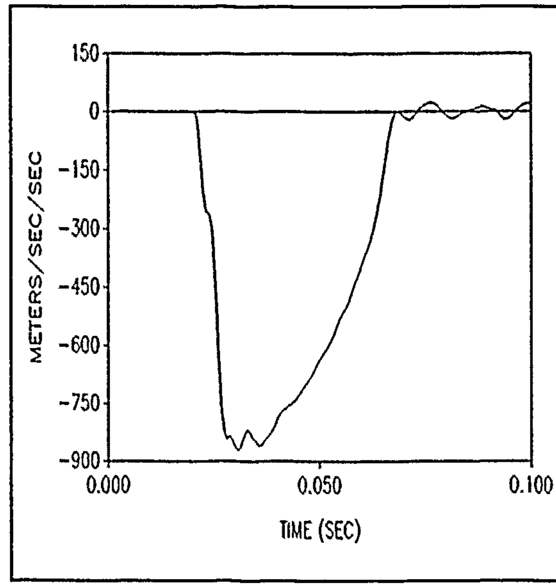

Figure 2. Sled acceleration profile for 89 g, -X animal NUCU run.

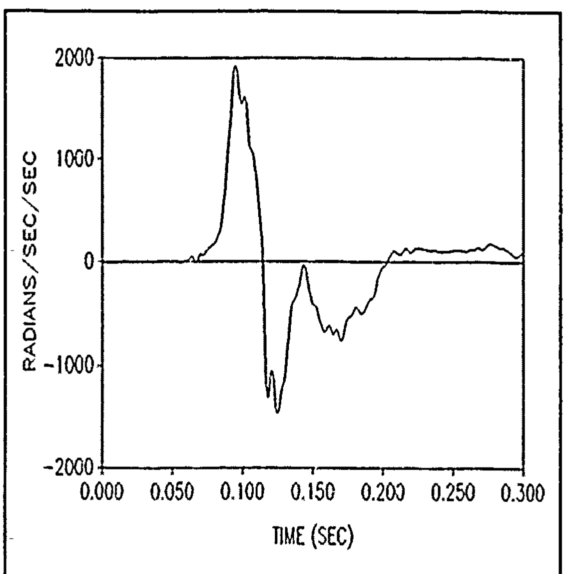

Figure 3. Head angular acceleration (Y-axis) for 15 g, -X human NUCU run.

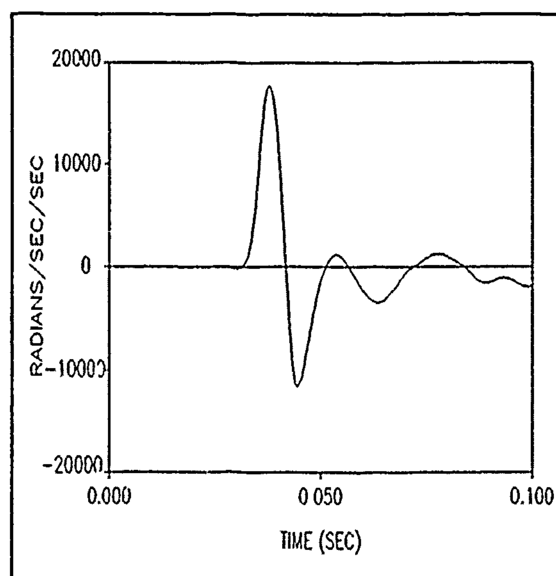

Figure 4. Head angular acceleration (Y-axis) for 89 g, -X animal NUCU run.

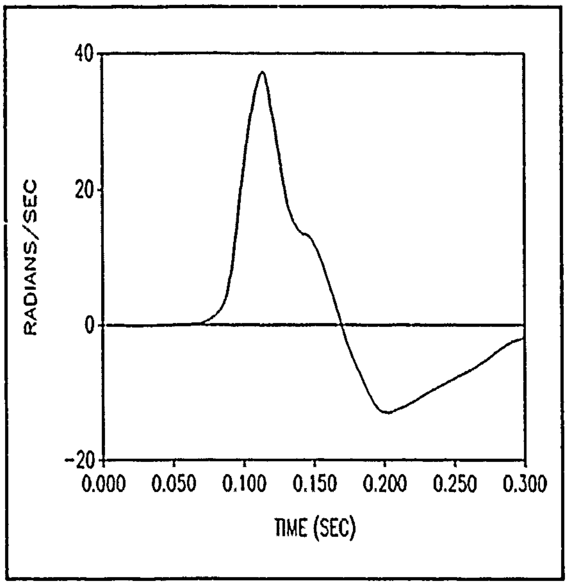

Figure 5. Head angular velocity (Y- axis) for 15 g, -X human, NUCU run.

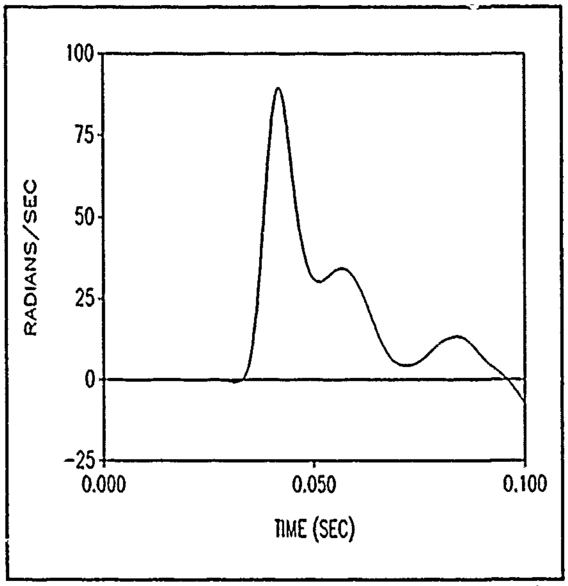

Figure 6. Head angular velocity (Y- axis) for 89 g, -X animal, NUCU run.

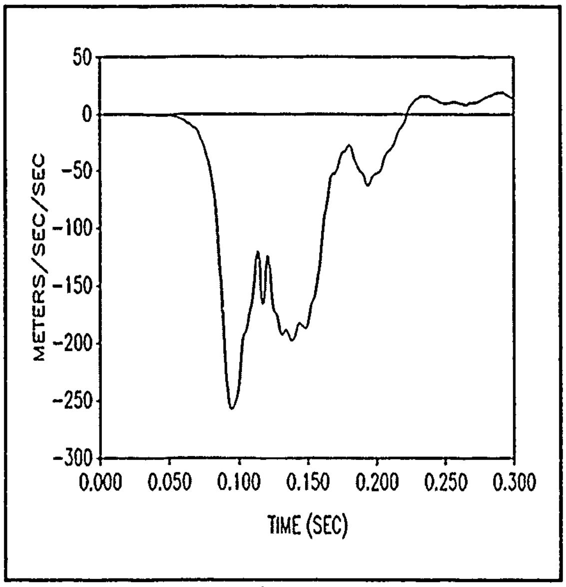

Figure 7. Head linear acceleration (X-component) for 15 g, -X human, NUCU run.

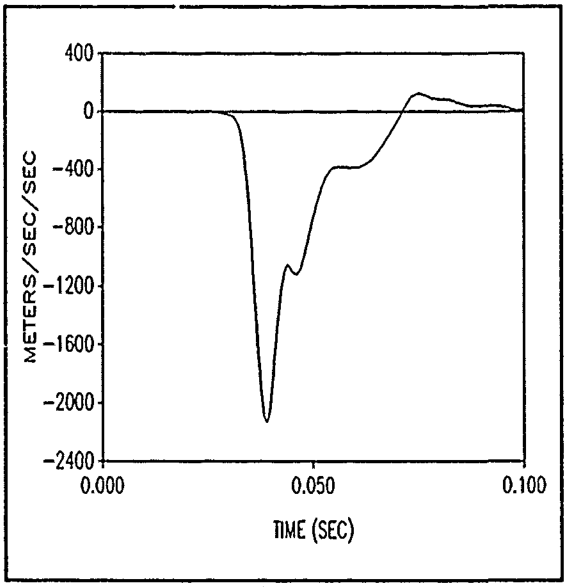

Figure 8. Head linear acceleration (X-component) for 89 g, -X animal, NUCU run.

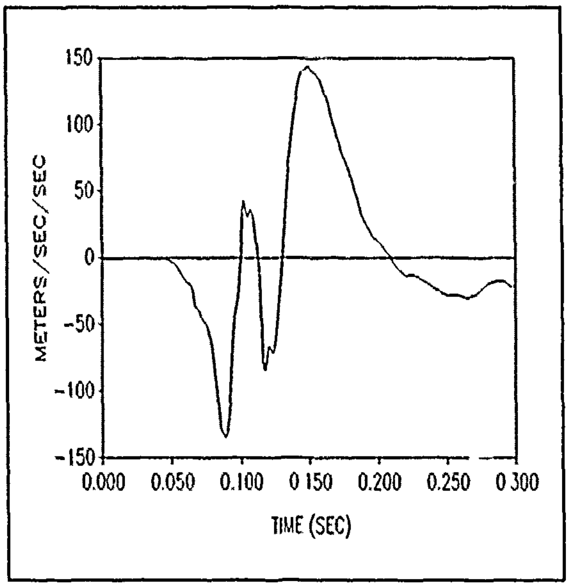

Figure 9. Head linear acceleration (Z-component) for 15 g, -X human, NUCU run.

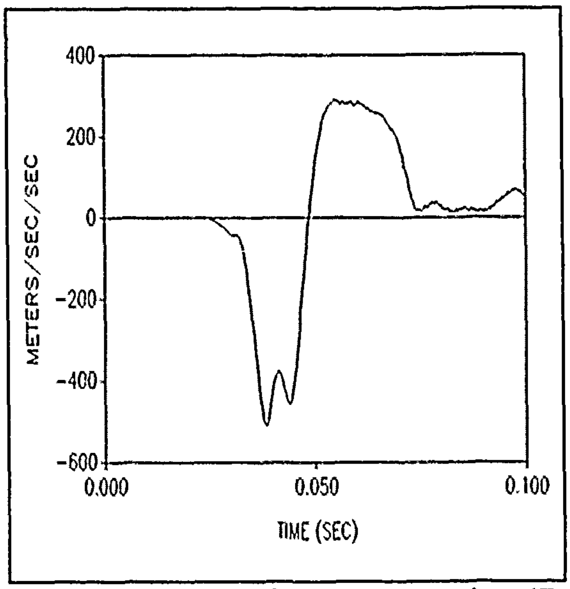

Figure 10. Head linear acceleration (Z-component) for 89 g, -X animal, NUCU run.

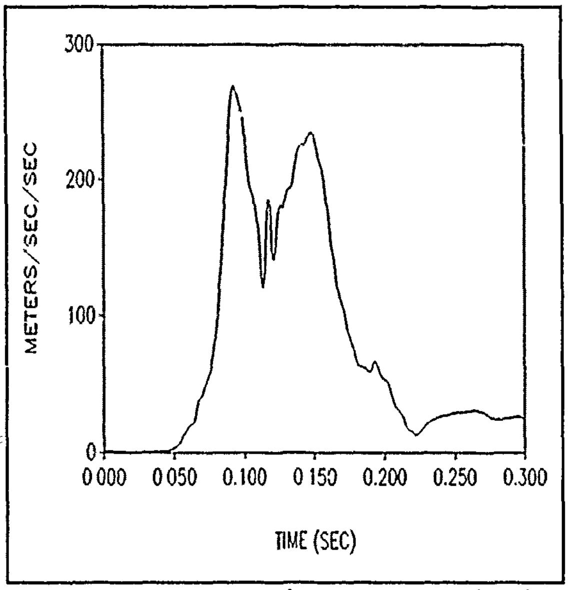

Figure 11. Resultant linear acceleration (X-Z plane) for 15 g, -X human NUCU run.

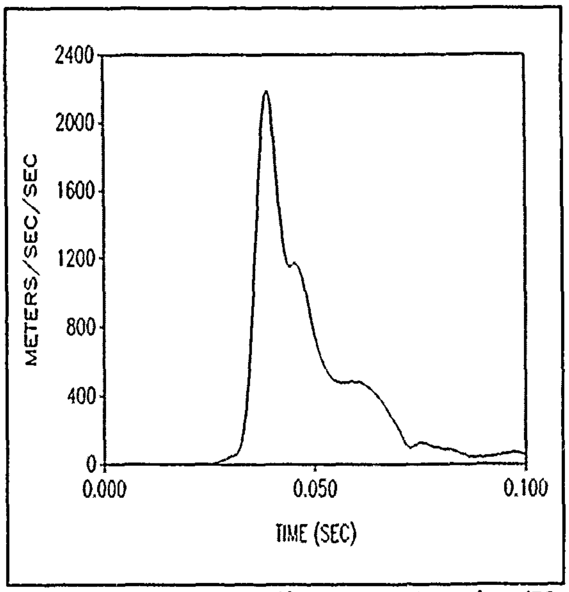

Figure 12. Resultant linear acceleration (X-Z plane) for 89 g, -X animal, NUCU run.

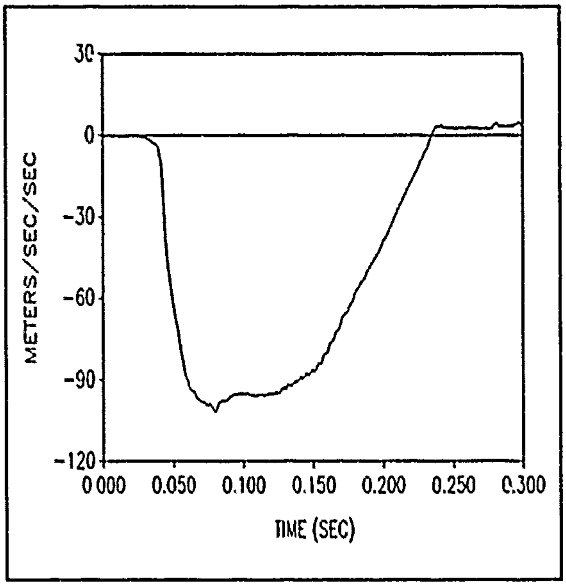

Figure 13. Sled acceleration profile for 10 g, -X human, NFCD run.

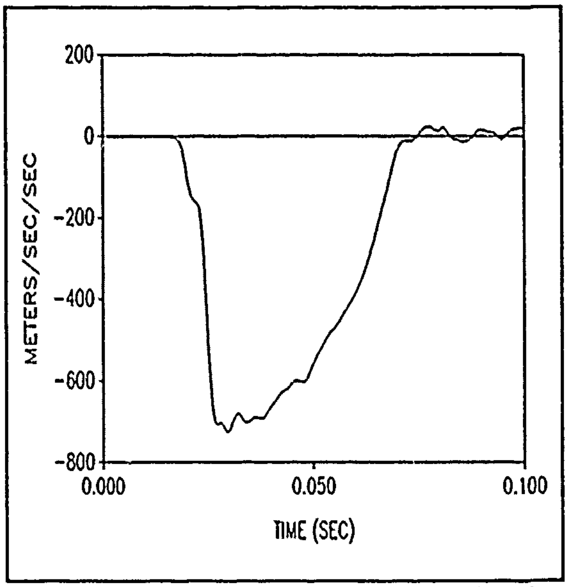

Figure 14. Sled acceleration profile for 74 g, -X animal, NFCD run.

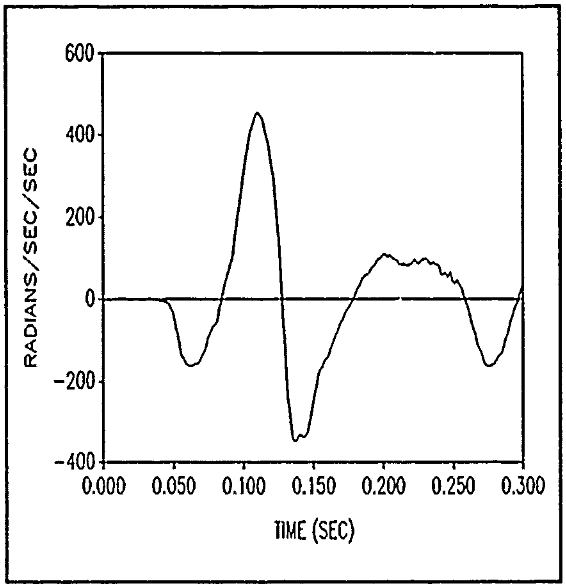

Figure 15. Head angular acceleration (Y-axis) for 10 g, -X human, NFCD run.

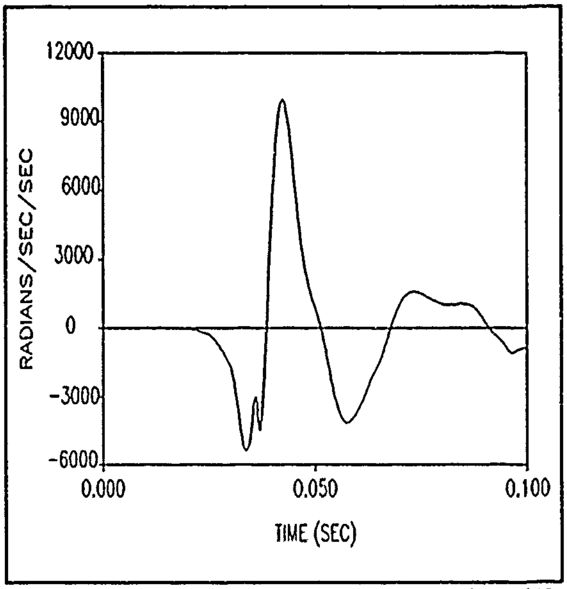

Figure 16. Head angular acceleration (Y-axis) for 74 g, -X animal, NFCD run.

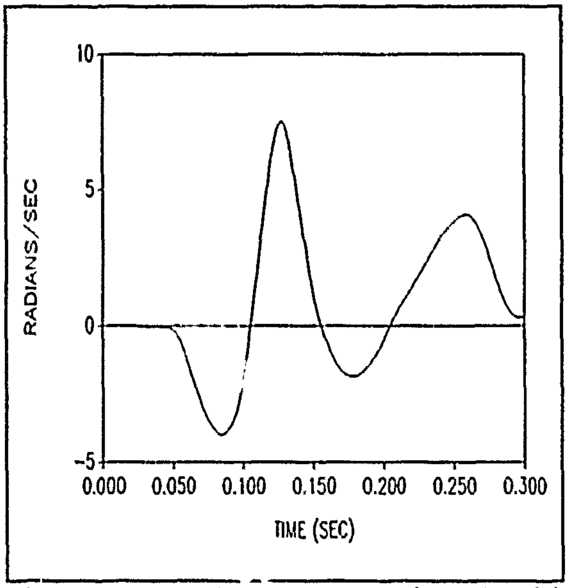

Figure 17. Head angular velocity (Y-axis) for 10 g, -X human, NFCD run.

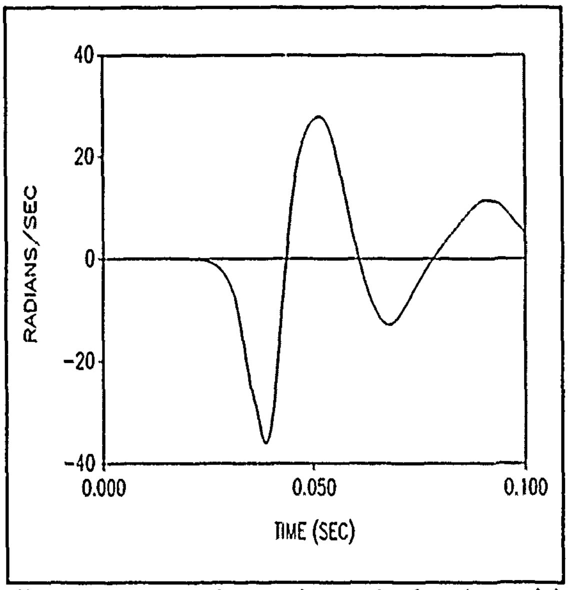

Figure 18. Head angular velocity (Y-axis) for 74 g, -X animal, NFCD run.

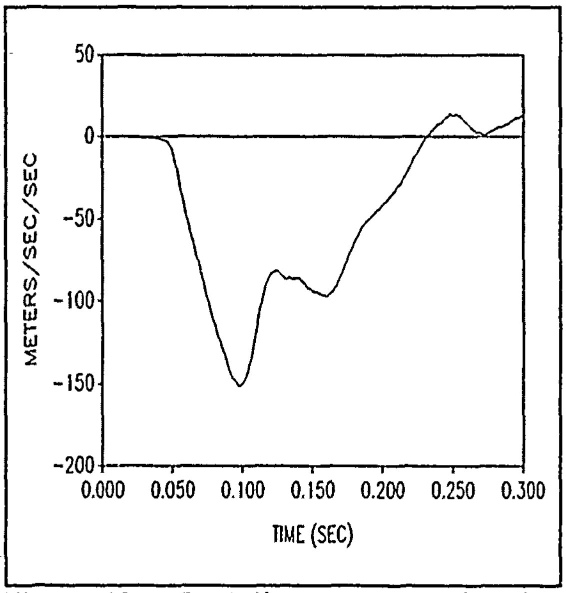

Figure 19. Head linear acceleration (X-component) for 10 g, -X human, NFCD run.

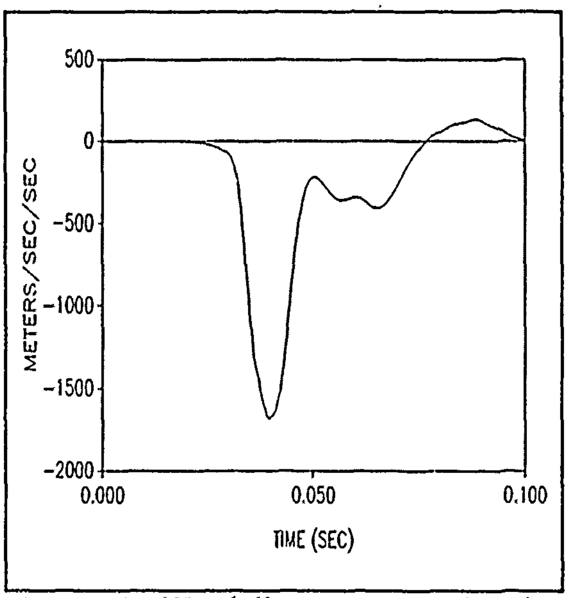

Figure 20. Head linear acceleration (X-component) for 74 g, -X animal, NFCD run.

Human vs. Rhesus Head Kinematics Comparison

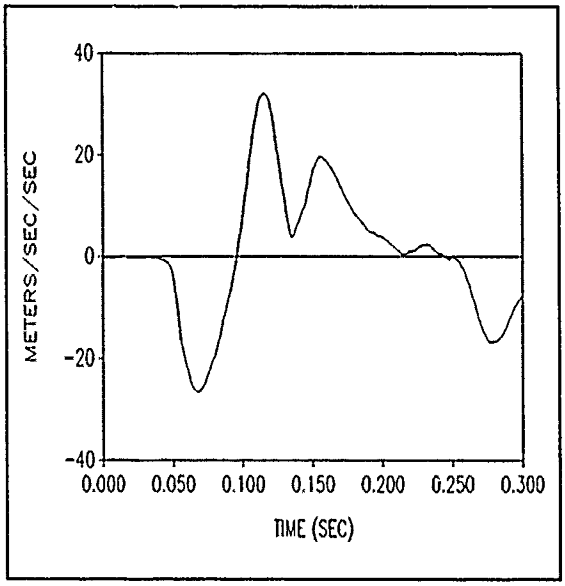

Figure 21. Head linear acceleration (Z-component) for 10 g, -X human, NFCD run.

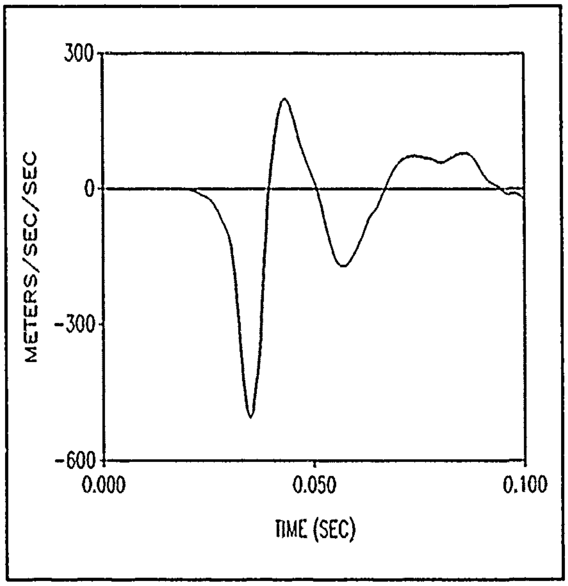

Figure 22. Head linear acceleration (Z-component) for 74 g, -X animal, NFCD run.

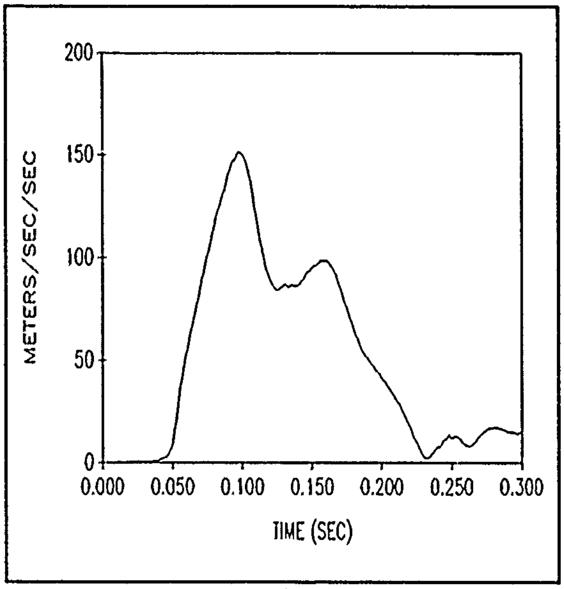

Figure 23. Resultant linear acceleration (X-Z plane) for 10 g, -X human, NFCD run.

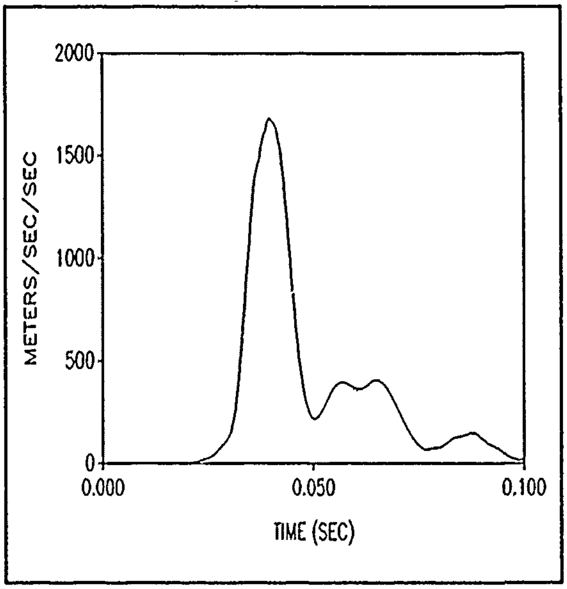

Figure 24. Resultant linear acceleration (X-Z plane) for 74 g, -X animal, NFCD run.

TABLE B1.

TEST	SUBJECT	PHB	COND.	QHB	RHB	AAX	AAZ	AAR
LX5782	AR5851	.144	NUCU	5417 -4236	77 --*	-1612	-530	1691
LX5161	AR0016	.505	NFCD	-6225	-33 24*	-1660	-529	1677

* Occurs very late.

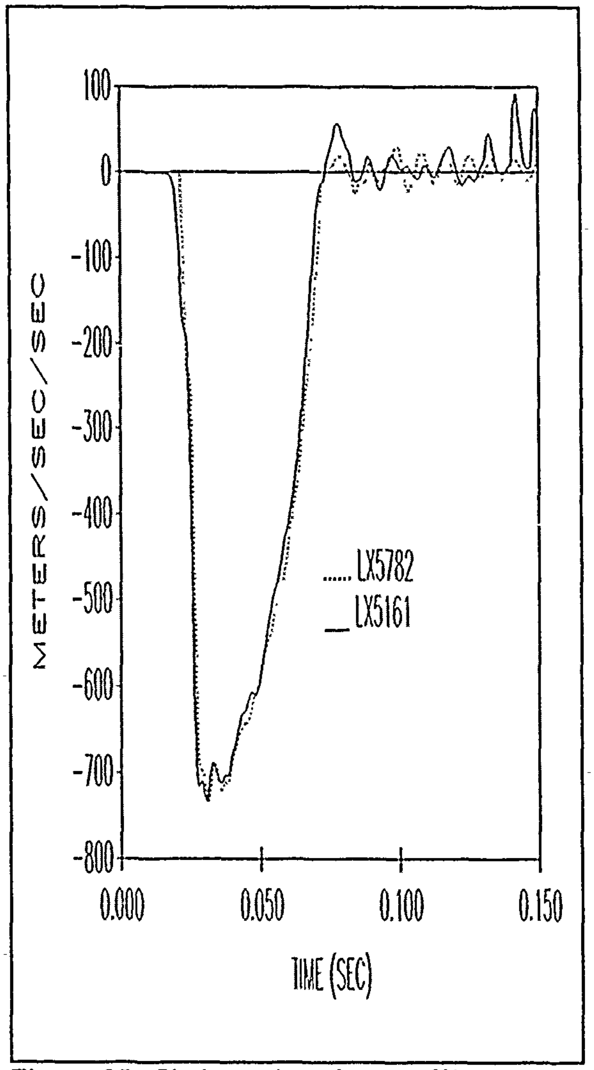

Figure 25. Sled acceleration profiles.

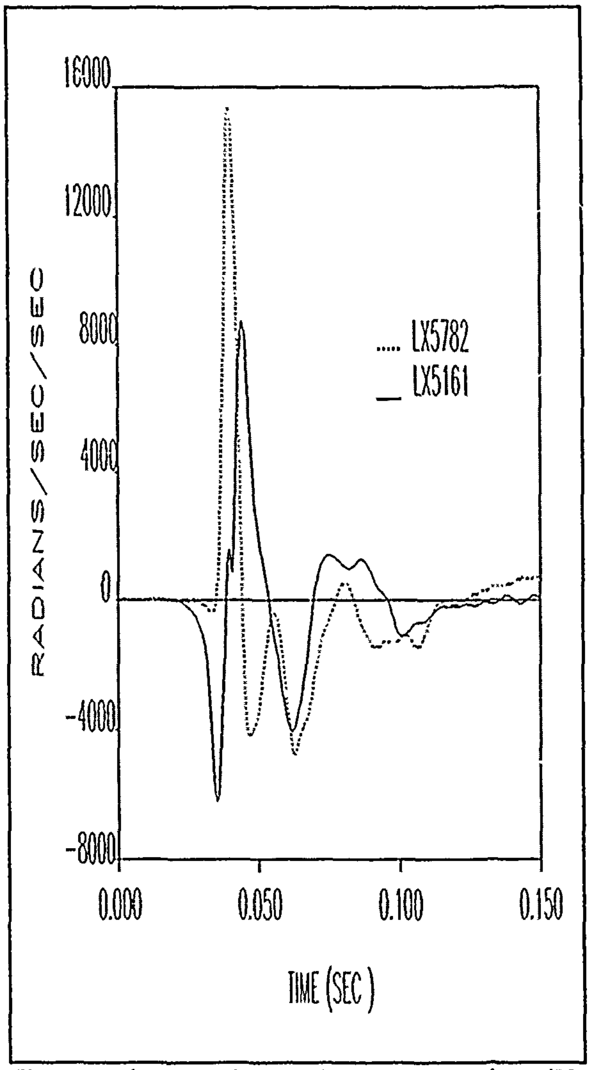

Figure 26. Head angular acceleration (Y-axis).

Rhesus 75 g, In-Plane, NUCU vs. NFCD

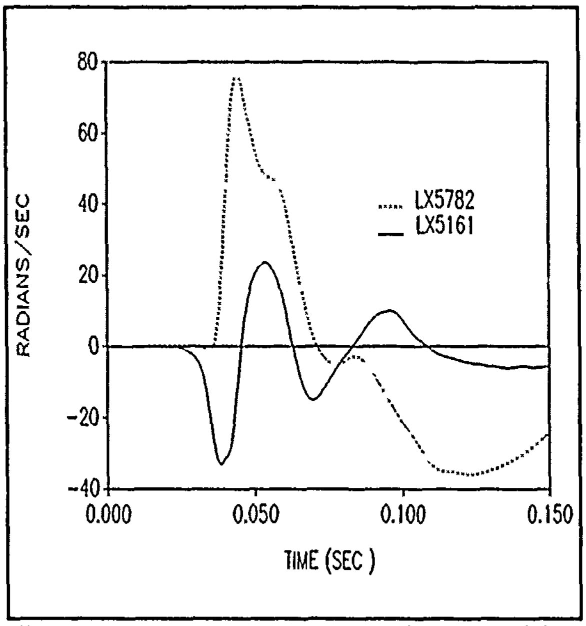

Figure 27. Head angular velocity (Y-axis).

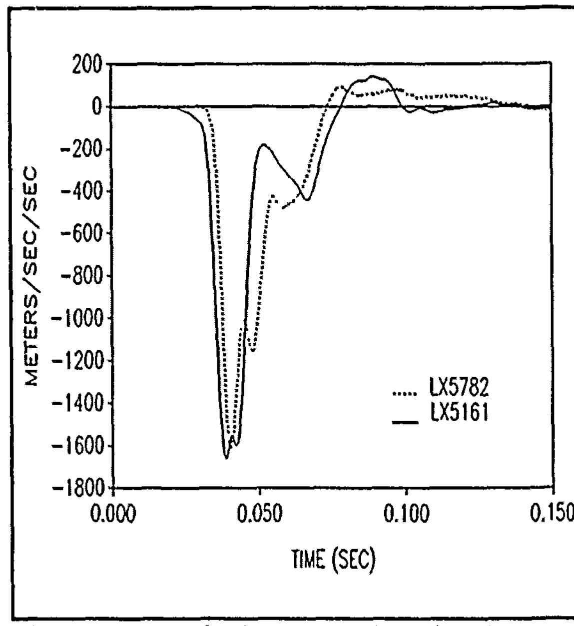

Figure 28. Head linear acceleration (X-component).

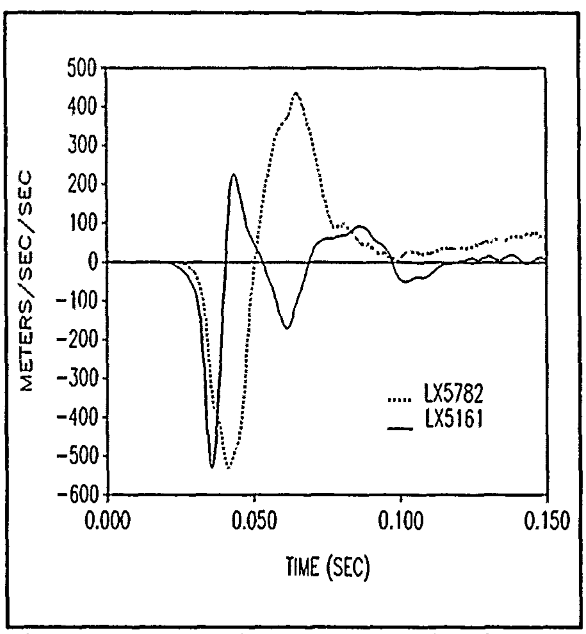

Figure 29. Head linear acceleration (Z-component).

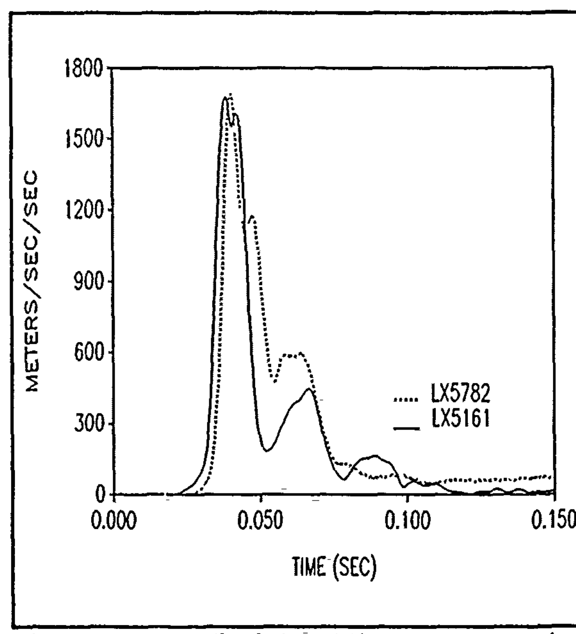

Figure 30. Resultant head linear acceleration (X-Z plane).

Rhesus 75 g, In-Plane, NUCU vs. NFCD

TABLE B2.

TEST	SUBJECT	G LEVEL	PHB	QHB	RHB	AAX	AAZ	AAR
LX5135	AR8845	42	0.094	9546	55	-1120	-214	121
LX5772	AR986B	57	-0.008	12256	56	-1374	-385	140
LX5782	AR5851	75	-0.144*	15417	77	-1612	-530	169
LX5786	AR894C	89	-0.063	17661	89	-2132	-511	218

* Slightly more backward pitch than the rest.

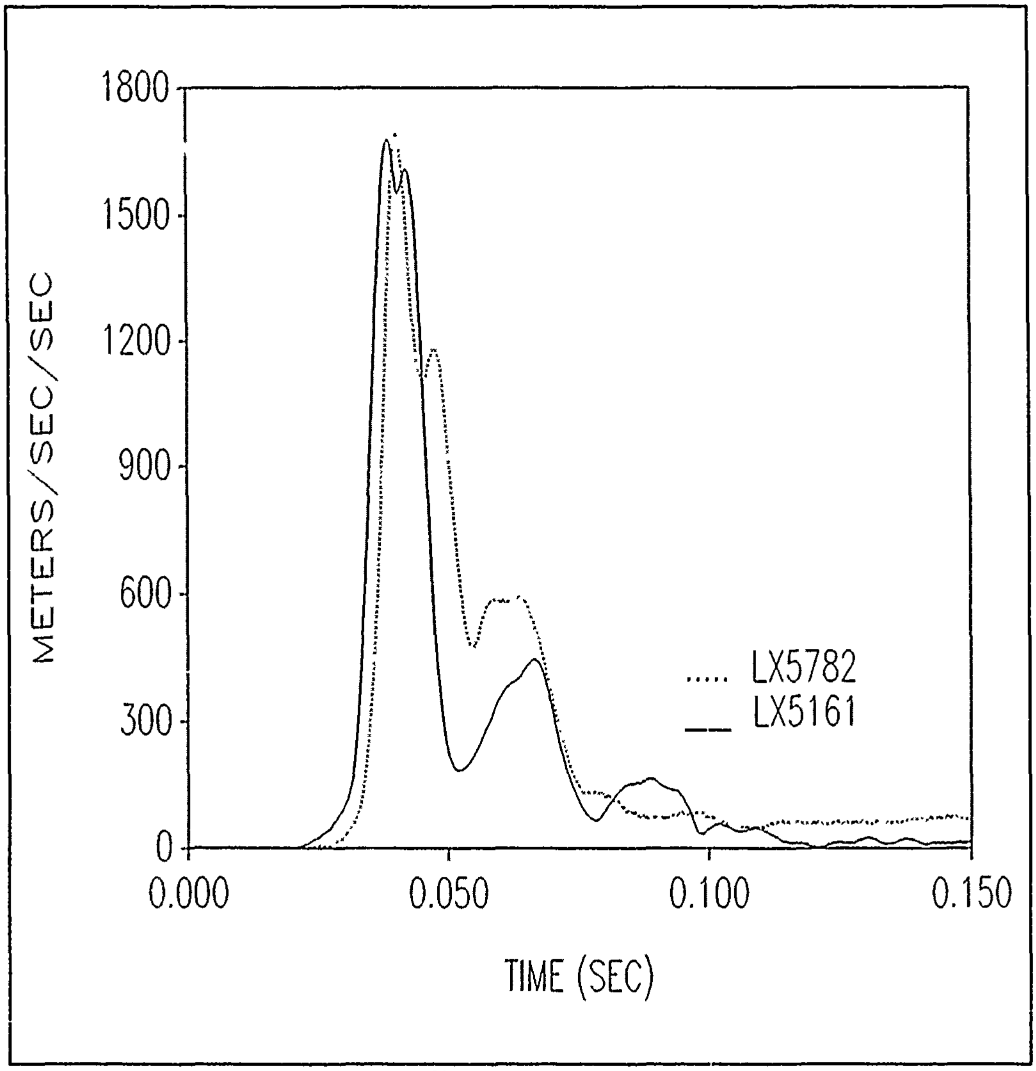

Figure 31. Sled acceleration profiles.

Effect of Increasing G Level, Pure NUCU, In-Plane.

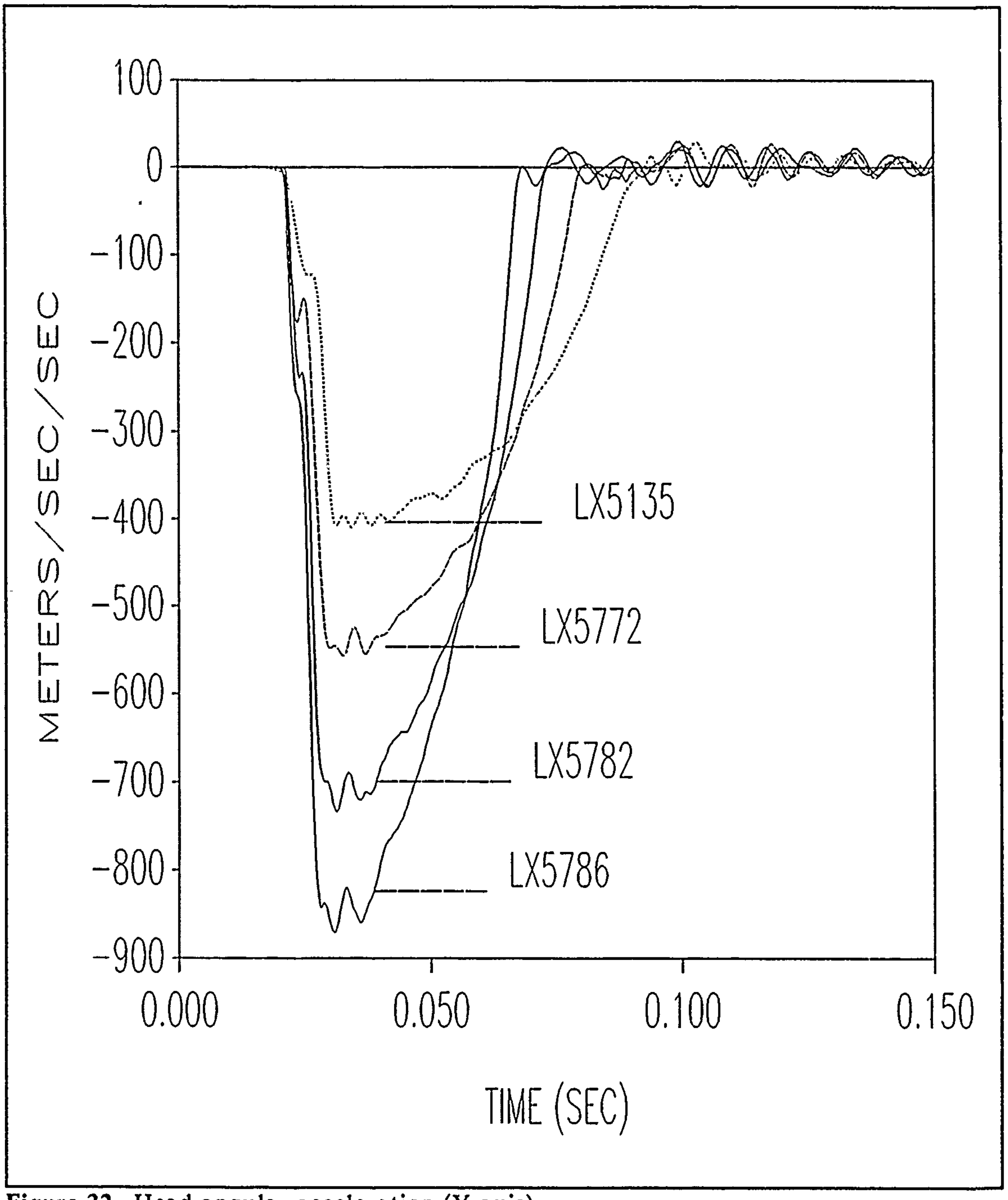

Figure 32. Head angular acceleration (Y-axis).

Effect of Increasing G Level, Pure NUCU, In-Plane.

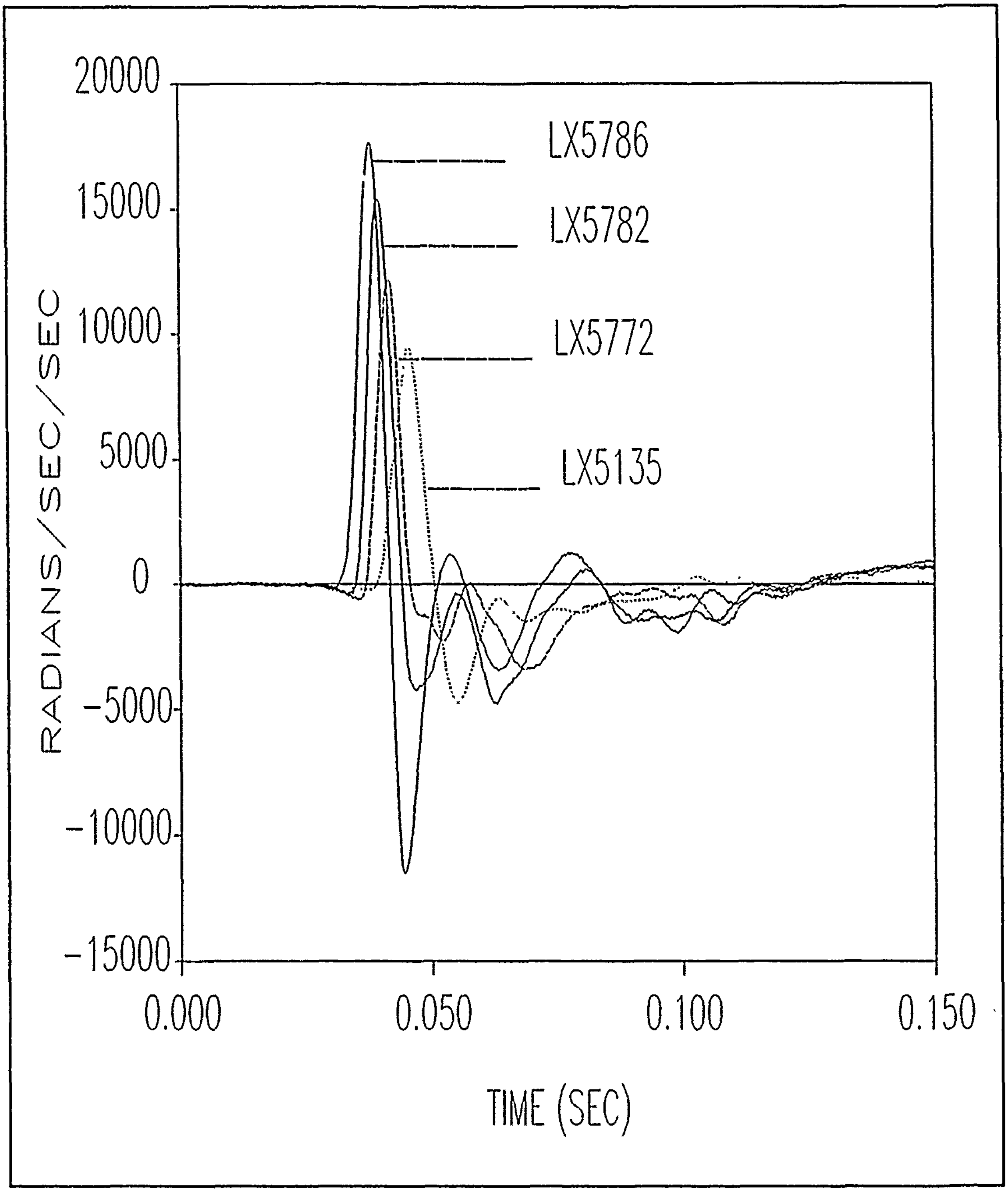

Figure 33. Head angular velocity (Y-axis).

Effect of Increasing G Level, Pure NUCU, In-Plane.

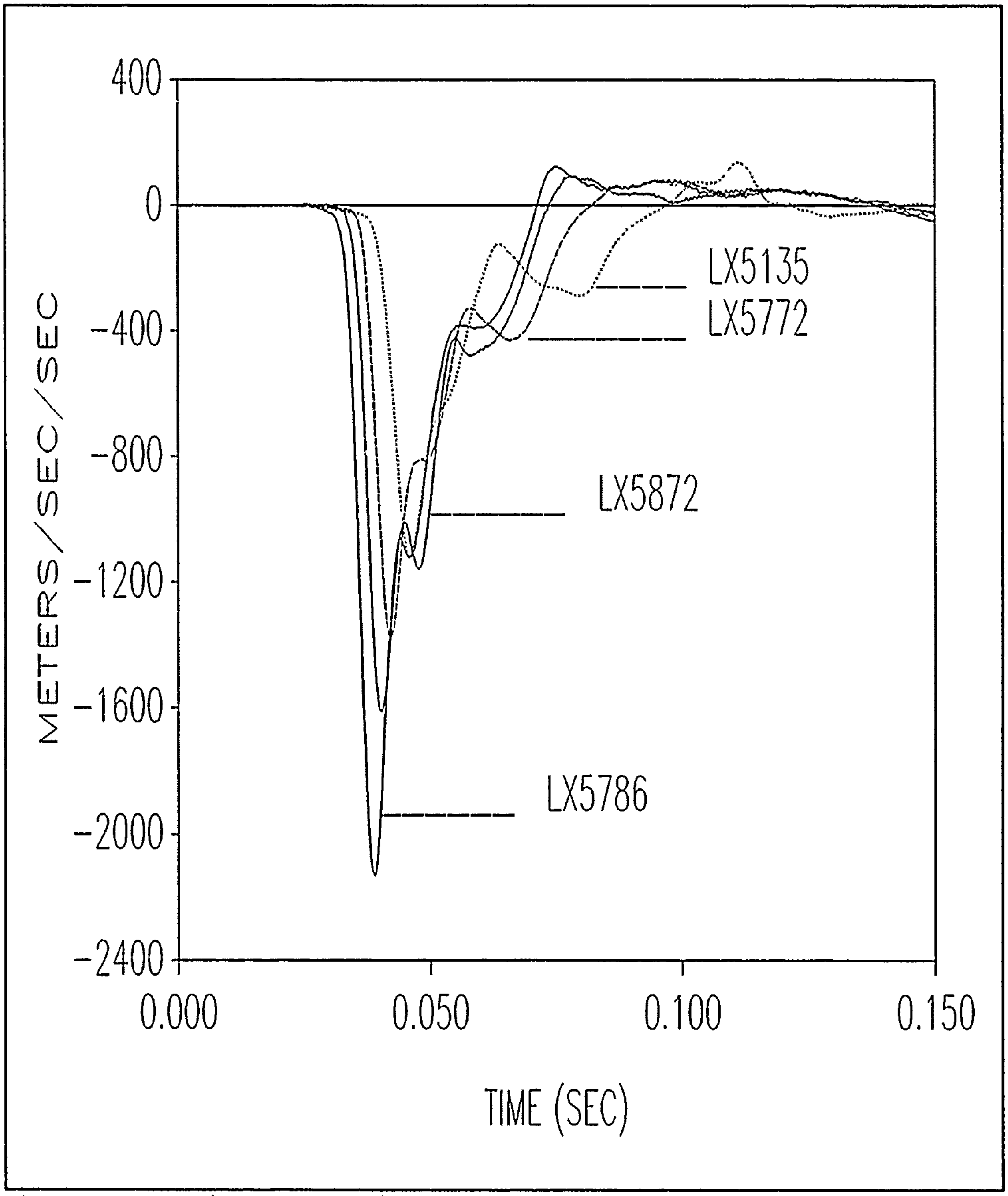

Figure 34. Head linear acceleration (X-component).

Effect of Increasing G Level, Pure NUCU, In-Plane.

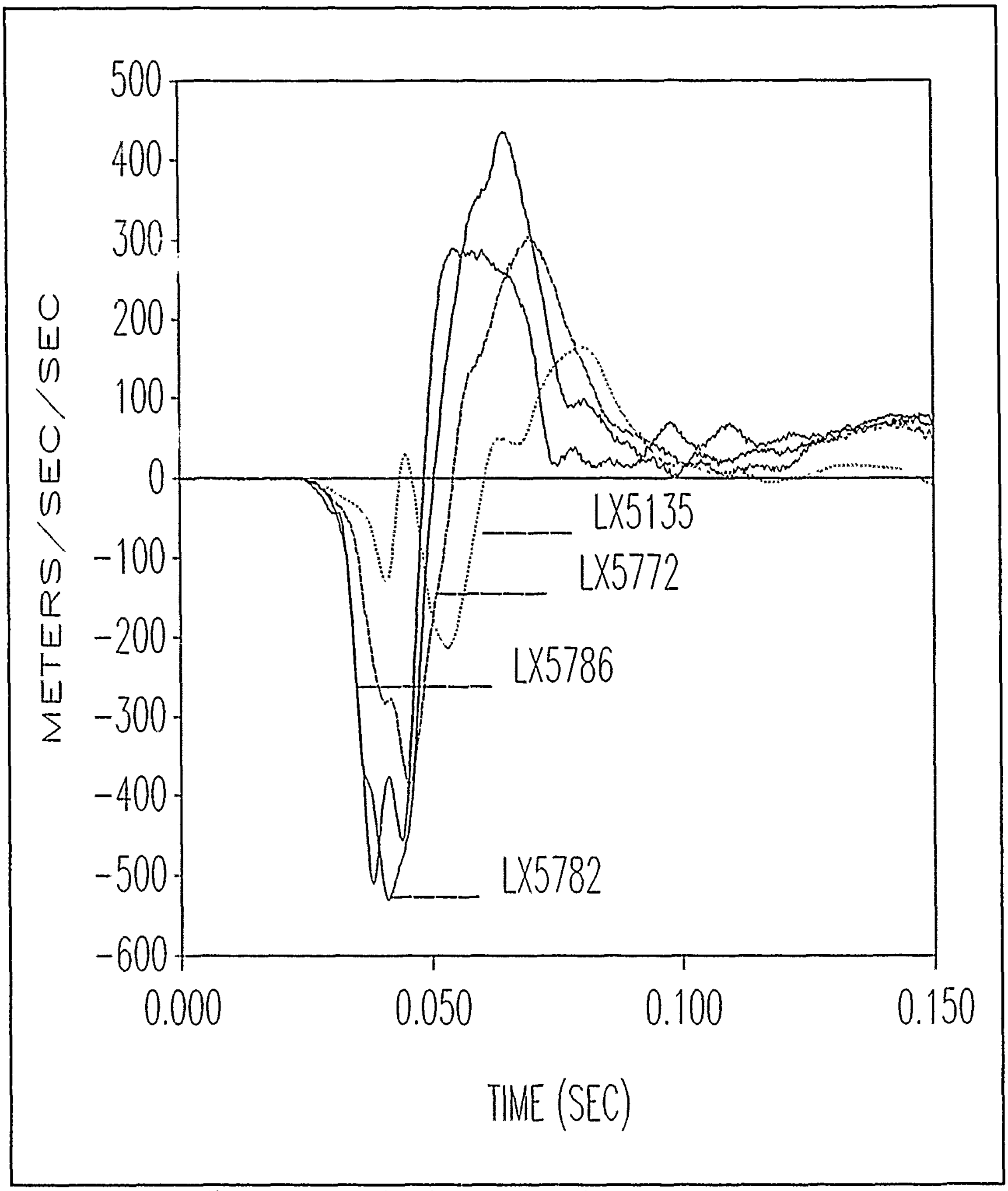

Figure 35. Head linear acceleration (Z-component).

Effect of Increasing G Level, Pure NUCU, In-Plane.

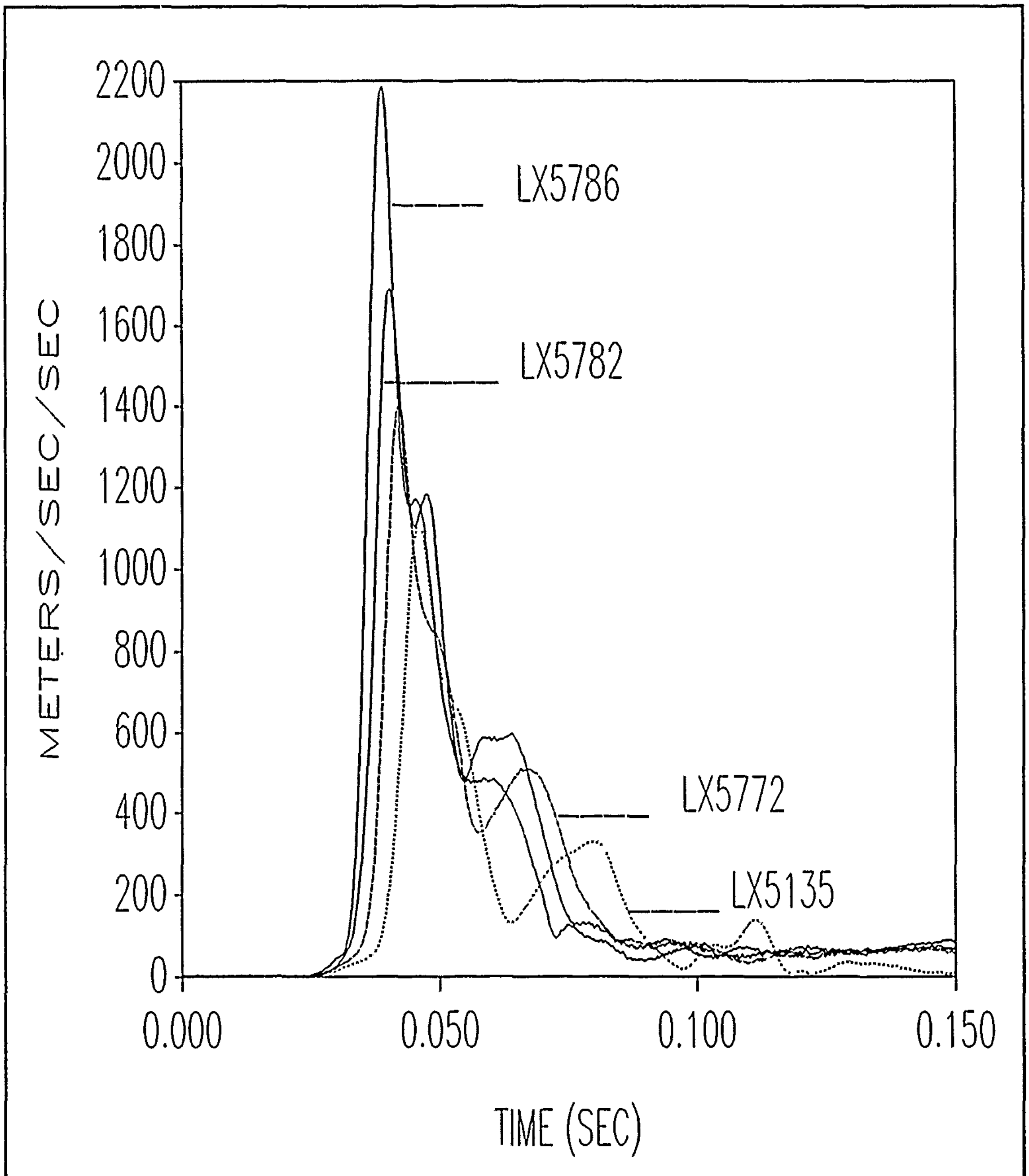

Figure 36. Resultant head linear acceleration (X-Z plane).

Effect of Increasing G Level, Pure NUCU, In-Plane.

TABLE B3.							
TEST	**SUBJECT**	**PHB**	**QHB**	**RHB**	**AAX**	**AAZ**	**AAR**
LX5782	AR5851	-0.144	15417	77	-1612	-530	1691
LX5784	AR5852	-0.213	18868	94	-1827	-552	1838
LX5777	AR8776	-0.433	22637	123	-1522	-808	1613
LX5165	AR0016	-0.820	28123	153	-1500	-1124	*

* Double peak.

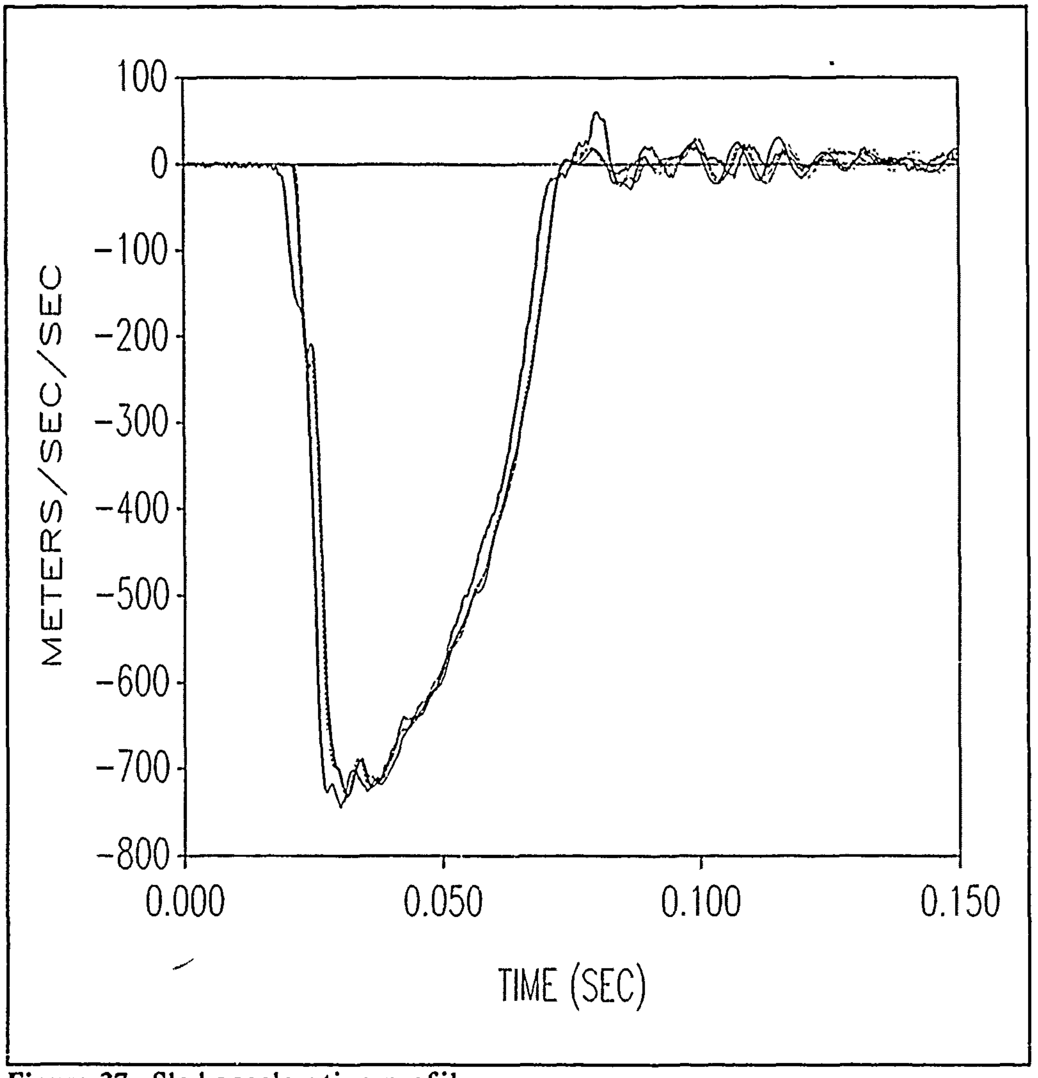

Figure 37. Sled acceleration profile.

Effect of Increasing Negative Pitch (PHB), 75 g, In-Plane, NUCU.

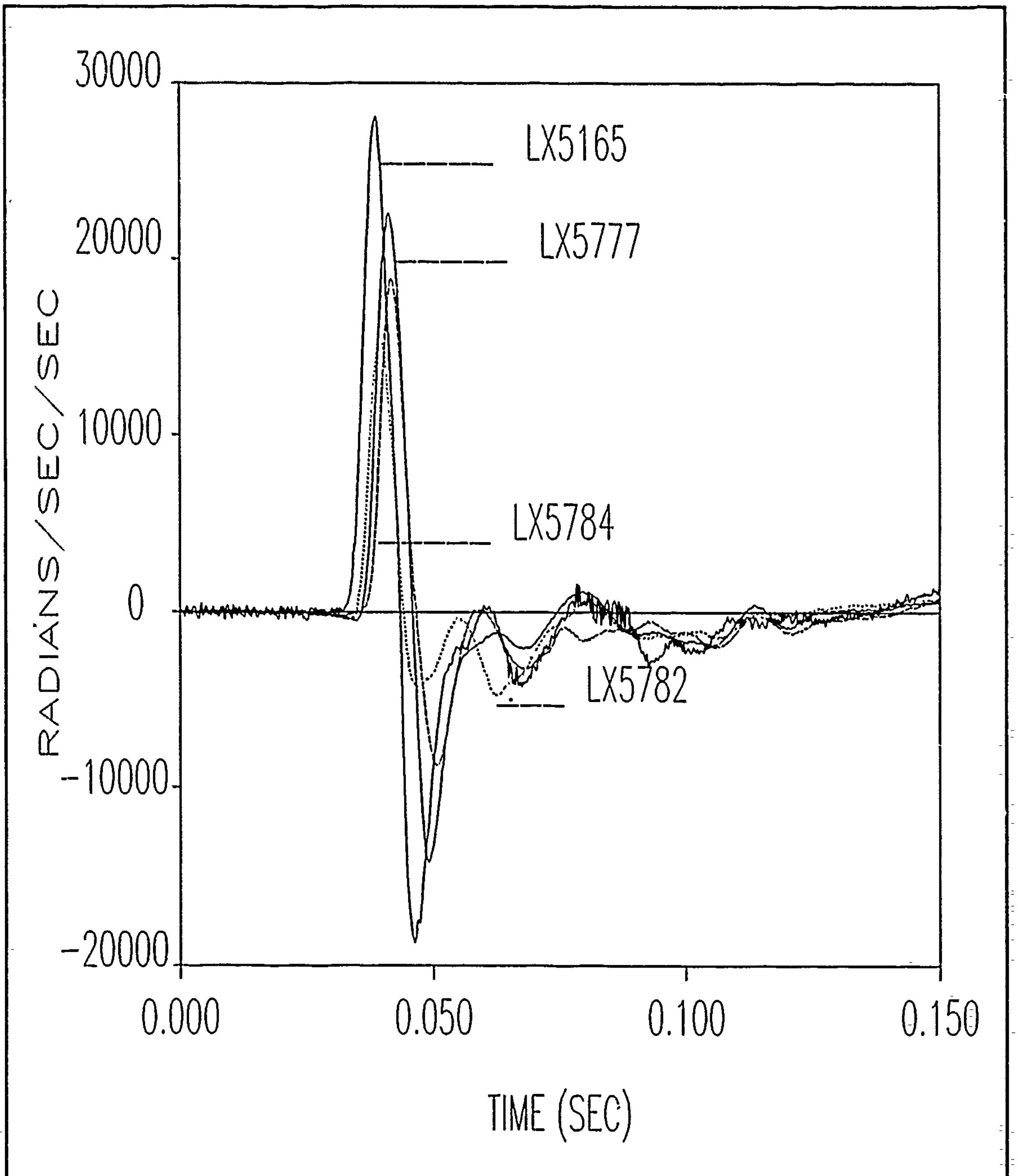

Figure 38. Head angular acceleration (Y-axis).

Effect of Increasing Negative Pitch (PHB), 75 g, In-Plane, NUCU.

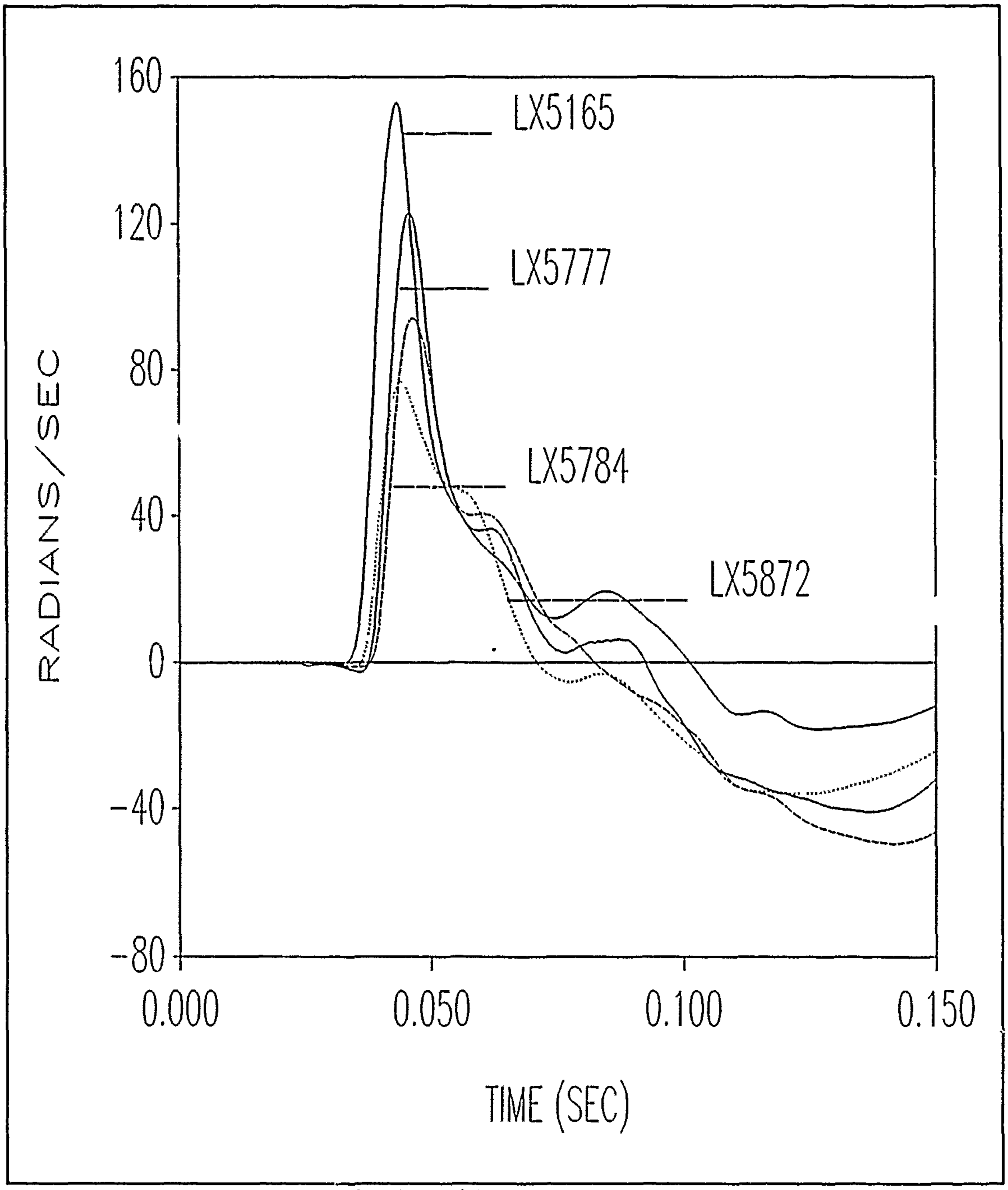

Figure 39. Head angular velocity (Y-axis).

Effect of Increasing Negative Pitch (PHB), 75 g, In-Plane, NUCU.

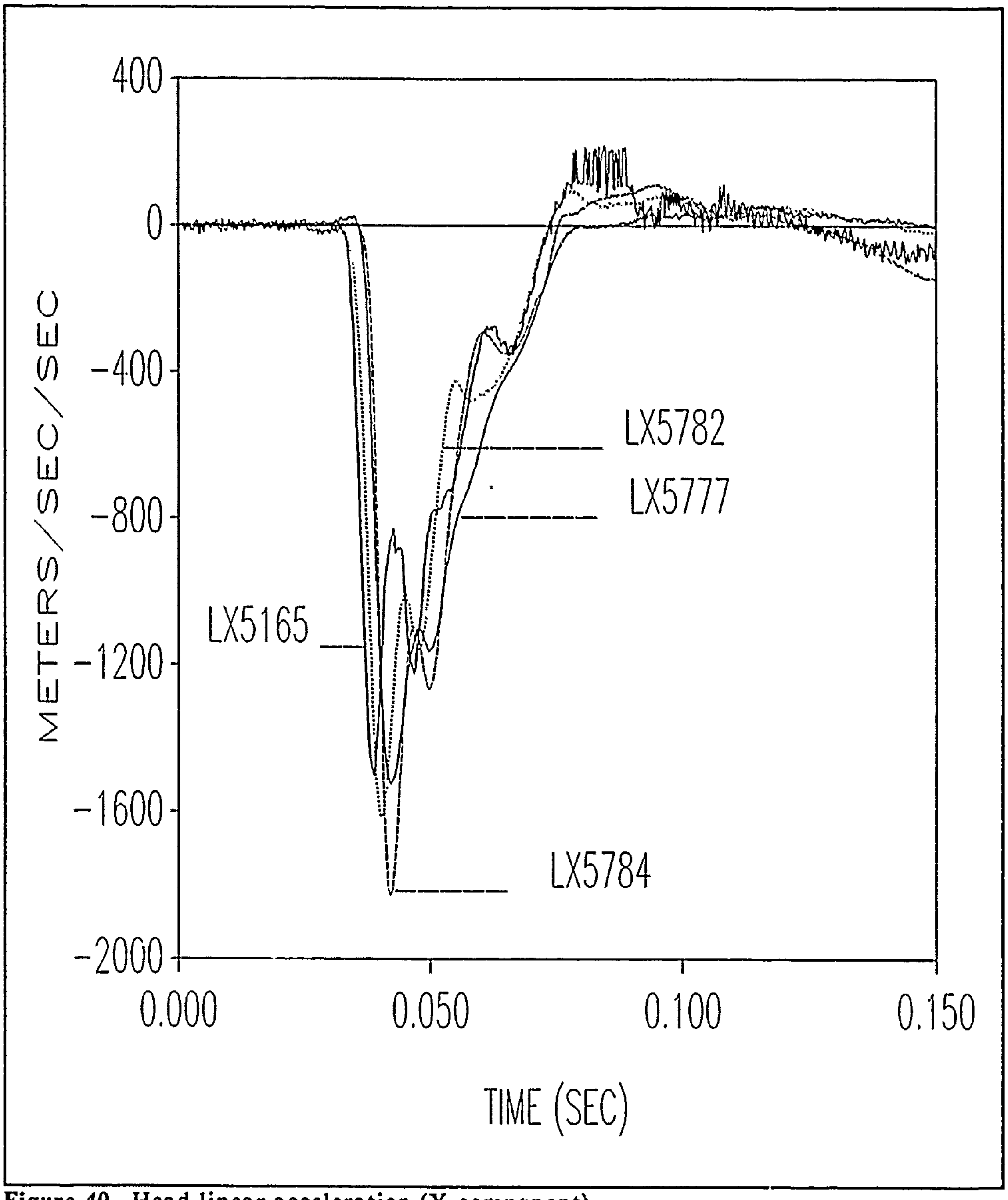

Figure 40. Head linear acceleration (X-component).

Effect of Increasing Negative Pitch (PHB), 75 g, In-Plane, NUCU.

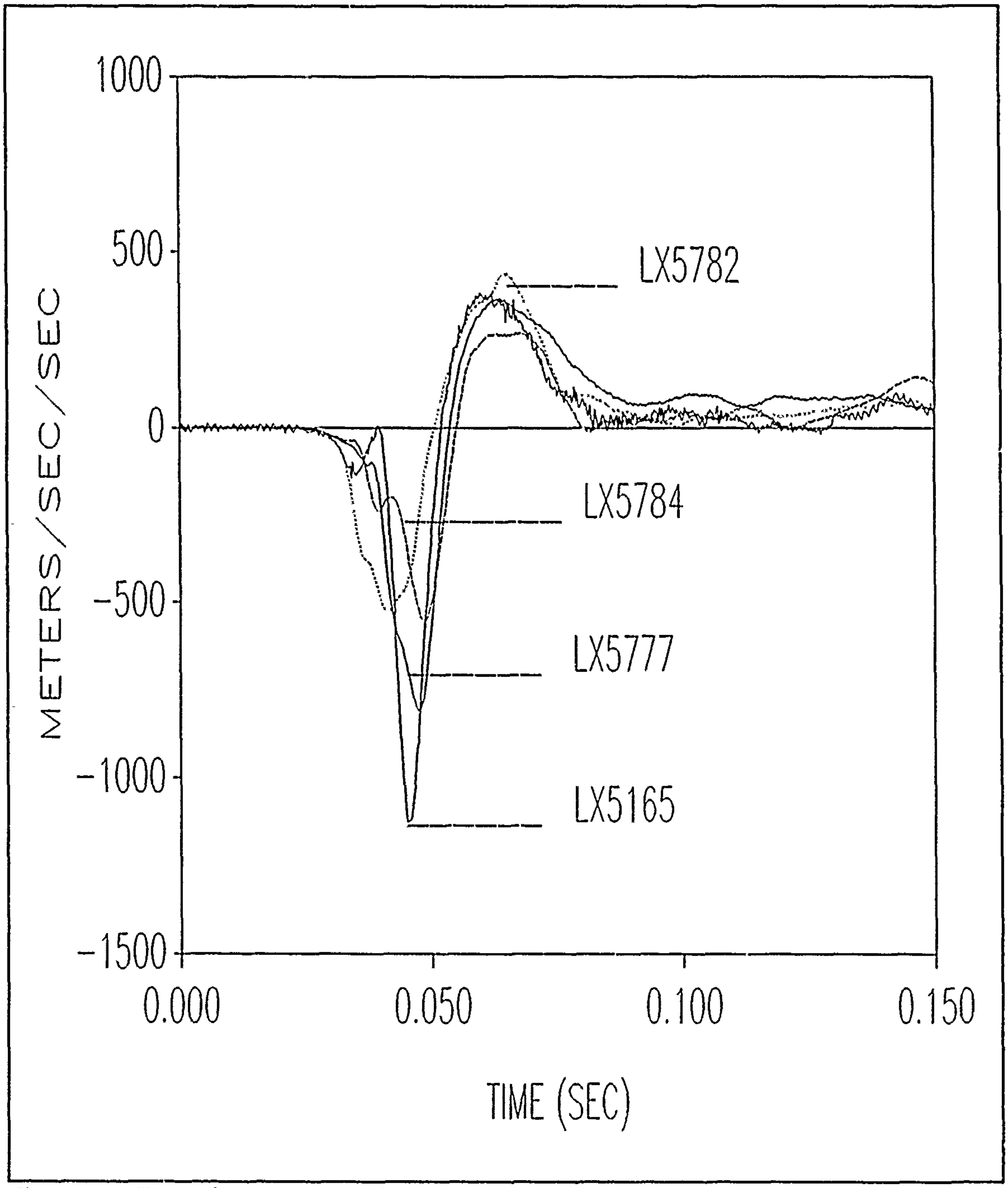

Figure 41. Head linear acceleration (Z-component).

Effect of Increasing Negative Pitch (PHB), 75 g, In-Plane, NUCU.

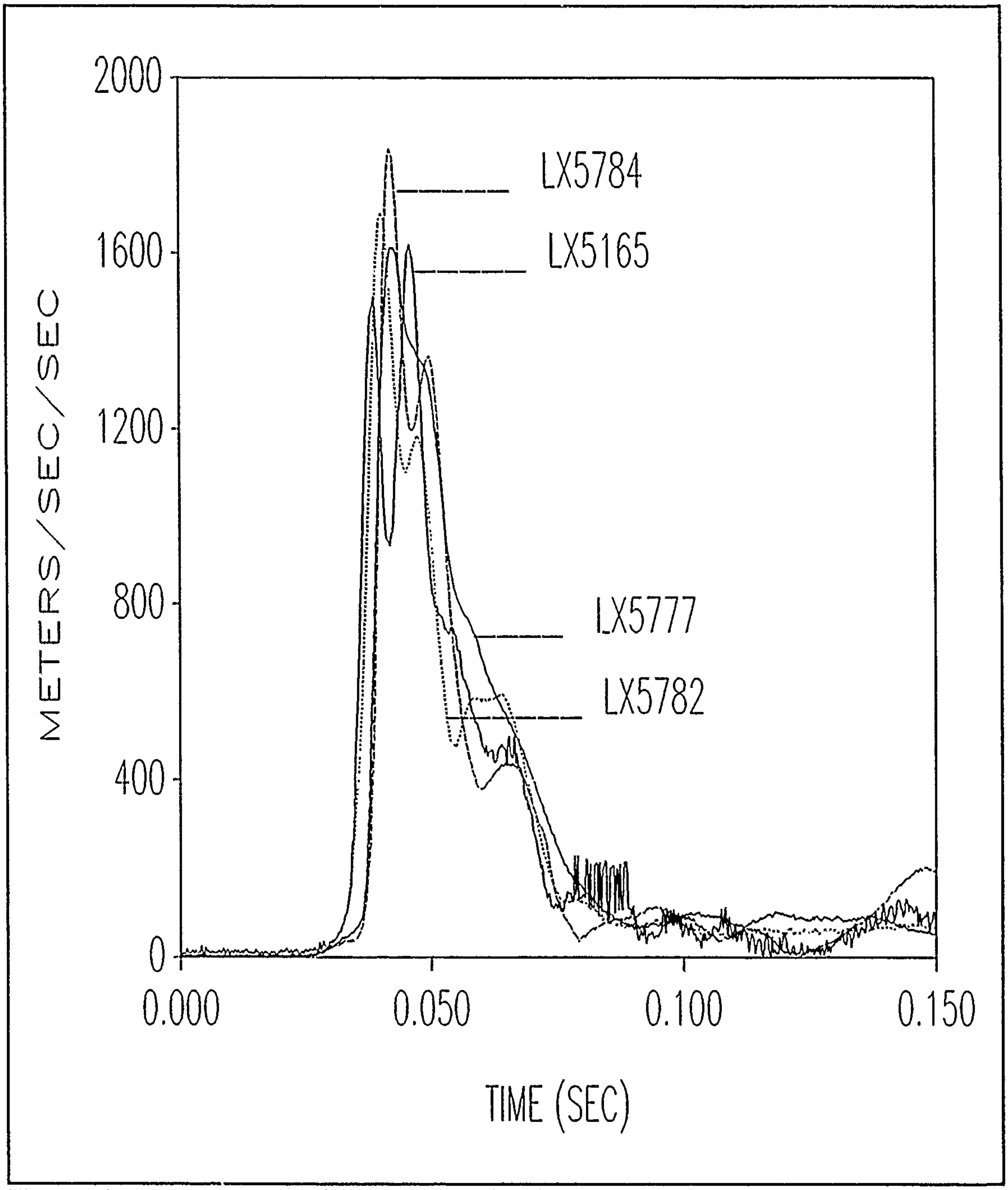

Figure 42. Resultant head linear acceleration (X-Z plane).

Effect of Increasing Negative Pitch (PHB), 75 g, In-Plane, NUCU.

TABLE B4.							
TEST	**SUBJECT**	**PHB**	**QHB**	**RHB**	**AAX**	**AAZ**	**AAR**
LX5770	AR5852	-0.042	10113	64	-1435	-253	1435
LX5772	AR986B	-0.008	12256	56	-1374	-385	1403

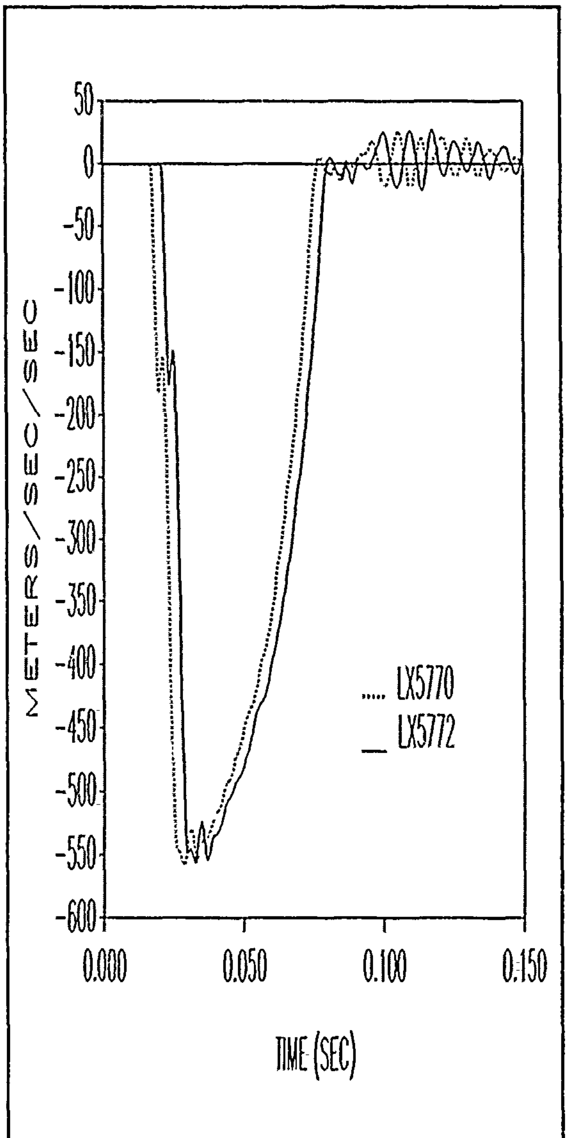

Figure 43. Sled acceleration profile.

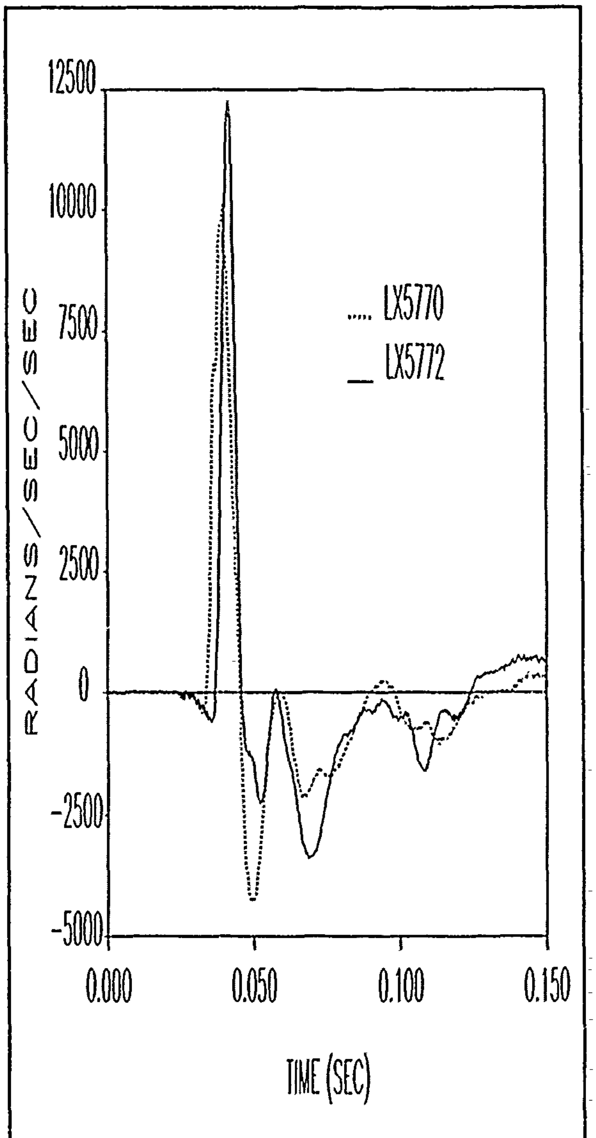

Figure 44. Head angular acceleration (Y-axis).

Between Animal Comparison, 57 g, In-Plane, NUCU.

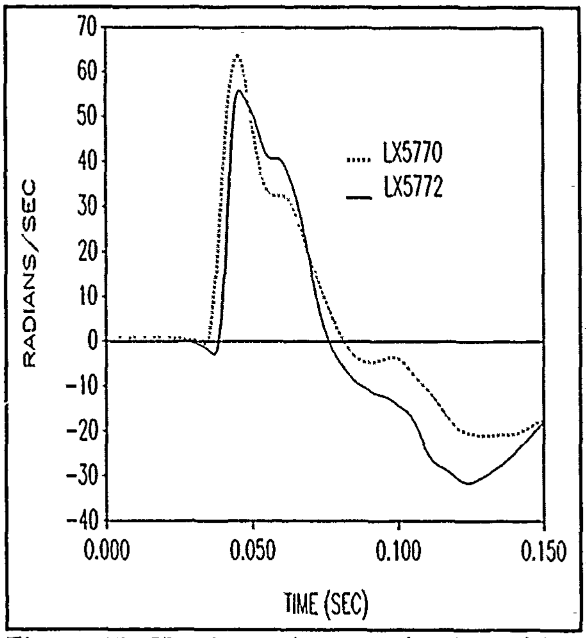

Figure 45. Head angular velocity (Y-axis).

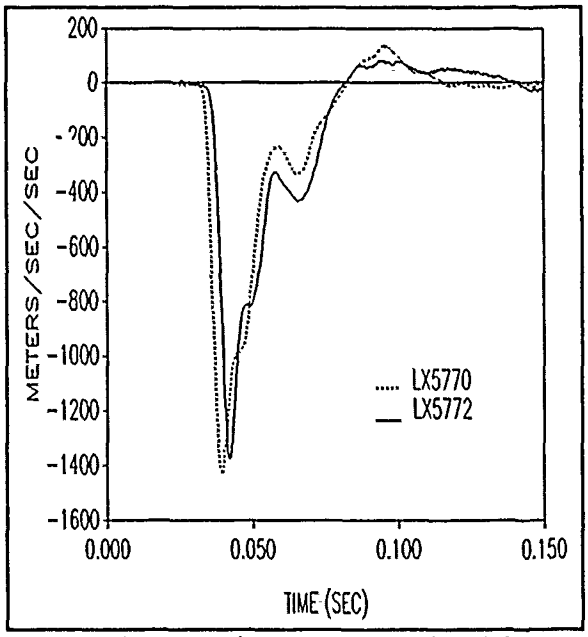

Figure 46. Head linear acceleration (X-component).

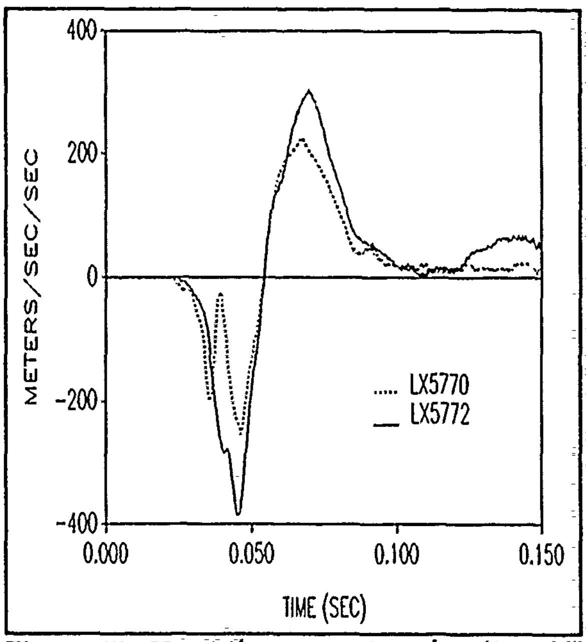

Figure 47. Head linear acceleration (Z-component).

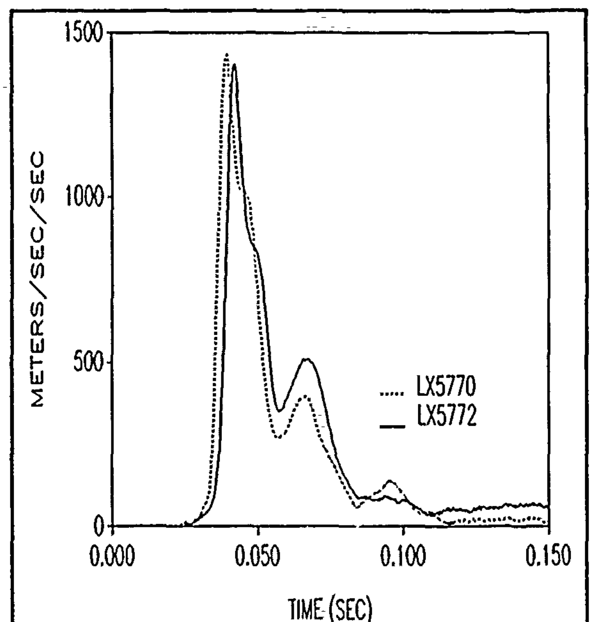

Figure 48. Resultant head linear acceleration (X-Z plane).

Between Animal Comparison, 57 g, In-Plane, NUCU.

TABLE B5.							
TEST	**SUBJECT**	**PHB**	**QHB**	**RHB**	**AAX**	**AAZ**	**AAR**
LX5786	AR894C	-0.063	17611	89	-2132	-511	2186
LX5797	ARNR20	-0.129	20052	87	-2347	-748	2388

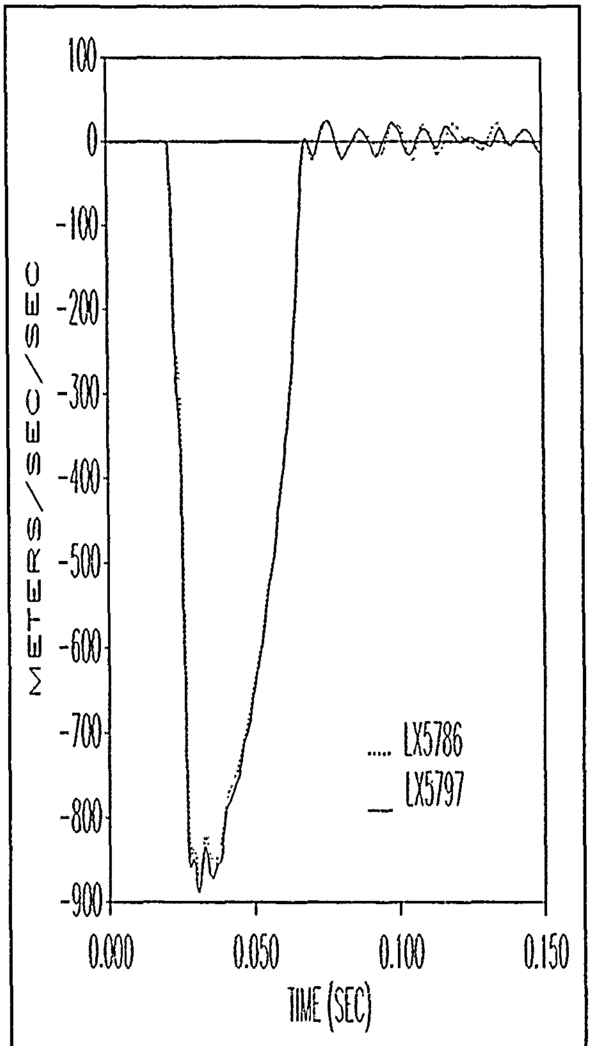

Figure 49. Sled acceleration profile.

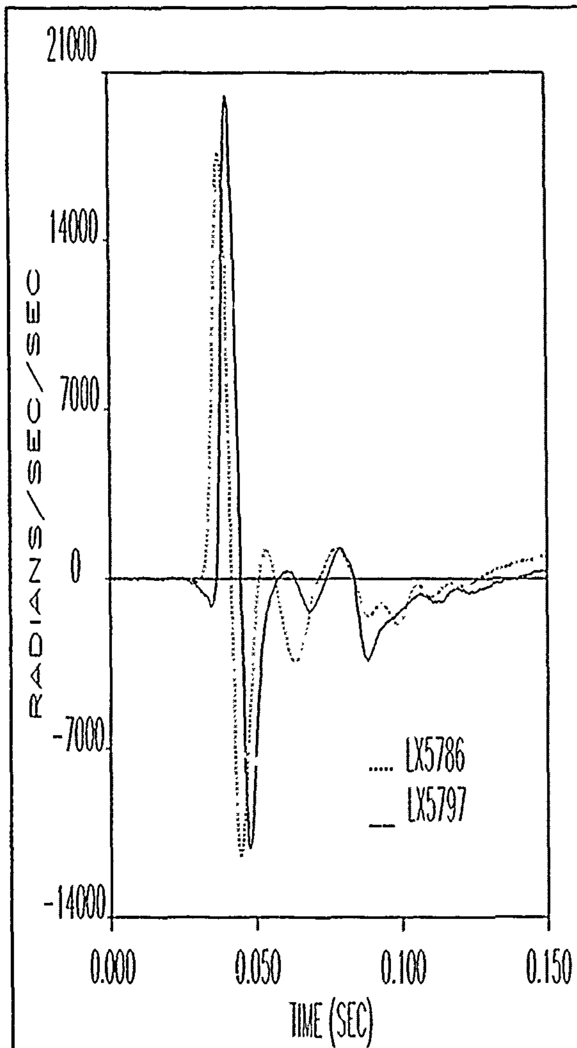

Figure 50. Head angular acceleration (Y-axis).

Between Animal Comparison, 90 g, In-Plane, NUCU.

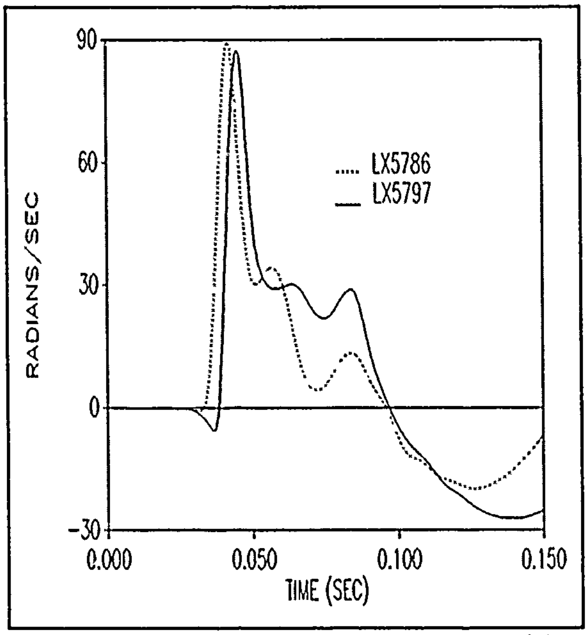

Figure 51. Head angular velocity (Y-axis).

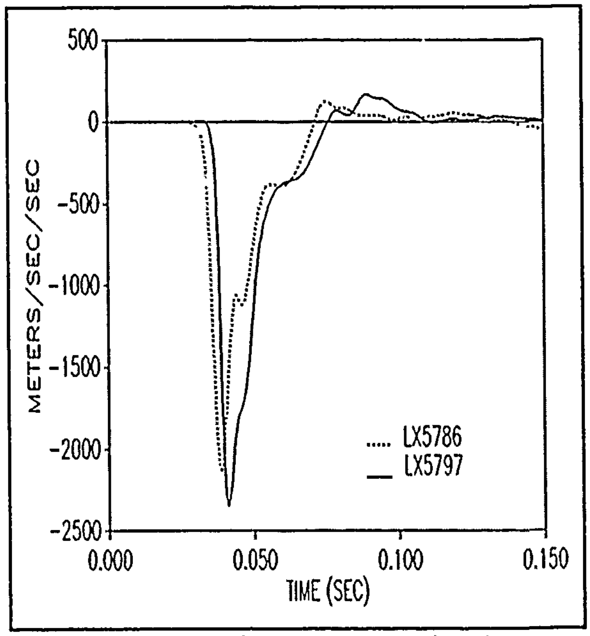

Figure 52. Head linear acceleration (X-component).

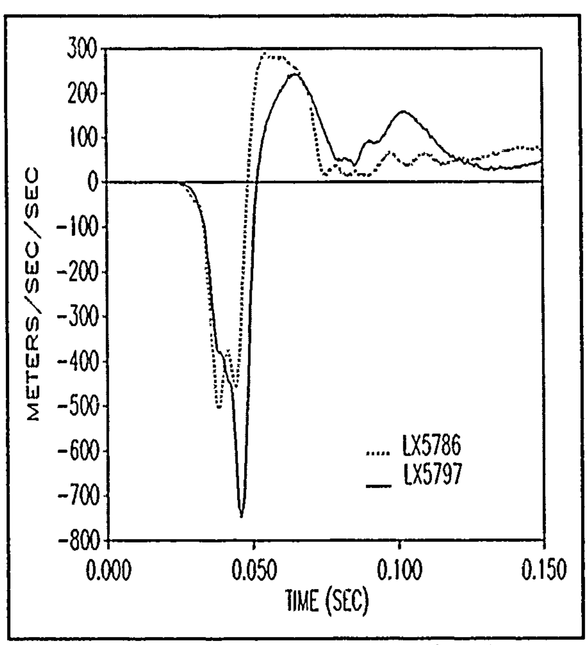

Figure 53. Head linear acceleration (Z-component).

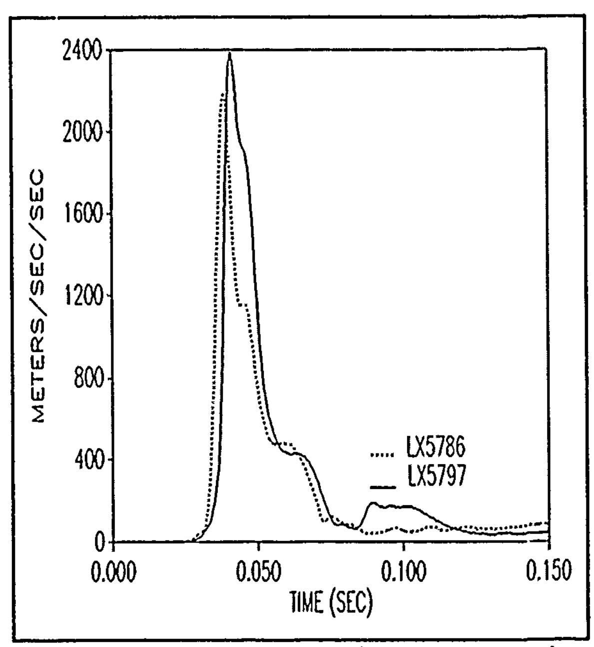

Figure 54. Resultant head linear acceleration (X-Z plane).

Between Animal Comparison, 90 g, In-Plane, NUCU.

TABLE B6.						
TEST	**SUBJECT**	**G LEVEL**	**PHA**	**PHB**	**PHC**	**CONDITION**
LX5786	AR894C	89	0.024	-0.063	-0.022	In-Plane
LX4799	ARNR18*	106	0.029	-0.019	-0.893	Out-of-Plane

TEST	QHB	RHB	AAX	AAZ	AAR
LX5786	17661	89	-2132	-511	2186
LX4799	16726	74	-2821	-579	2879

* Sled acceleration profile not available.

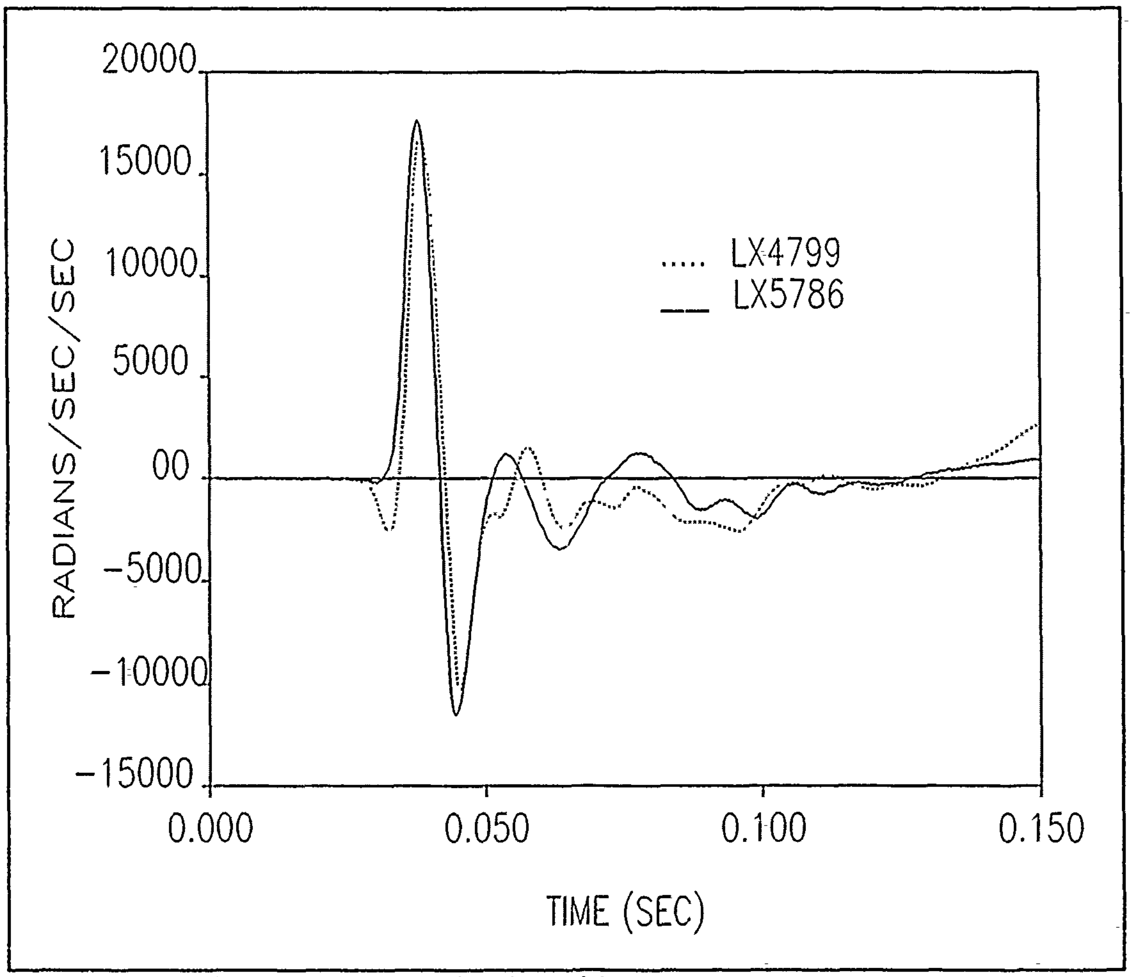

Figure 55. Head angular acceleration (Y-axis).

Effect of Out-of-Plane Behavior, NUCU.

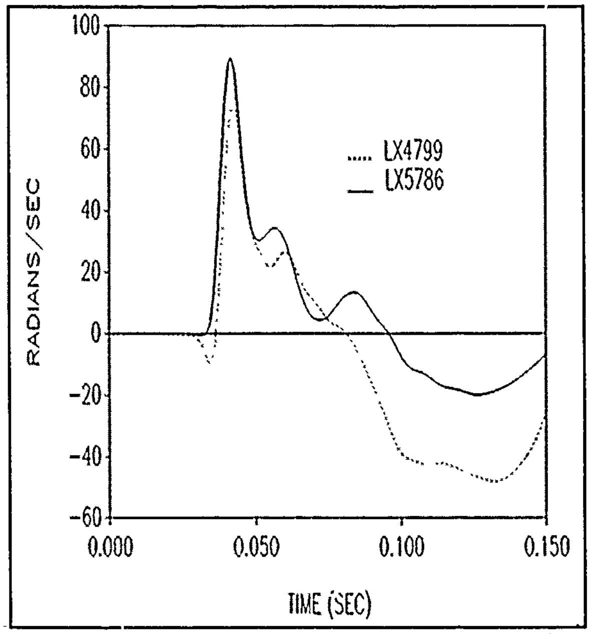

Figure 56. Head angular velocity (Y-axis).

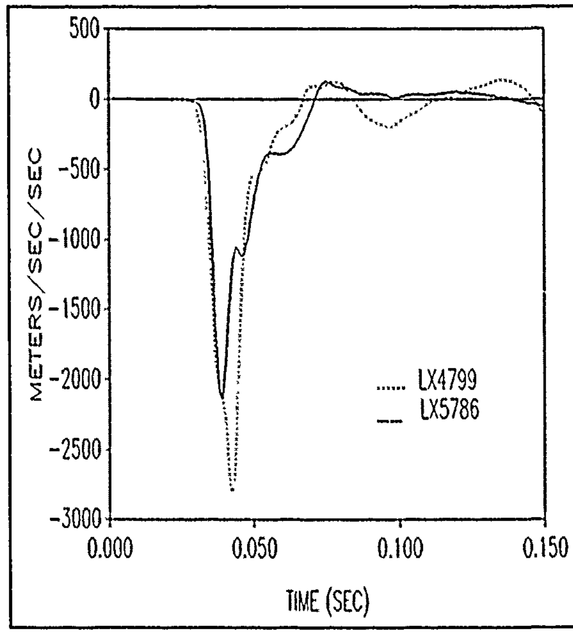

Figure 57. Head linear acceleration (X-component).

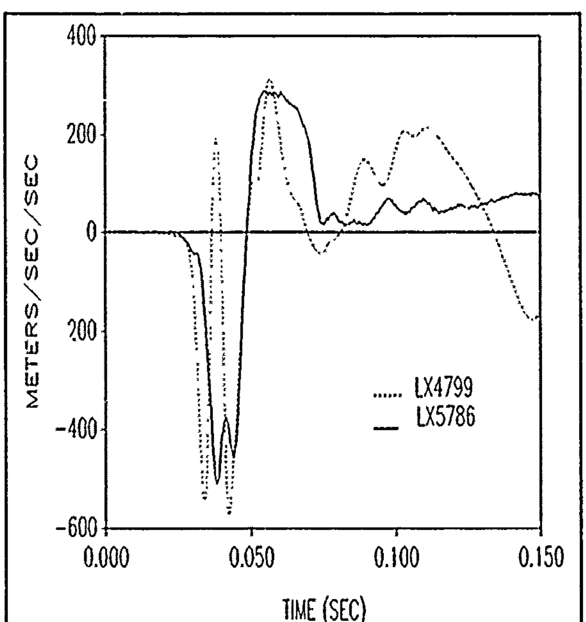

Figure 58. Head linear acceleration (Z-component).

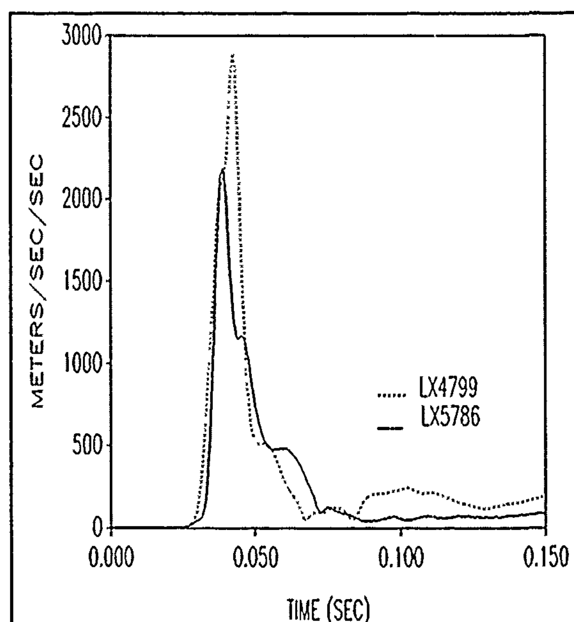

Figure 59. Resultant head linear acceleration (X-Z plane).

Effect of Out-of-Plane Behavior, NUCU.

TABLE B7.								
TEST	SUBJECT	G LEVEL	PHB	QHB	RHB	AAX	AAZ	AAR
LX4883	AR660B	57	.705	-6386	-53	*	-355	1416
LX5125	AR0016	74	.543	-8231	-48	-1844	-553	1851
LX4786	AR660B	96	.657	-12218	-58	-240	*	2411

* Not available.

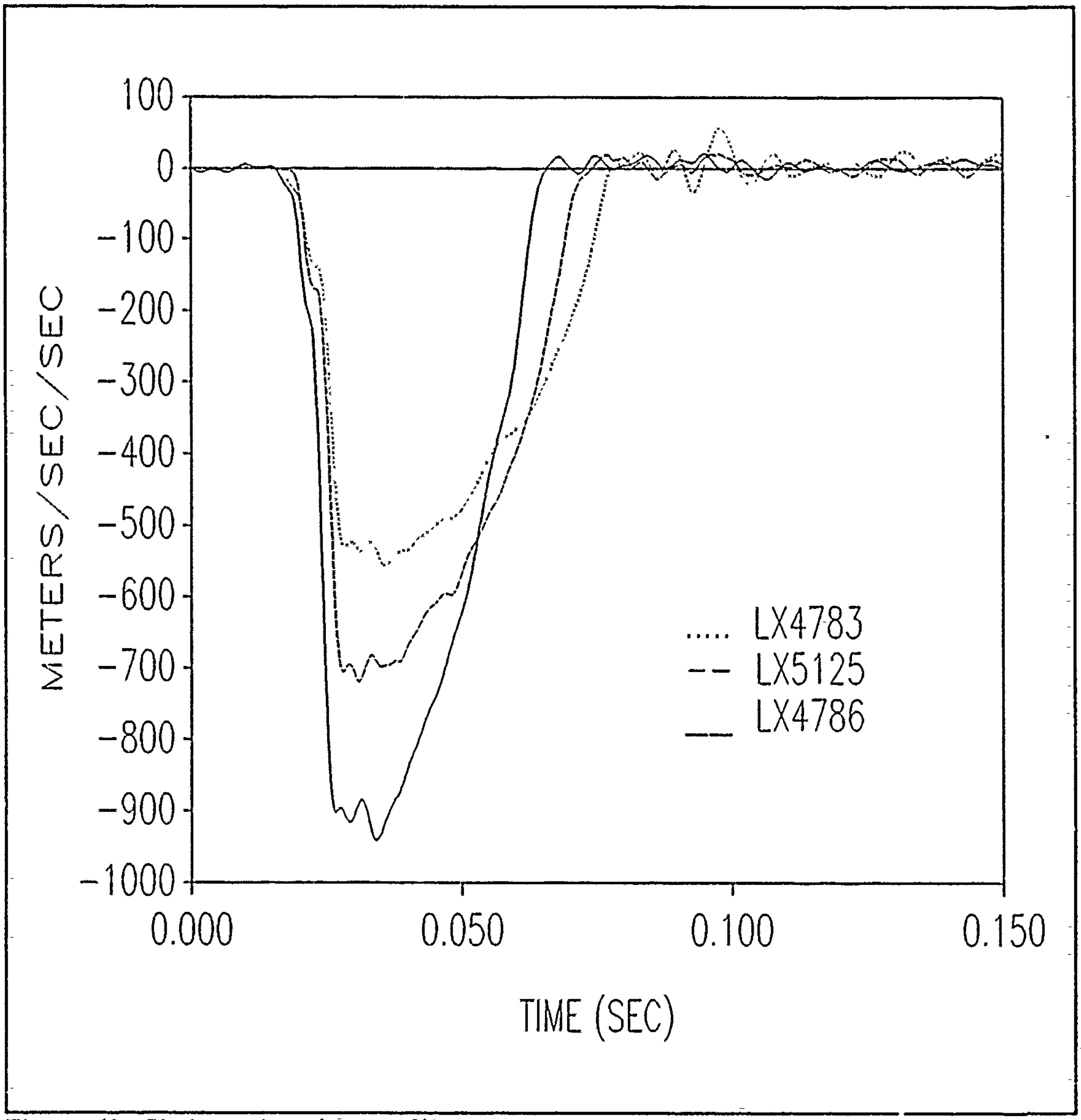

Figure 60. Sled acceleration profile.

Effect of Increasing G Level, In Plane, NFCD.

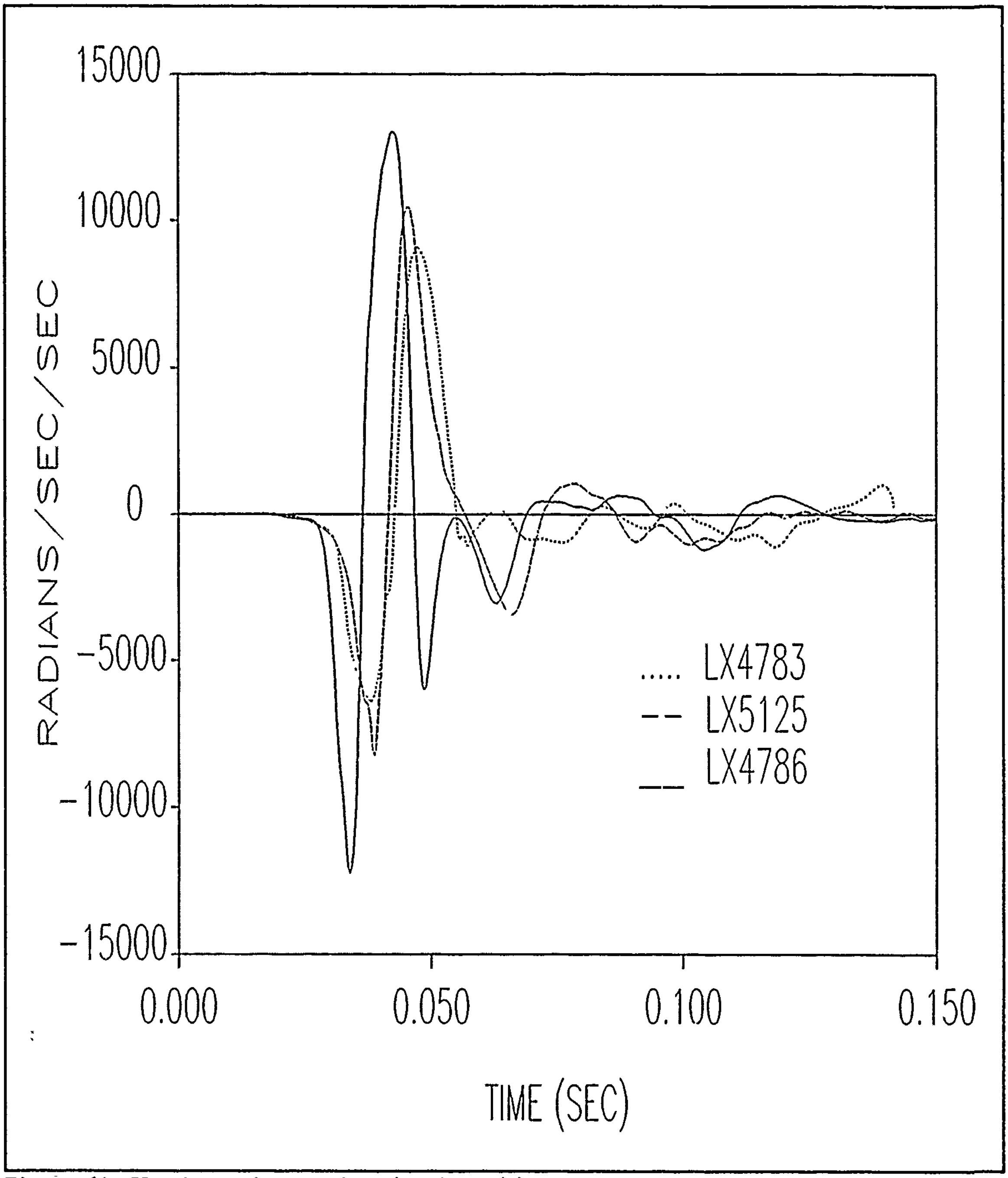

Figure 61. Head angular acceleration (Y-axis).

Effect of Increasing G Level, In Plane, NFCD.

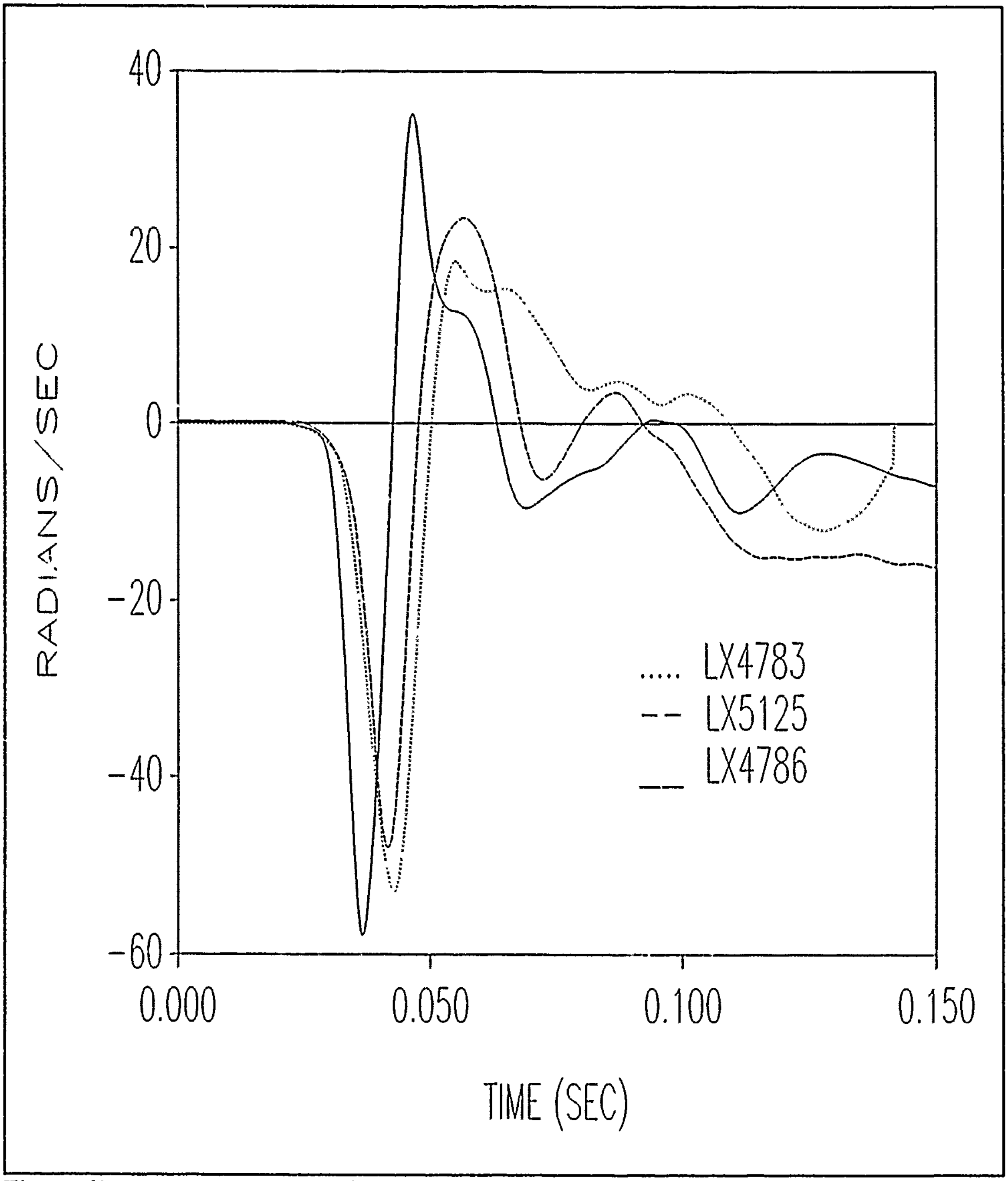

Figure 62. Head angular velocity (Y-axis).

Effect of Increasing G Level, In Plane, NFCD.

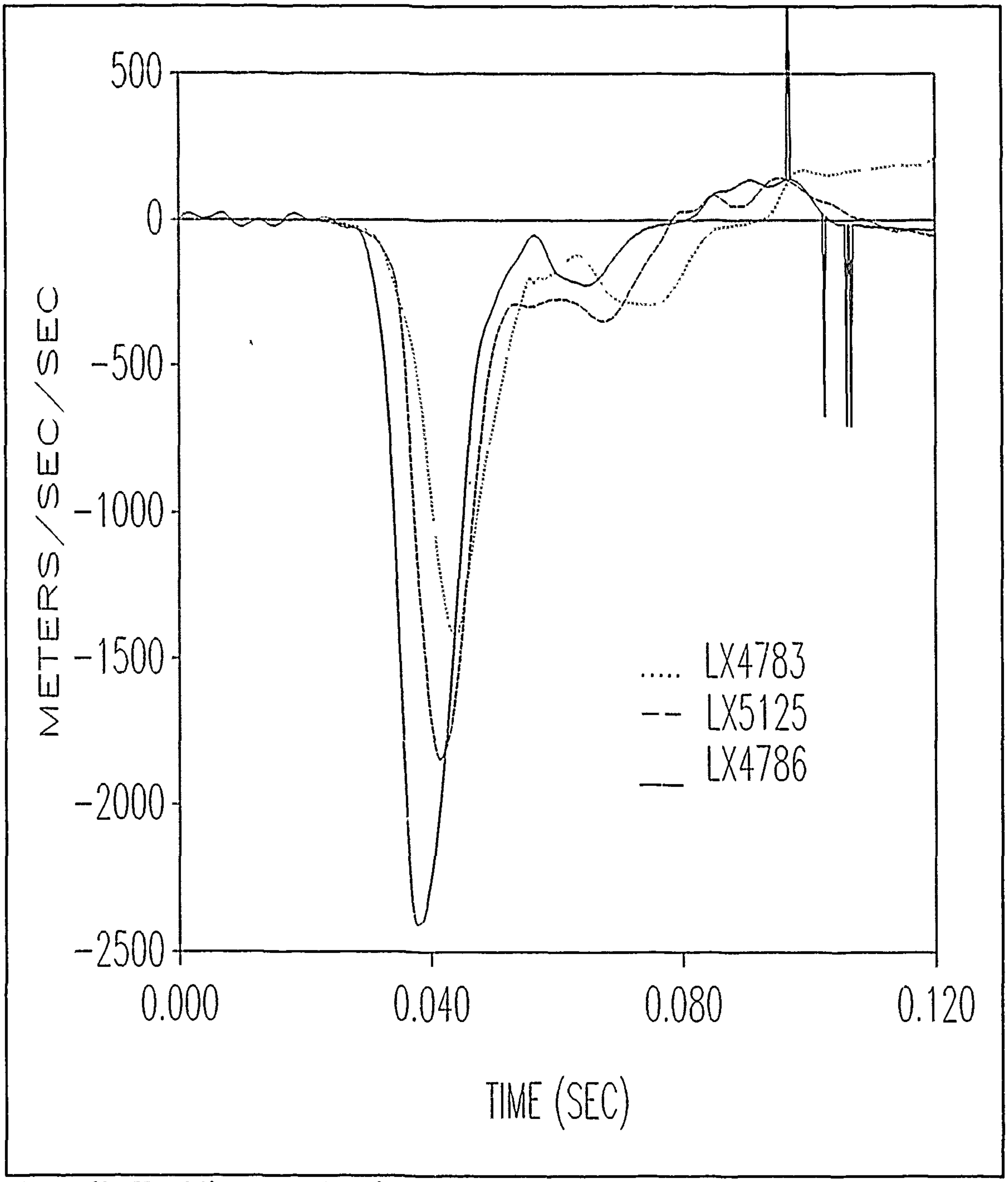

Figure 63. Head linear acceleration (X-component).

Effect of Increasing G Level, In Plane, NFCD.

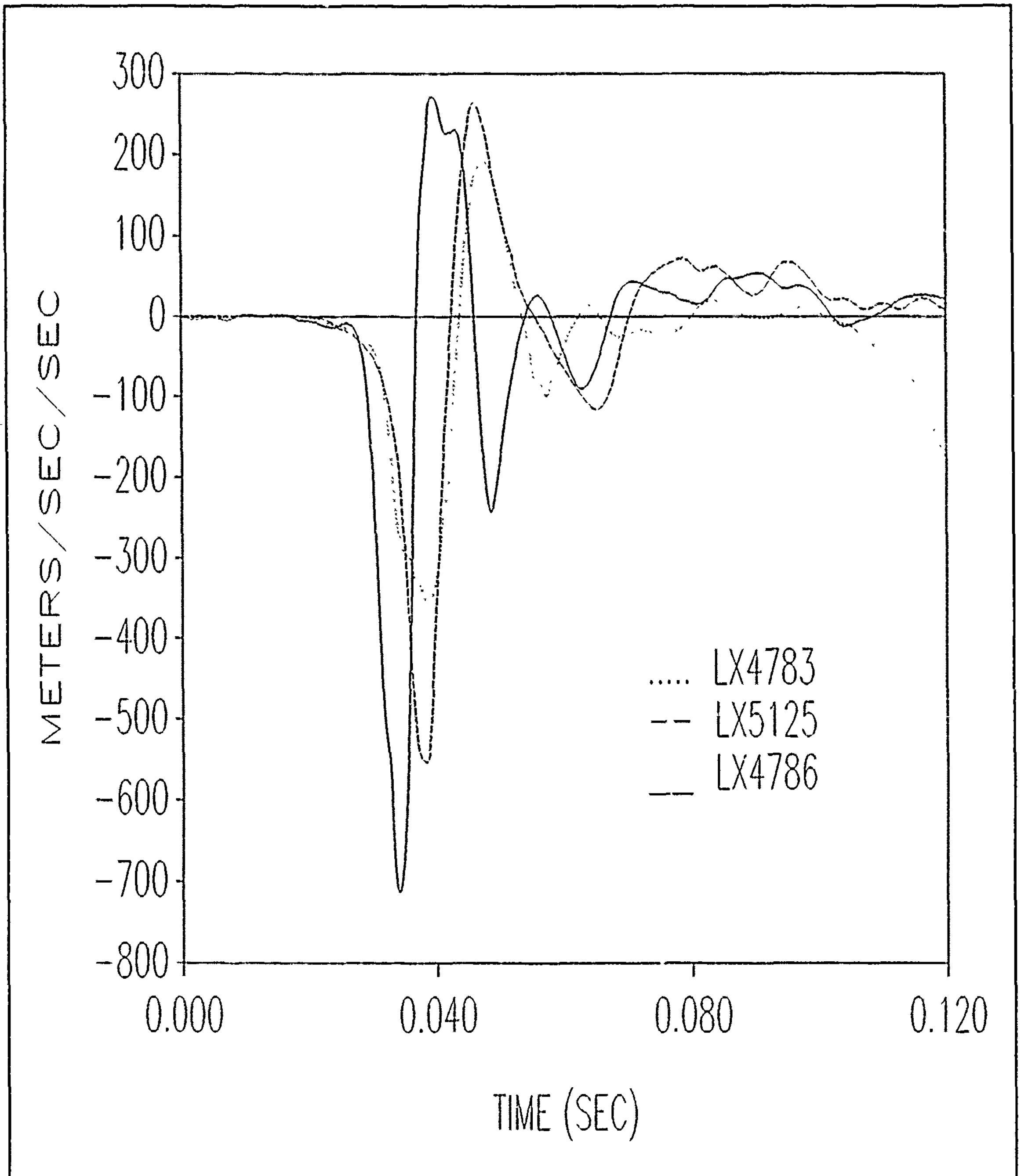

Figure 64. Head linear acceleration (Z-component).

Effect of Increasing G Level, In Plane, NFCD.

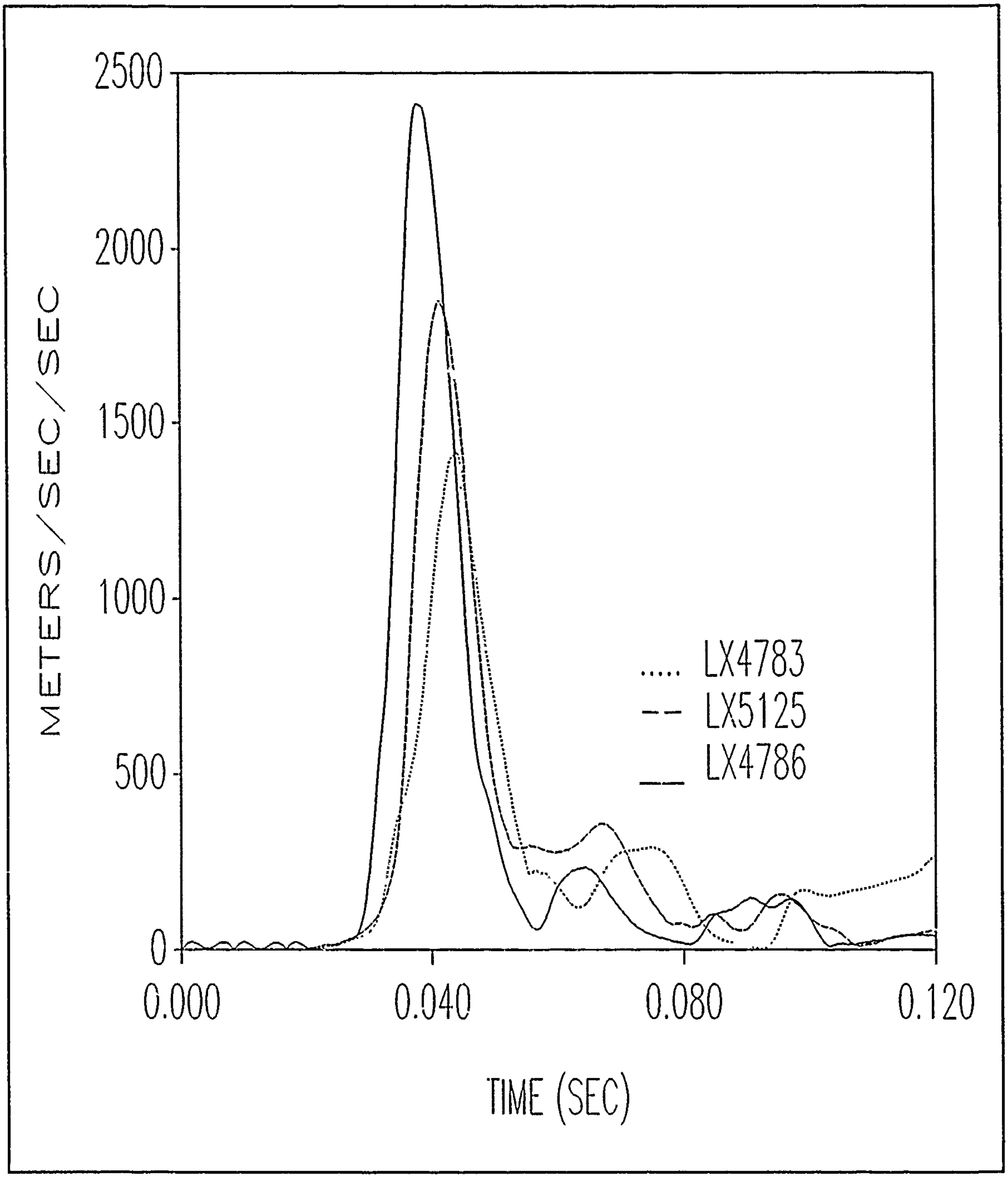

Figure 65. Resultant head linear acceleration (X-Z plane).

Effect of Increasing G Level, In Plane, NFCD.

TABLE B8.							
TEST	SUBJECT	PHB	QHB	RHB	AAX	AAZ	AAR
LX5160	AR0016	0.481	-5388	-36	-1679	-505	1679
LX5144	AR8858	0.358	-4824	-33	-2152	-722	2155
LX5161	AR0016	0.505	-6225	-33	-1660	-529	1677
LX5129	AR0016	0.632	-7004	-48	-1813	-416	1813

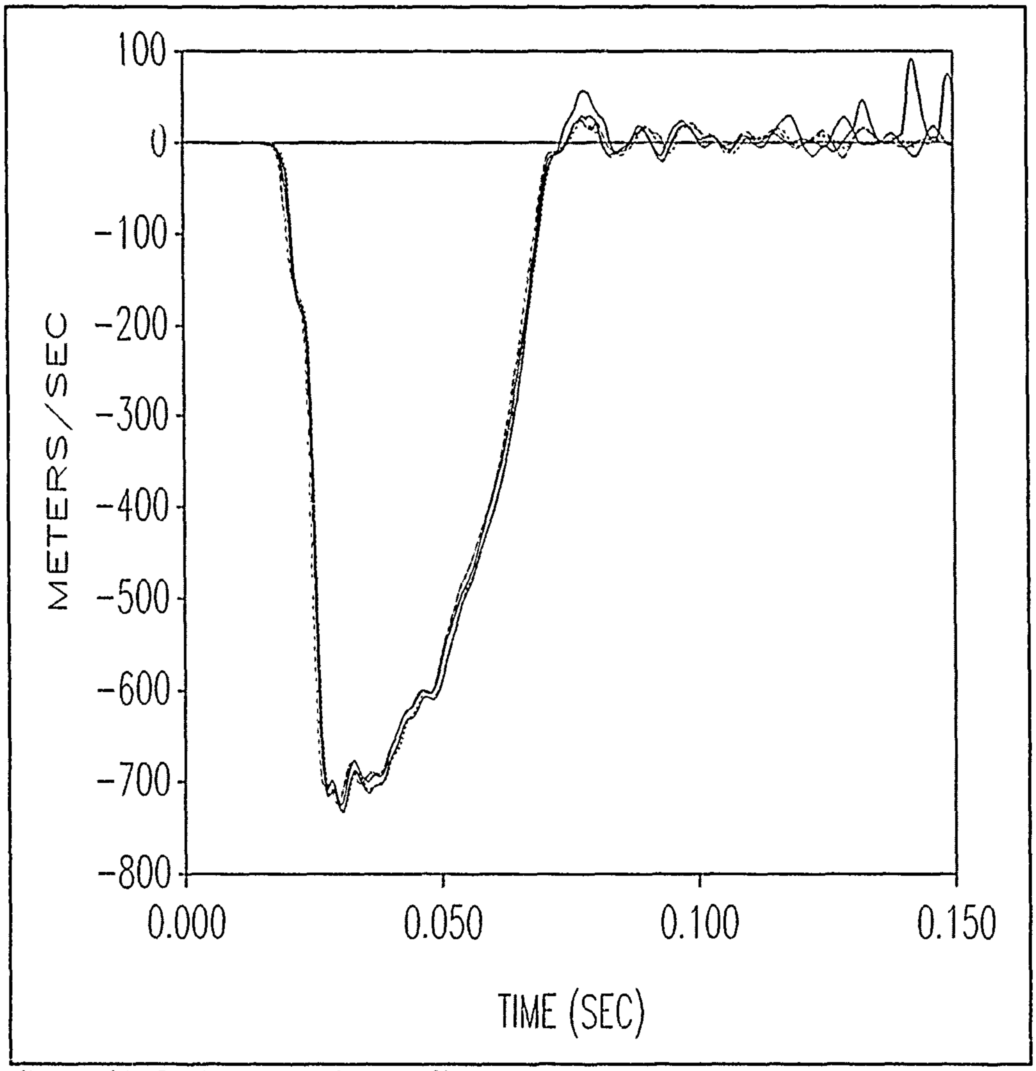

Figure 66. Sled acceleration profile.

Effect of Increasing Positive Pitch (PHB), 74 g, In-Plane, NFCD.

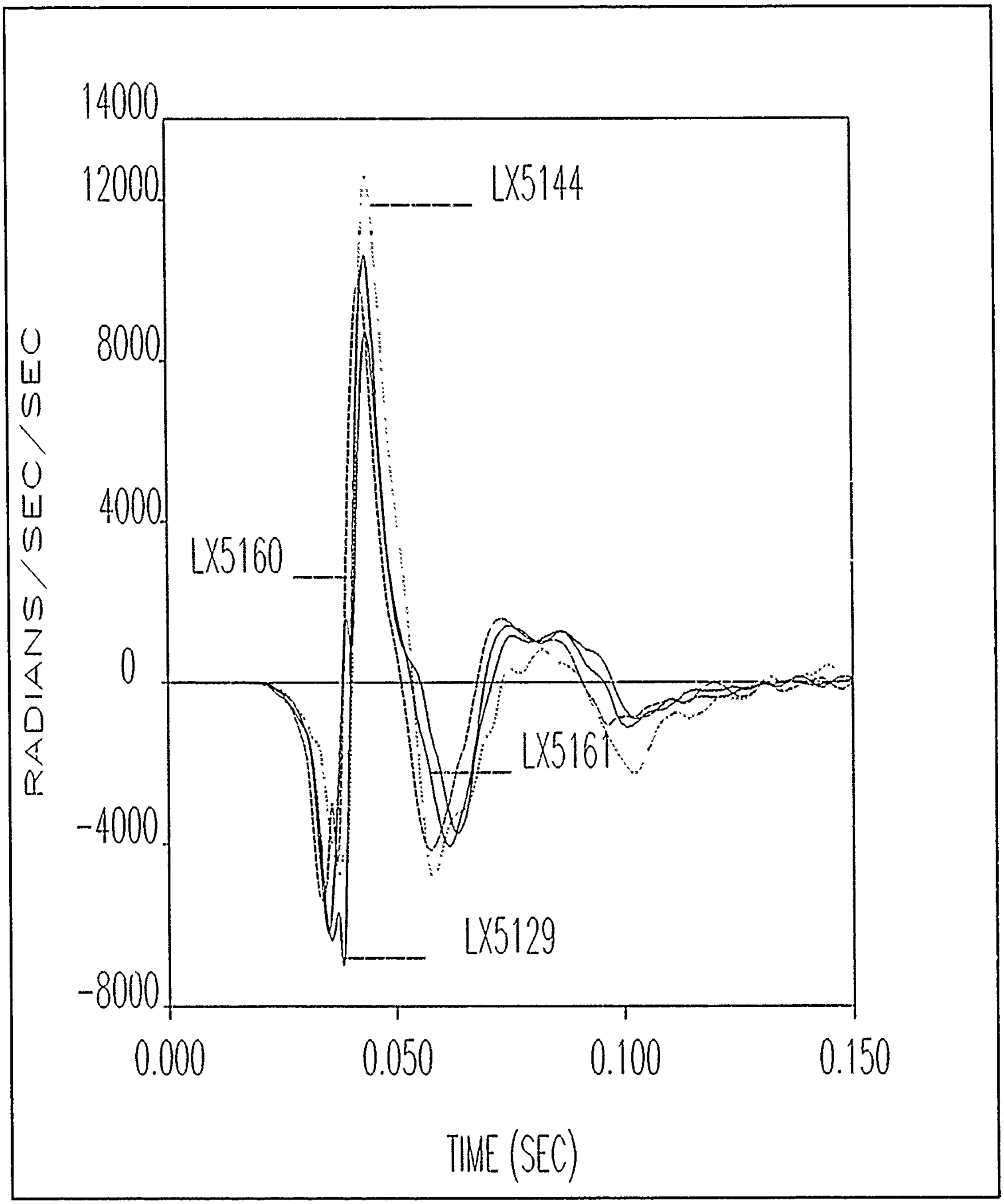

Figure 67. Head angular acceleration (Y-axis).

Effect of Increasing Positive Pitch (PHB), 74 g, In-Plane, NFCD.

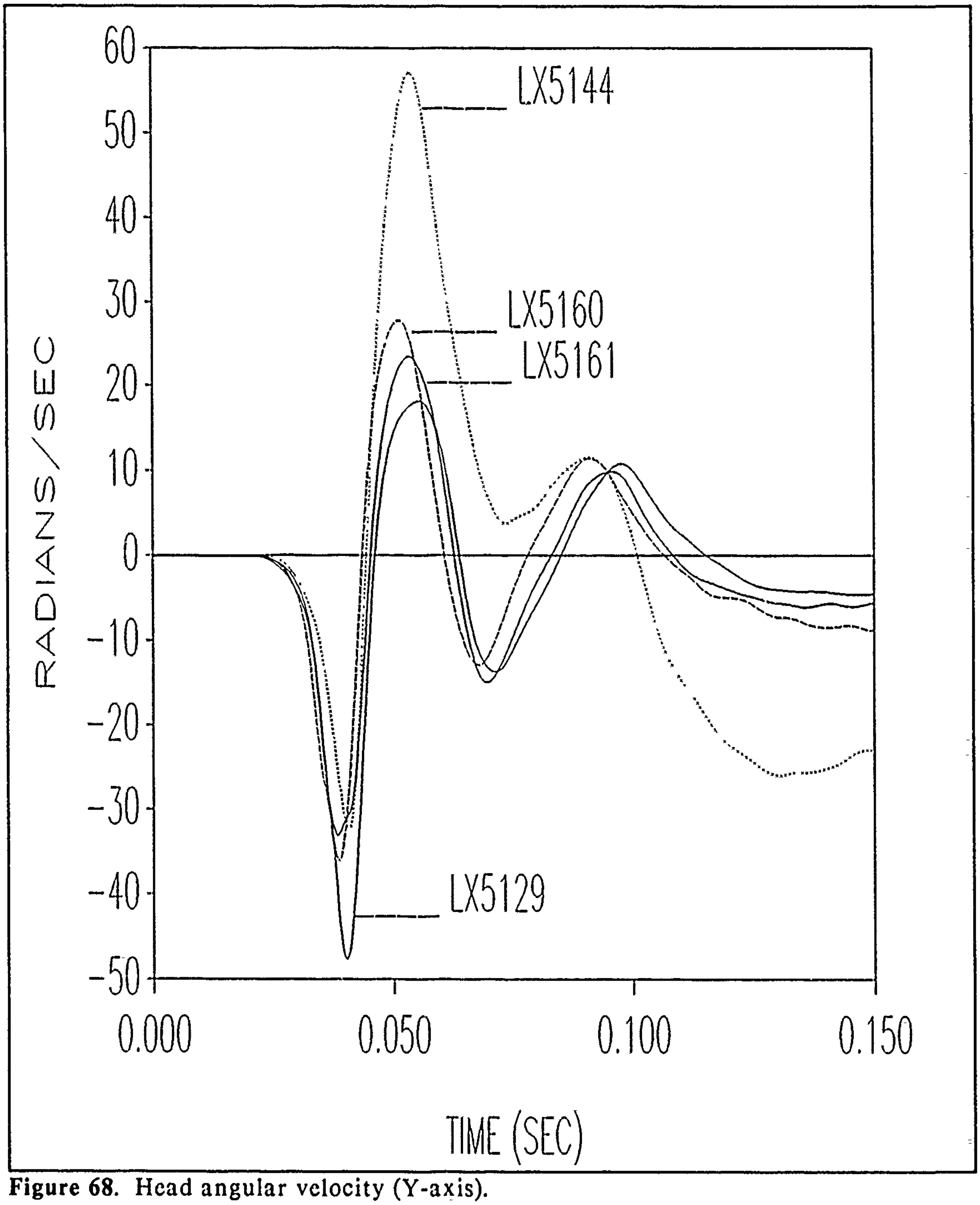

Figure 68. Head angular velocity (Y-axis).

Effect of Increasing Positive Pitch (PHB), 74 g, In-Plane, NFCD.

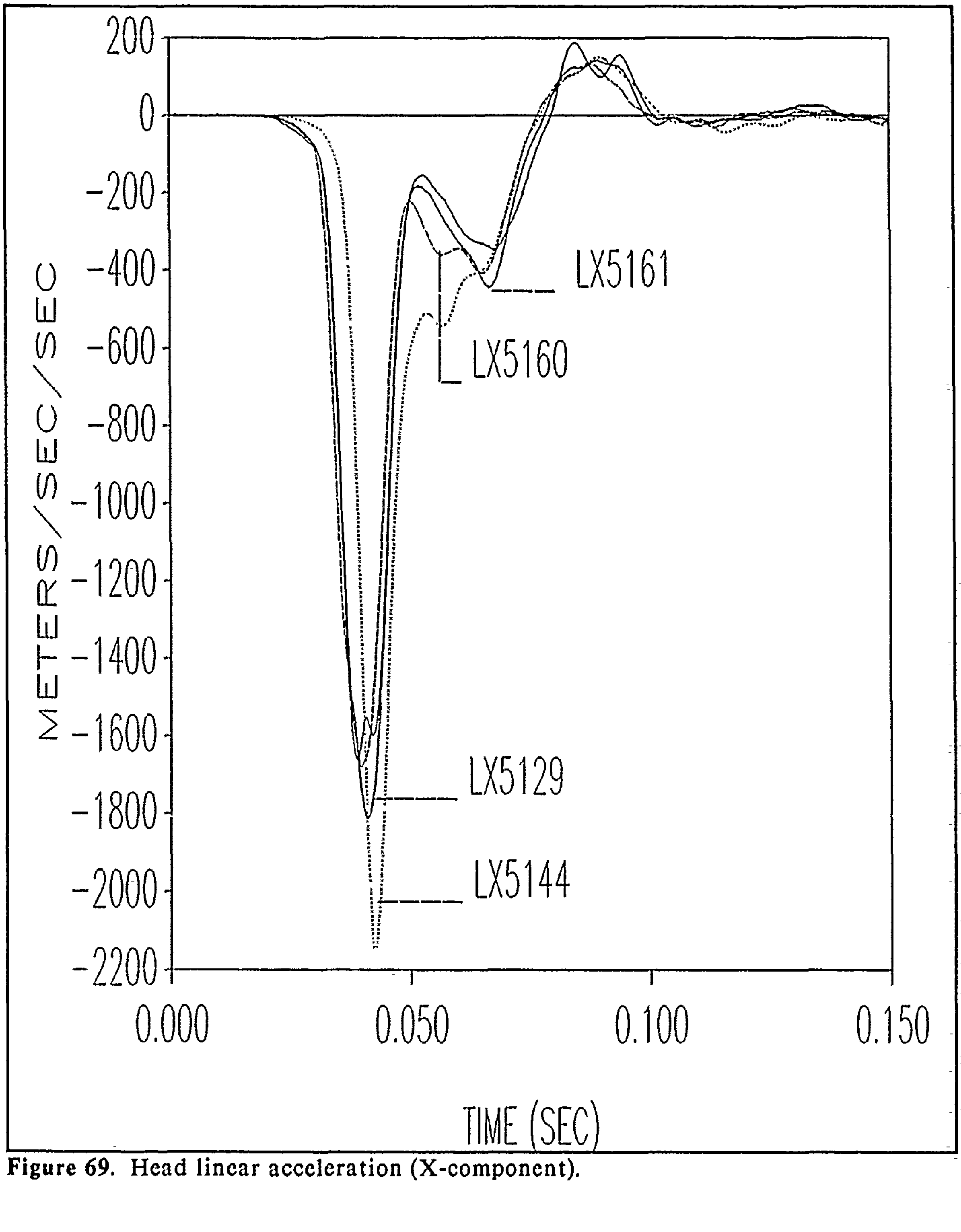

Figure 69. Head linear acceleration (X-component).

Effect of Increasing Positive Pitch (PHB), 74 g, In-Plane, NFCD.

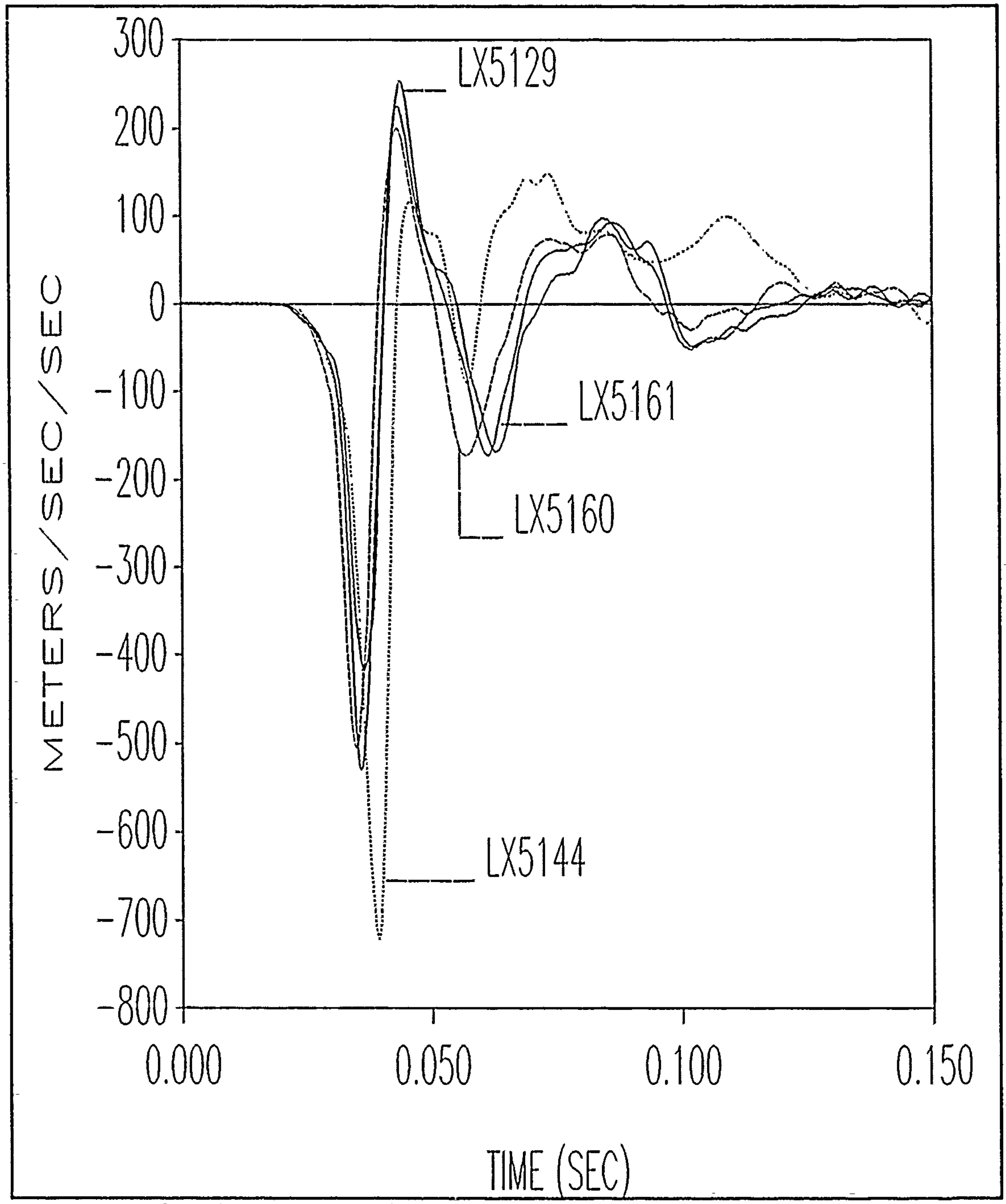

Figure 70. Head linear acceleration (Z-component).

Effect of Increasing Positive Pitch (PHB), 74 g, In-Plane, NFCD.

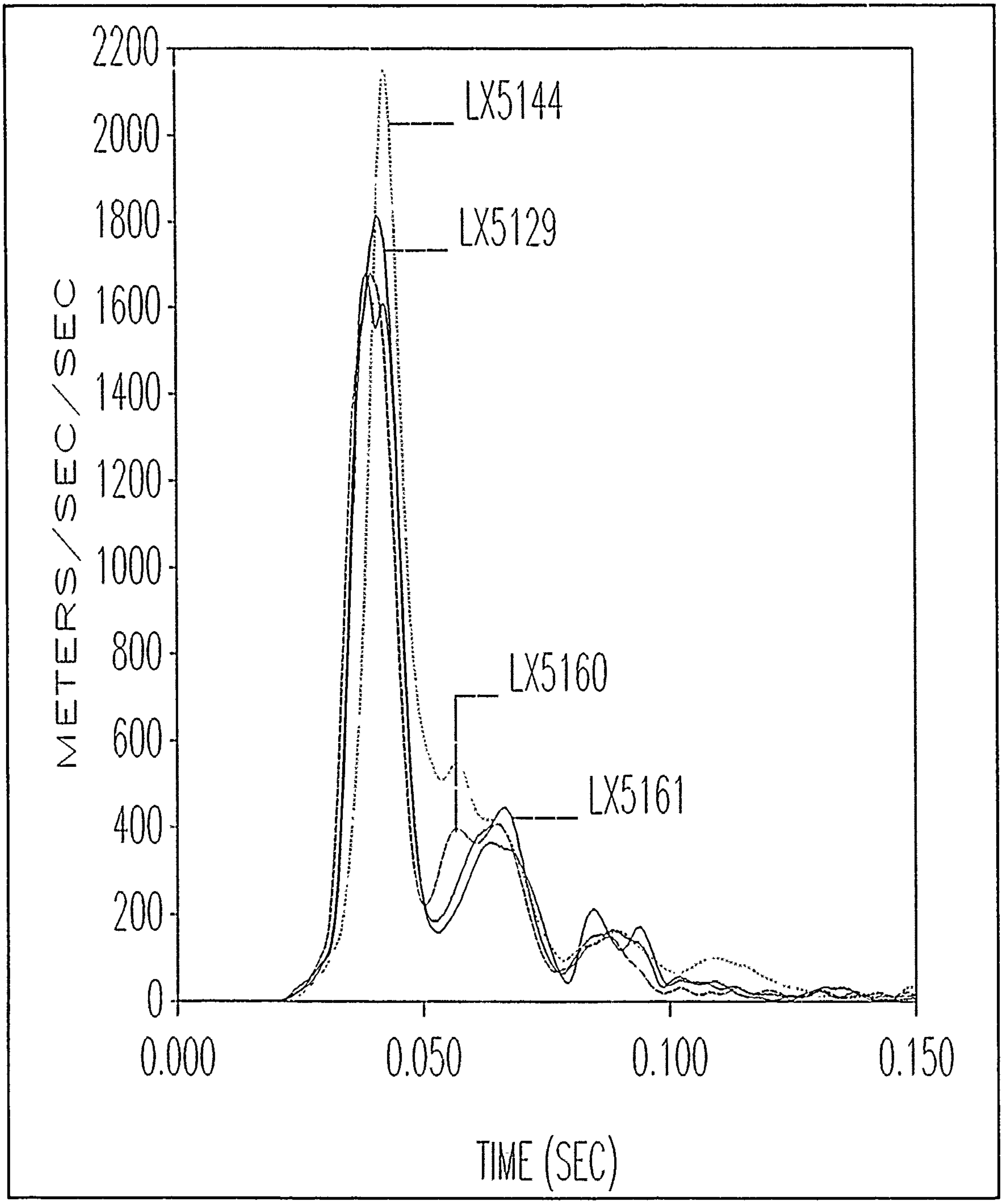

Figure 71. Resultant head linear acceleration (X-Z plane).

Effect of Increasing Positive Pitch (PHB), 74 g, In-Plane, NFCD.

TABLE B9.						
TEST	SUBJECT	G LEVEL	PHA	PHB	PHC	PLANARITY
LX4812	AR8696	86	0.111	0.364	0.411	Large yaw
LX5125	AR0016	73	0.062	0.543	-0.075	In-plane, more forward pitch
TEST	**SUBJECT**	**QHB**	**RHB**	**AAX**	**AAZ**	**AAR**
LX4812	AR8696	-8122	-37	-2544	-619	2546
LX5125	AR0016	-8231	-48	-1844	-553	1851

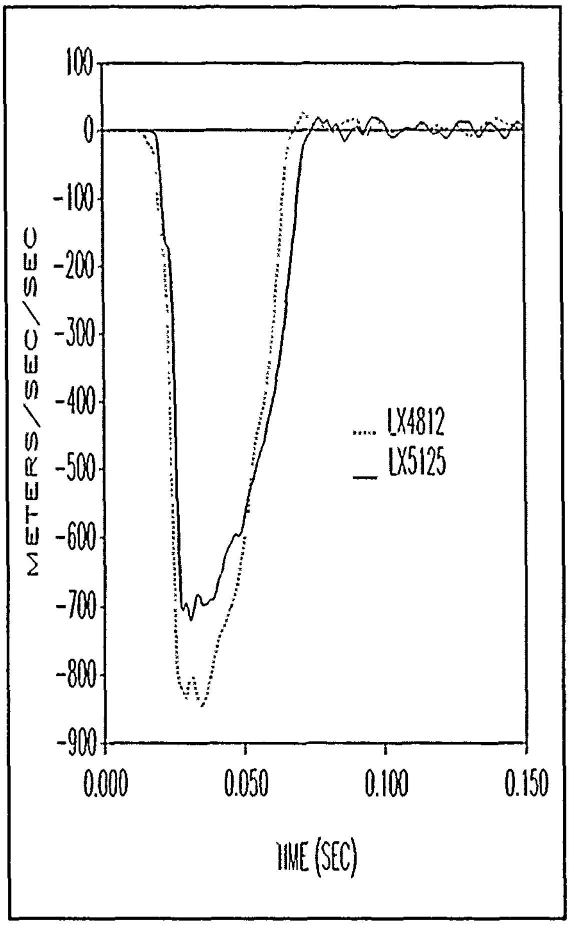

Figure 72. Sled acceleration profile.

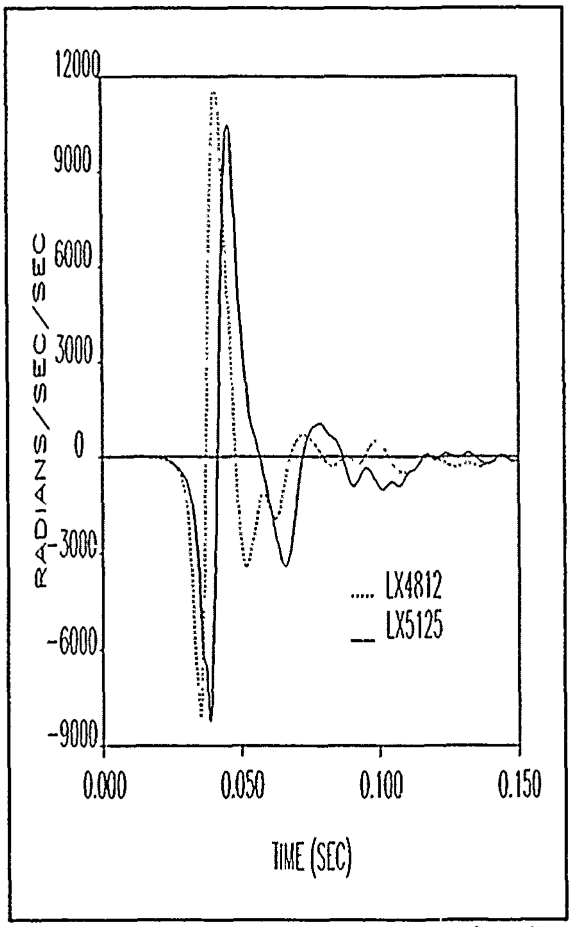

Figure 73. Head angular acceleration (Y-axis).

Effect of Out-of-Plane Behavior, NFCD.

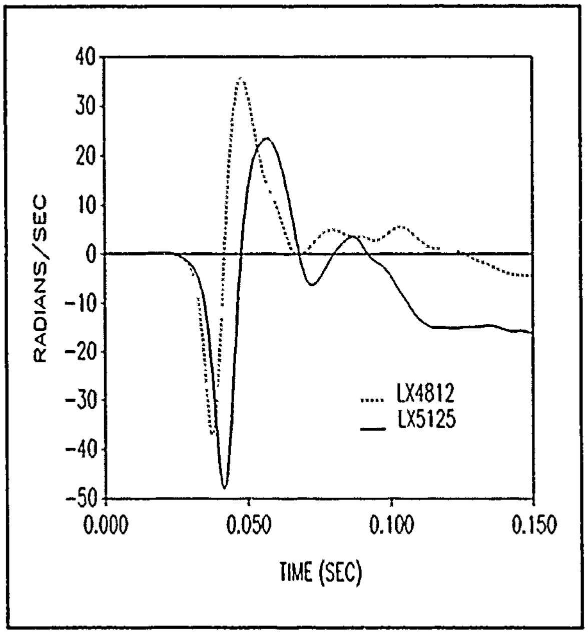

Figure 74. Head angular velocity (Y-axis).

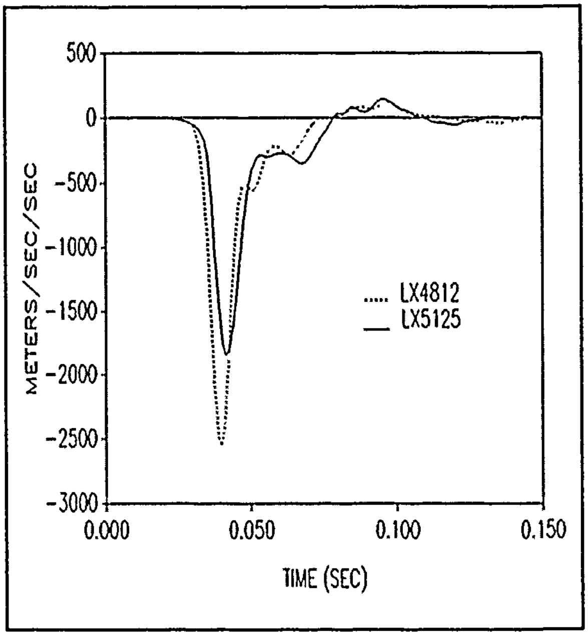

Figure 75. Head linear acceleration (X-component).

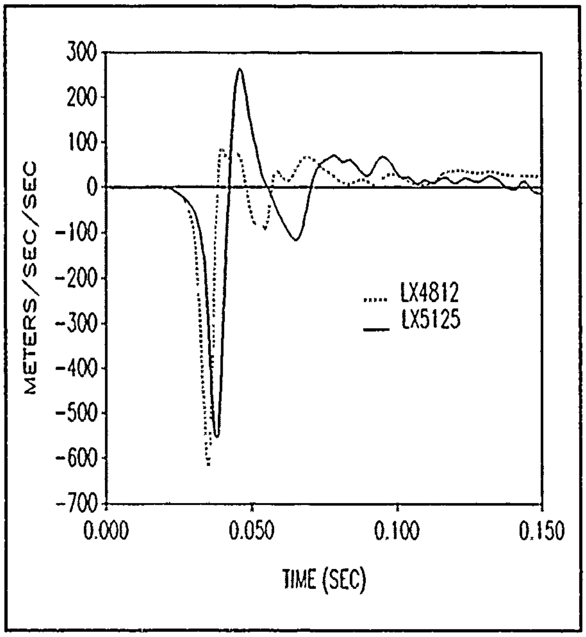

Figure 76. Head linear acceleration (Z-component).

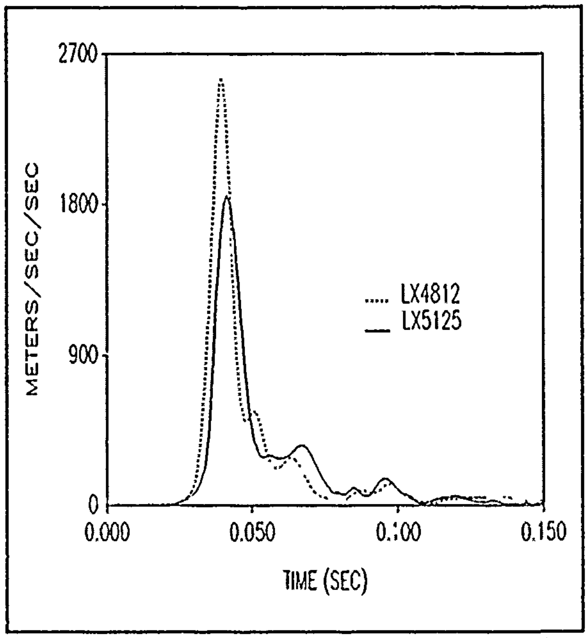

Figure 77. Resultant head linear acceleration (X-Z plane).

Effect of Out-of-Plane Behavior, NFCD.

TABLE B10.						
TEST	SUBJECT	G LEVEL	PHA	PHB	PHC	
LX5768	AR5855	58	0.076	-0.205*	0.128	
LX5774	AR5855	57	-0.027	-0.126	0.132	
TEST	SUBJECT	QHB	RHB	AAX	AAZ	AAR
LX5768	AR5855	9044	79	-1097	42	1121
LX5774	AR5855	9862	62	-1177	31	1200

* Slightly larger backward pitch inflates values somewhat.

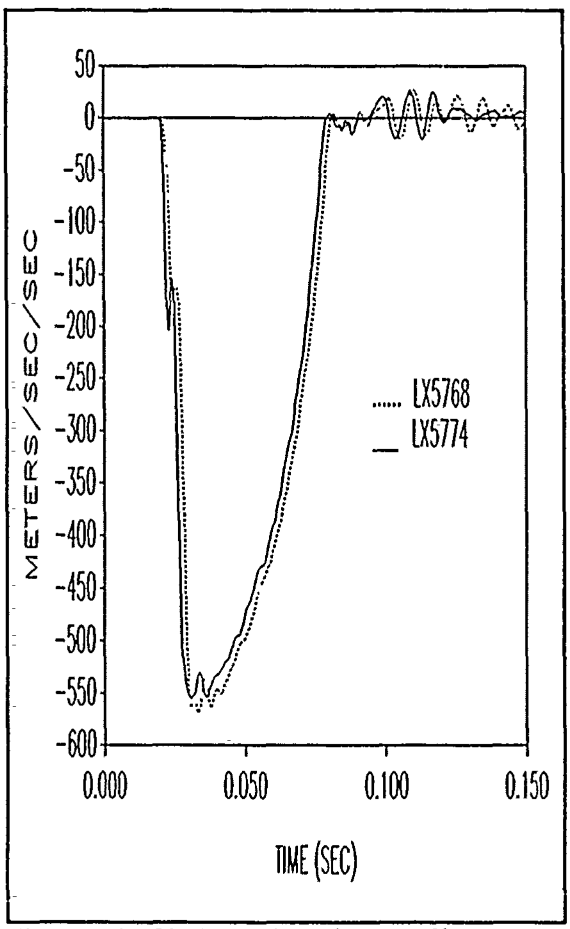

Figure 78. Sled acceleration profile.

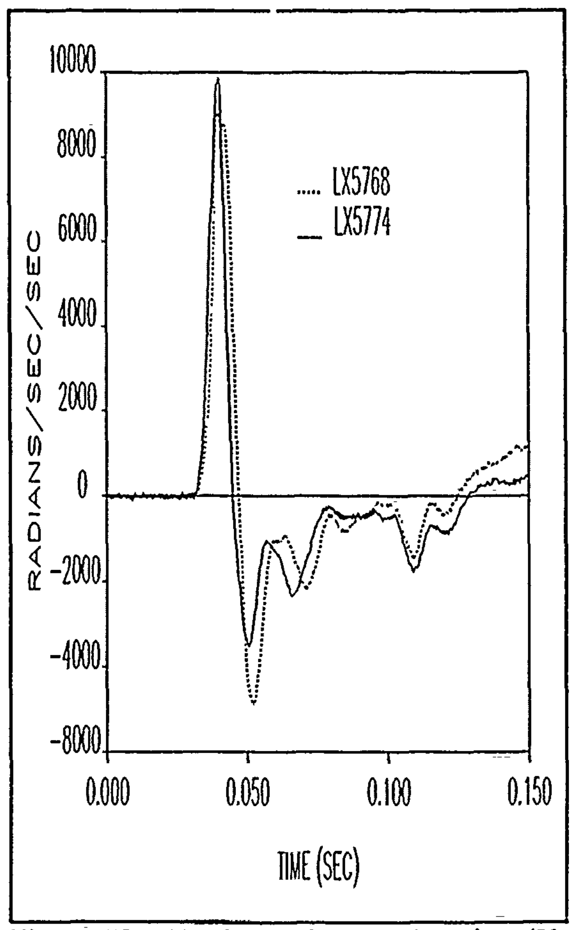

Figure 79. Head angular acceleration (Y-axis).

Within Animal Repeatability, Anesthetized, 57 g, NUCU.

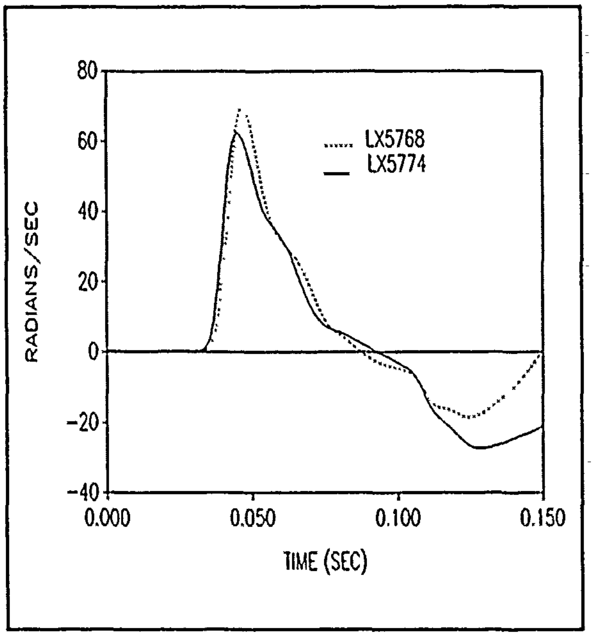

Figure 80. Head angular velocity (Y-axis).

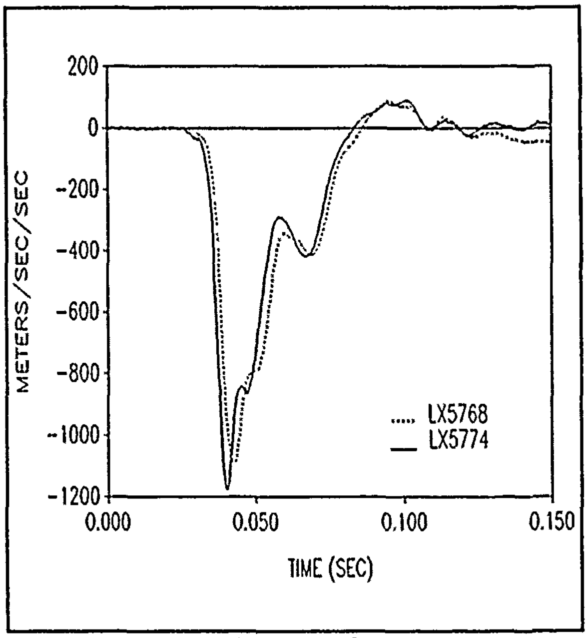

Figure 81. Head linear acceleration (X-component).

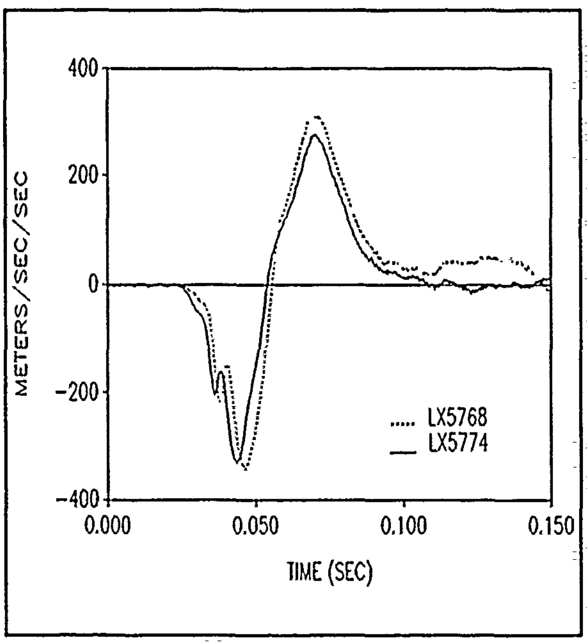

Figure 82. Head linear acceleration (Z-component).

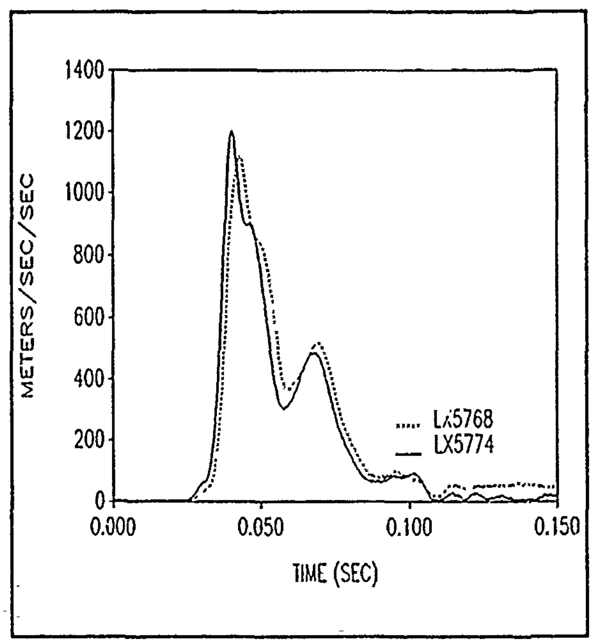

Figure 83. Resultant head linear acceleration (X-Z plane).

Within Animal Repeatability, Anesthetized, 57 g, NUCU.

TABLE B11.						
TEST	**SUBJECT**	**G LEVEL**	**PHA**	**PHB**	**PHC**	**QHB**
LX5151	ARNR16	42	-0.031	0.218	-0.490	-1674
LX5152	ARNR16	42	-0.052	0.225	-0.455	-1903
TEST	**SUBJECT**	**RHB**	**AAX**	**AAZ**	**AAR**	
LX5151	ARNR16	-11	-949	-242	954	
LX5152	ARNR16	-12	-950	-238	953	

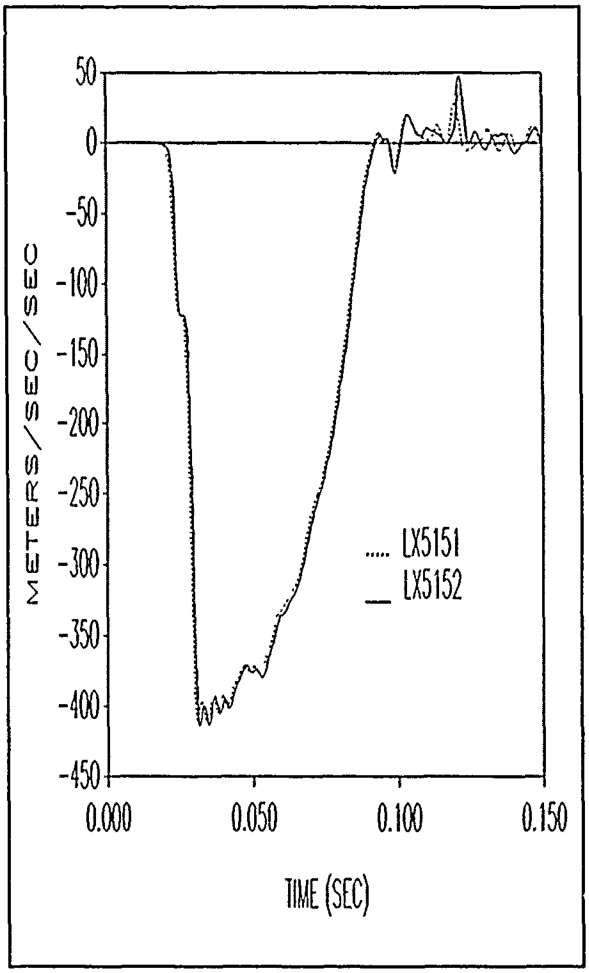

Figure 84. Sled acceleration profile.

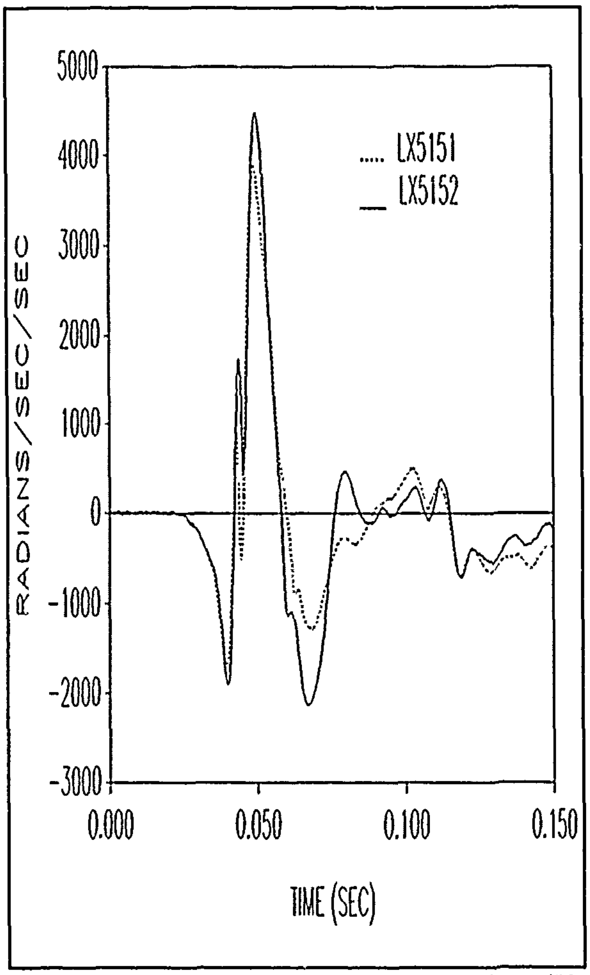

Figure 85. Head angular acceleration (Y-axis).

Within Animal Repeatability, Anesthetized, 42 g, NFCD.

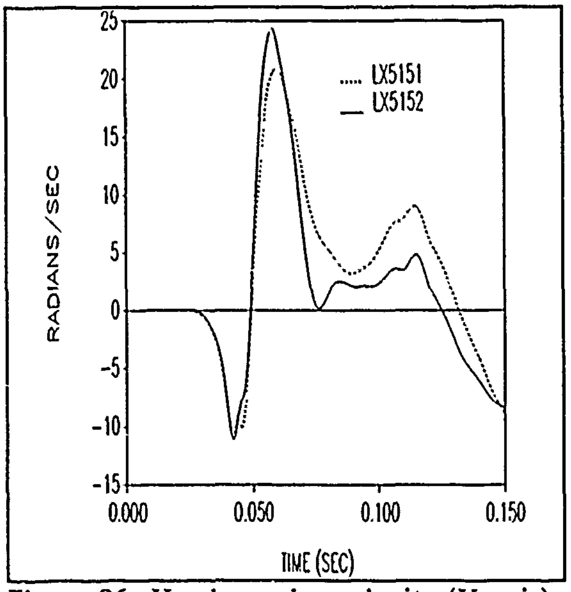

Figure 86. Head angular velocity (Y-axis).

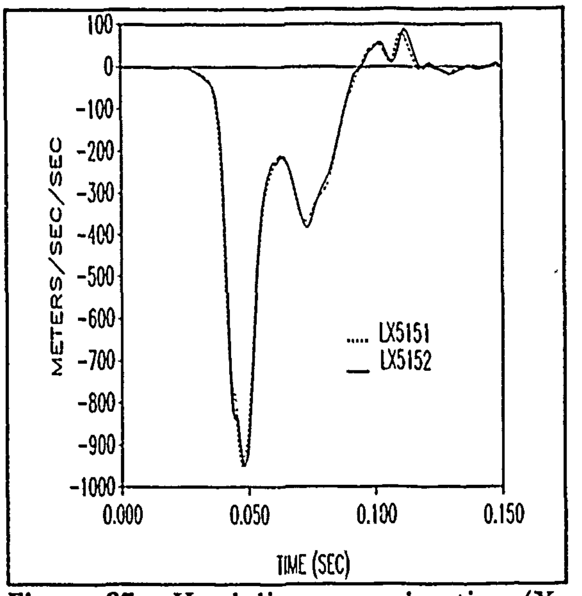

Figure 87. Head linear acceleration (X-component).

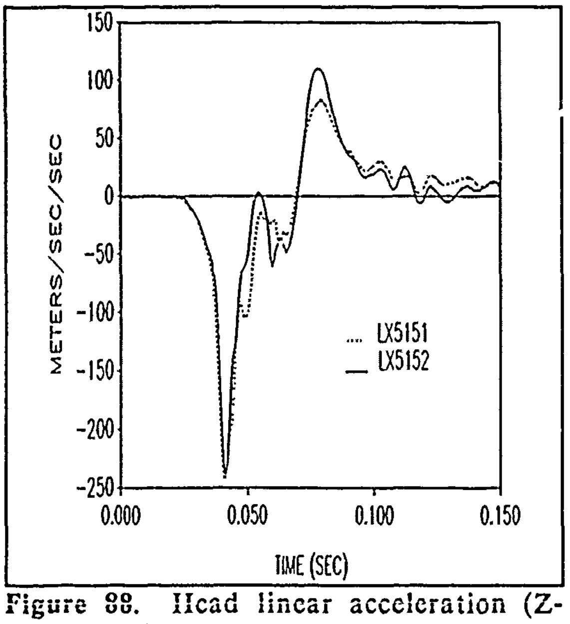

Figure 88. Head linear acceleration (Z-component).

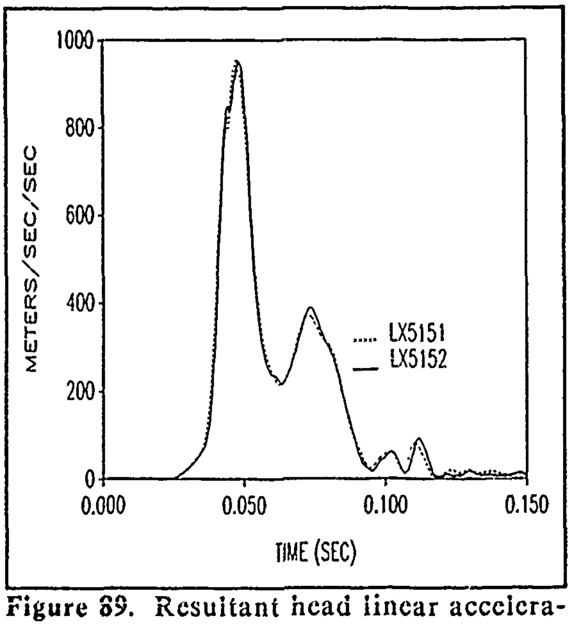

Figure 89. Resultant head linear acceleration (X-Z plane).

Within Animal Repeatability, Anesthetized, 42 g, NFCD.

TABLE B12.						
TEST	**SUBJECT**	**G LEVEL**	**PHA**	**PHB**	**PHC**	**QHB**
LX5160	AR0016	74	0.013	0.480	0.065	-5388
LX5161	AR0016	75	-0.108	0.505	0.070	-6225
LX5162	AR0016	75	-0.184	0.510	0.068	-7049
TEST	**SUBJECT**	**RHB**	**AAX**	**AAZ**	**AAR**	
LX5160	AR0016	-36	-1679	-505	1679	
LX5161	AR0016	-33	-1660	-529	1677	
LX5162	AR0016	-35	-1730	-514	1738	

Comments: Excellent replication in RHB, AAX, AAZ, and AXZ; QHB value for LX5162 seems a bit large.

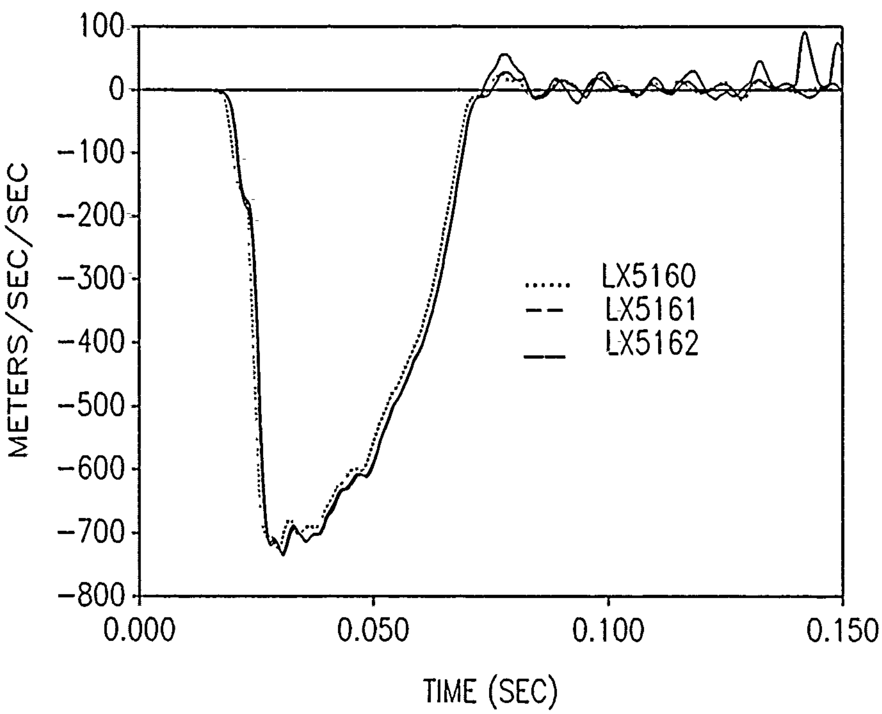

Figure 90. Sled acceleration profile.

Within Animal Repeatability, Anesthetized, 74 g, NFCD.

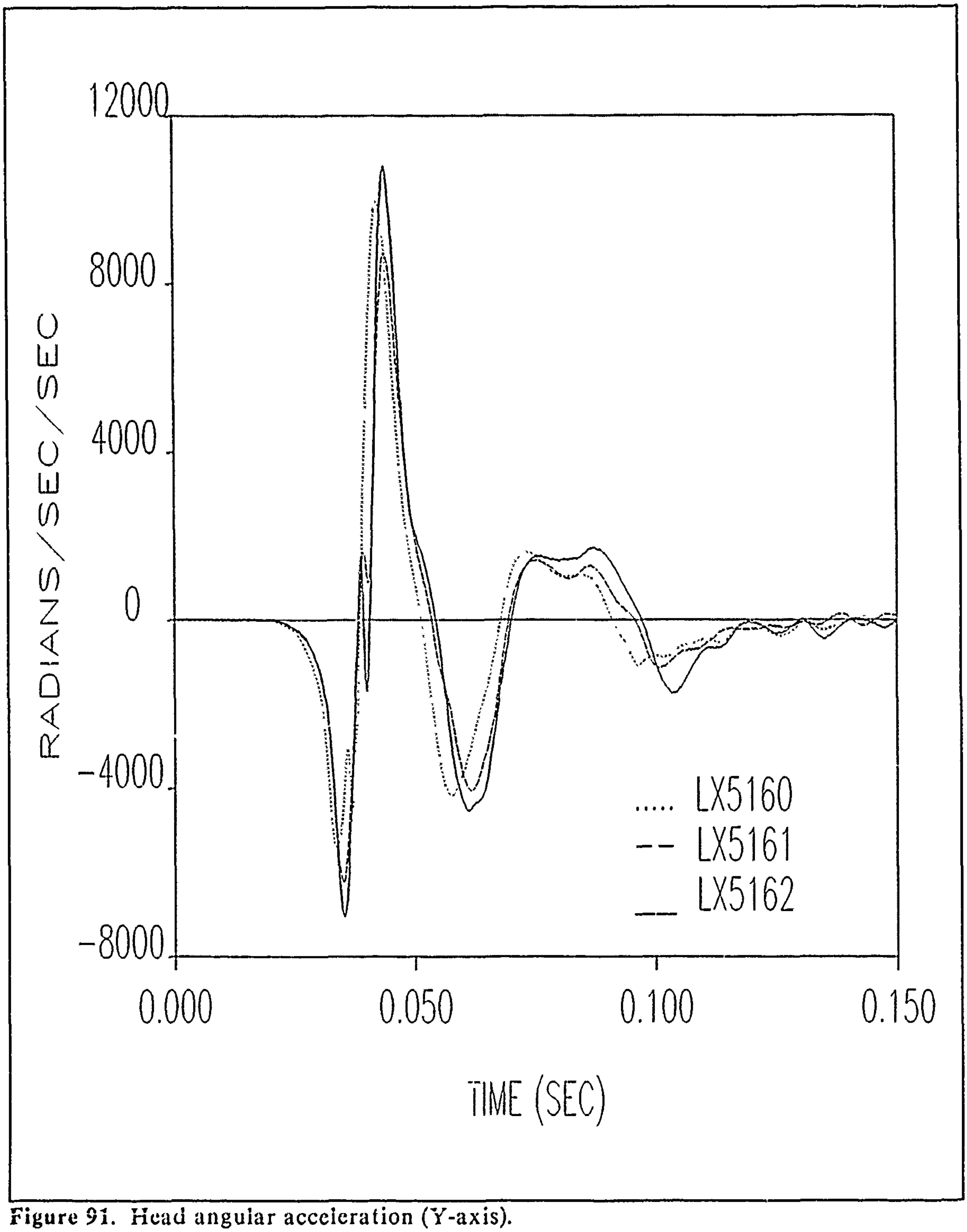

Figure 91. Head angular acceleration (Y-axis).

Within Animal Repeatability, Anesthetized, 74 g, NFCD.

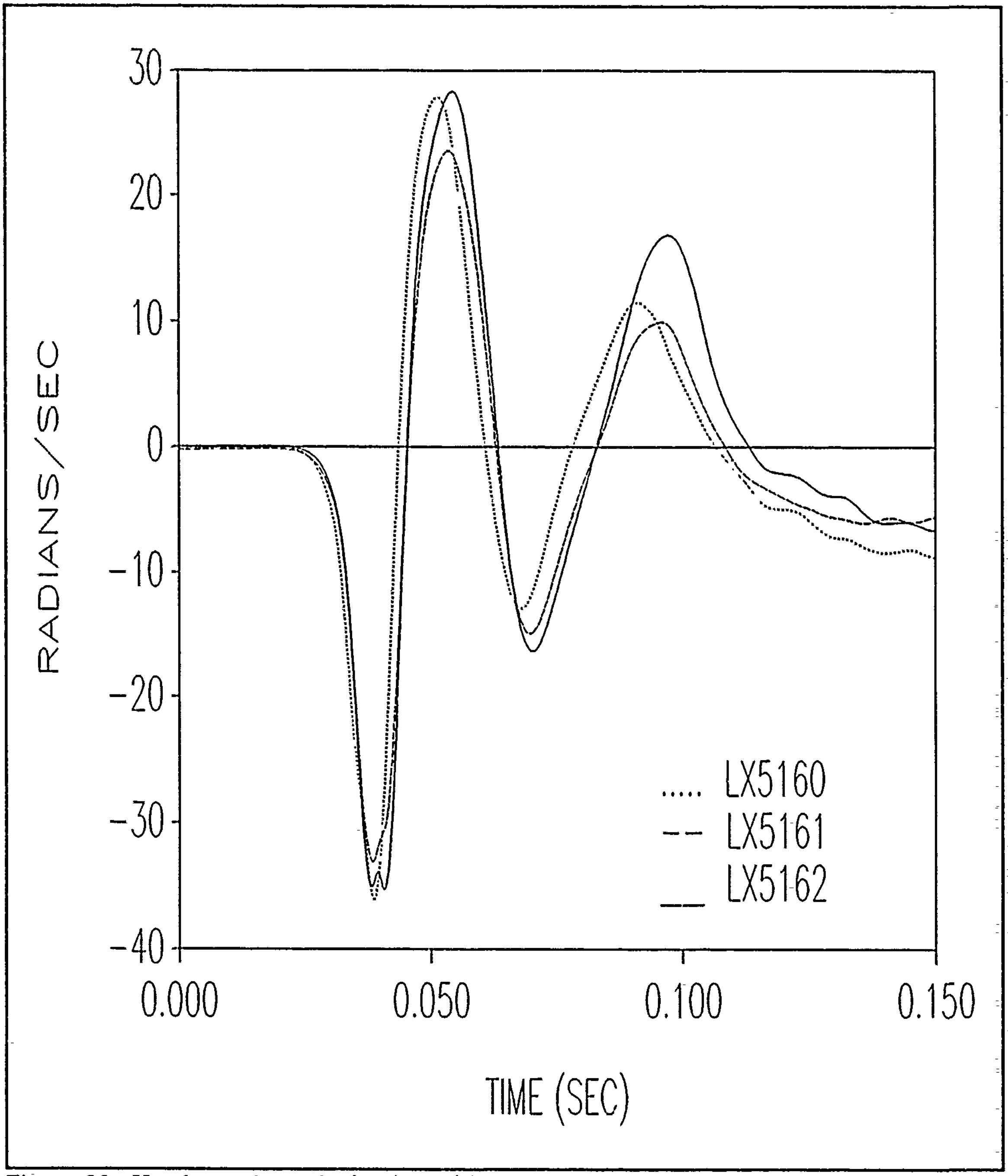

Figure 92. Head angular velocity (Y-axis).

Within Animal Repeatability, Anesthetized, 74 g, NFCD.

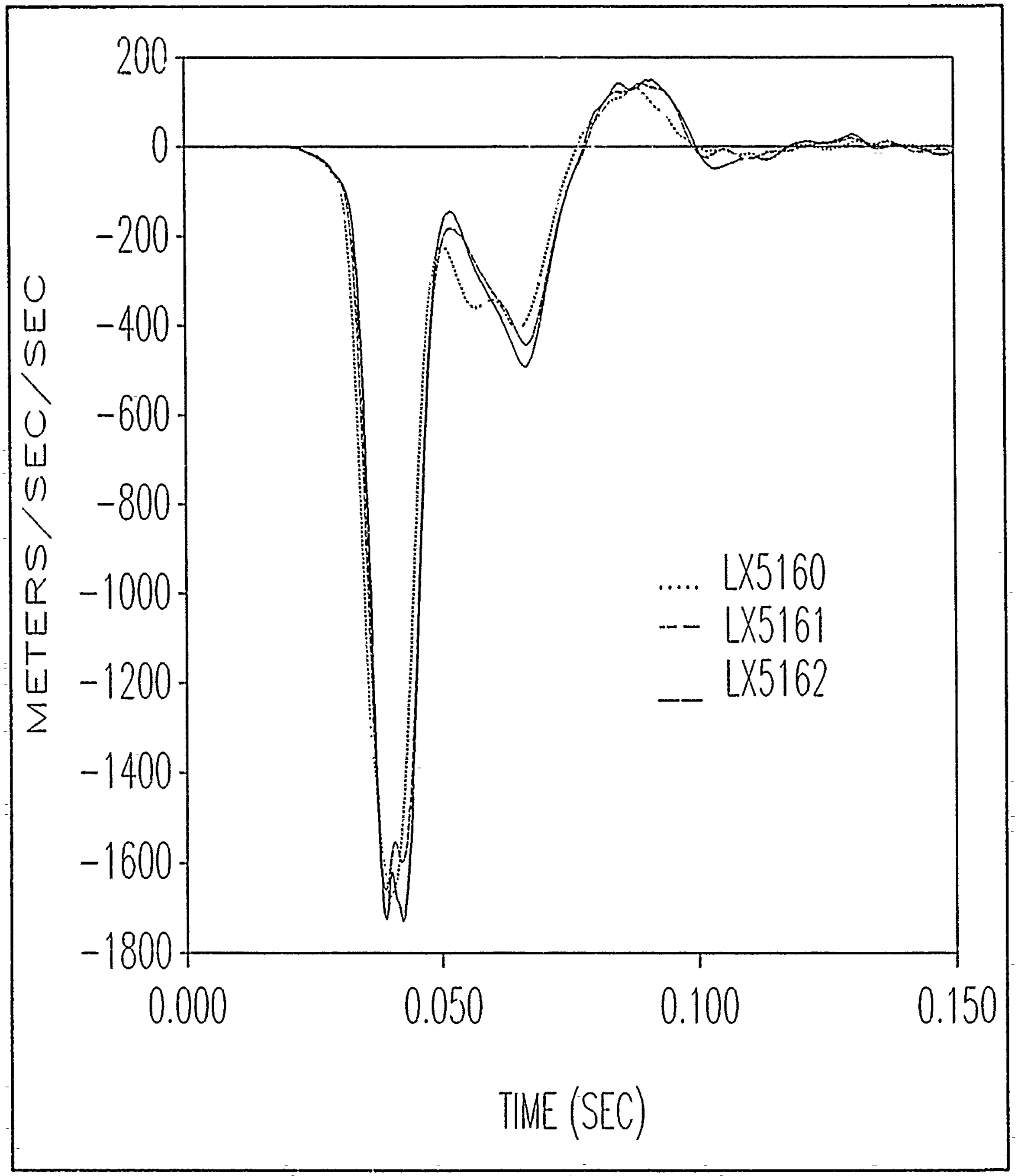

Figure 93. Head linear accelerations (X-component).

Within Animal Repeatability, Anesthetized, 74 g, NFCD.

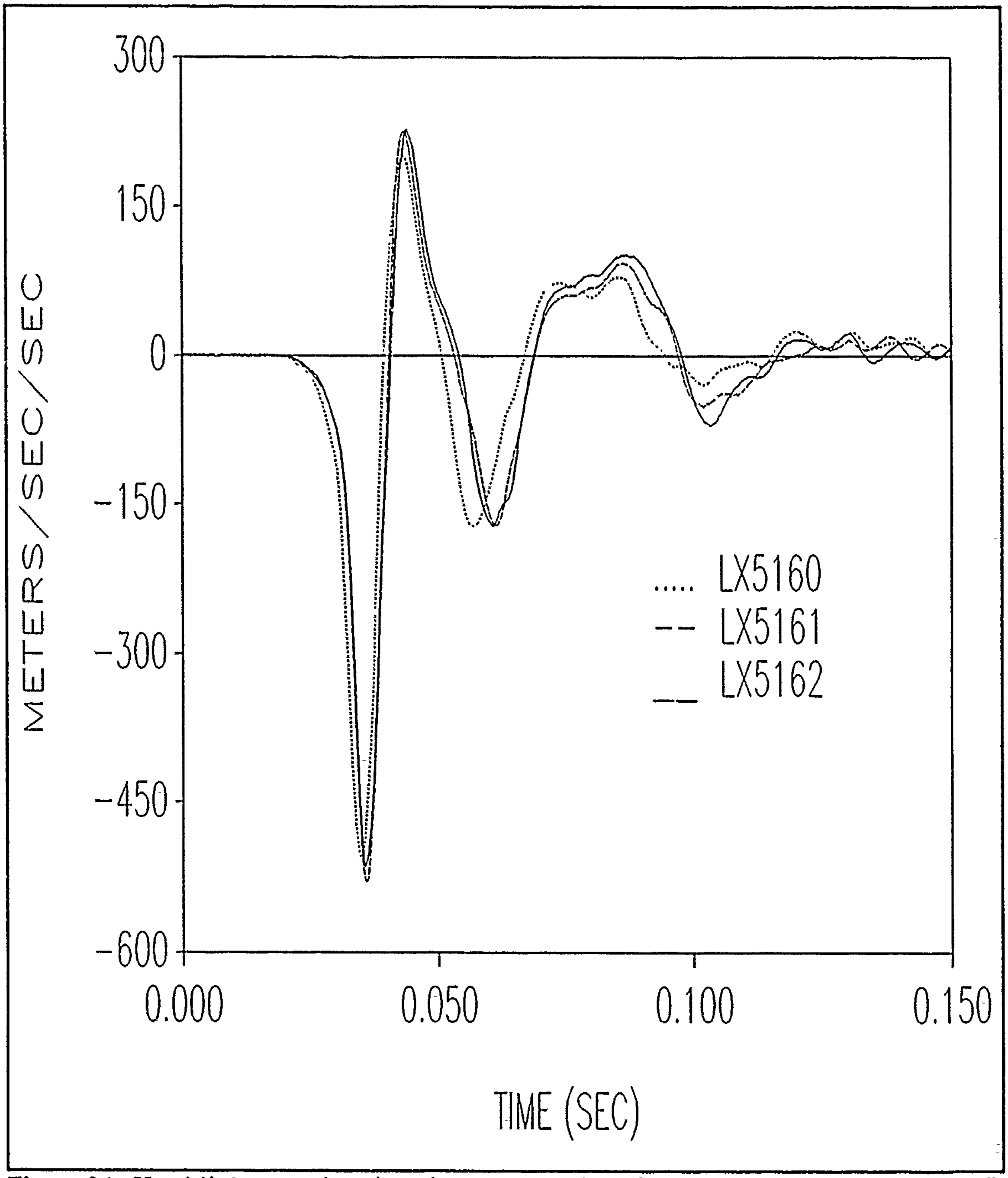

Figure 94. Head linear accelerations (Z-component).

Within Animal Repeatability, Anesthetized, 74 g, NFCD.

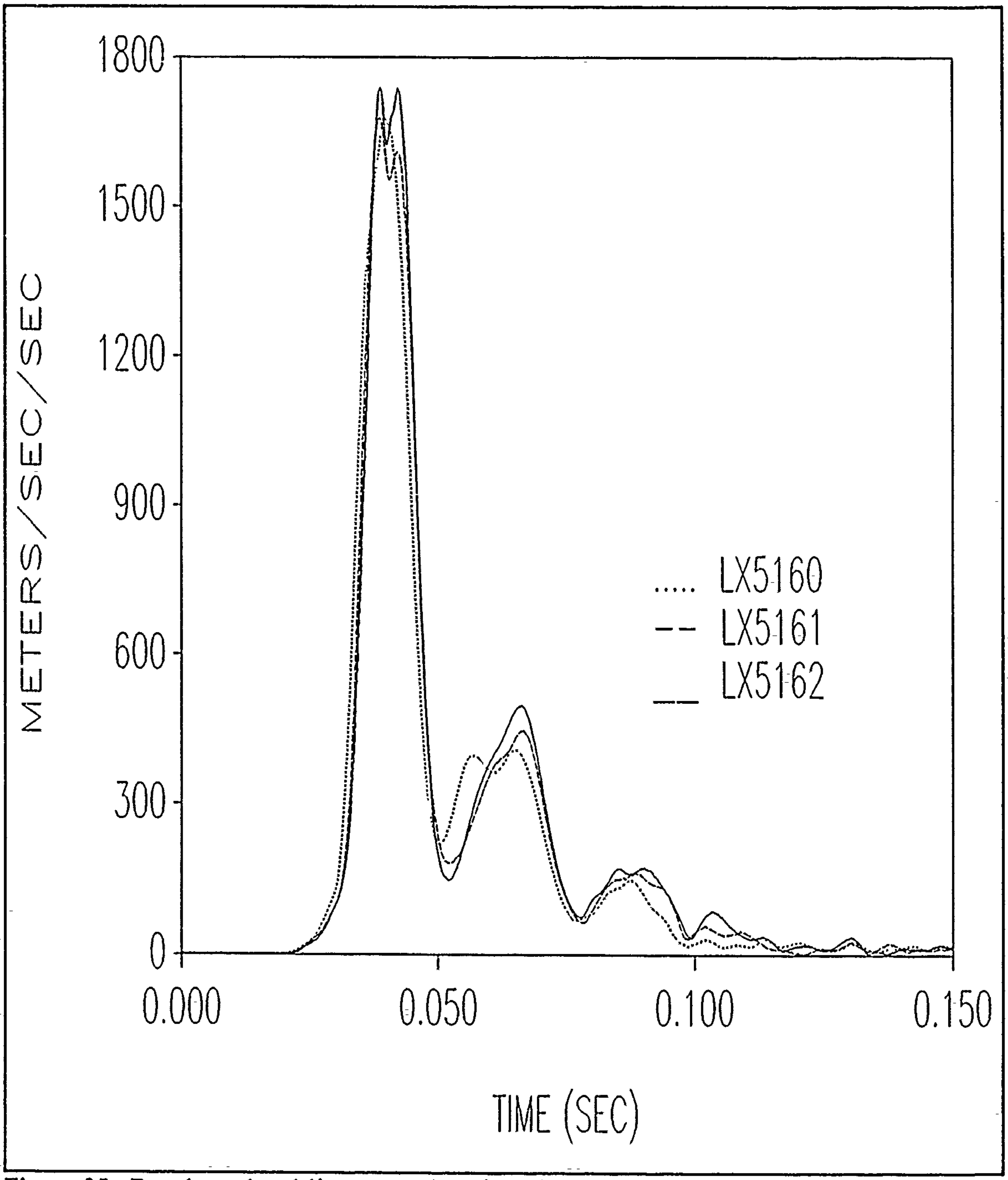

Figure 95. Resultant head linear accelerations (X-Z plane).

Within Animal Repeatability, Anesthetized, 74 g, NFCD.

TABLE B13.					
TEST	SUBJECT	G LEVEL	PHA	PHB	PHC
LX5125*	AR0016	73	0.062	0.543	-0.075
LX5129**	AR0016	74	-0.155	0.632	0.138
TEST	QHB	RHB	AAX	AAZ	AAR
LX5125*	-8231	-48	-1844	-553	1851
LX5129**	-7004	-48	-1813	-416	1813

* Unanesthetized.
** Anesthetized.

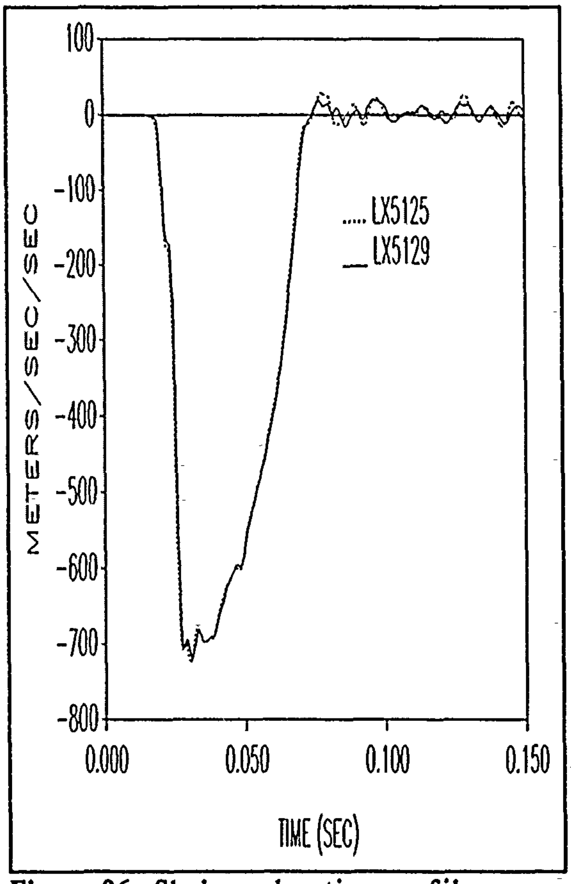

Figure 96. Sled acceleration profile.

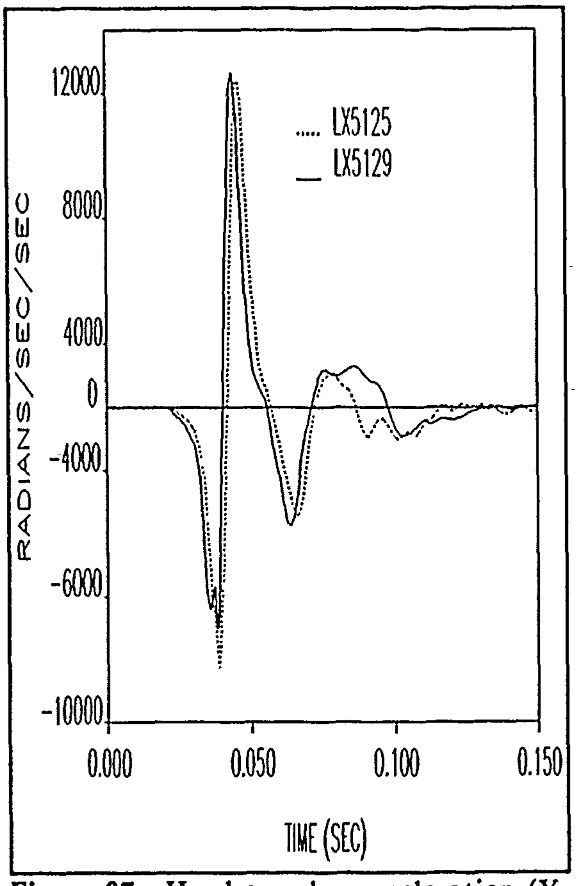

Figure 97. Head angular acceleration (Y-axis).

Anesthetized vs. Unanesthetized Subjects, 74 g, NFCD.

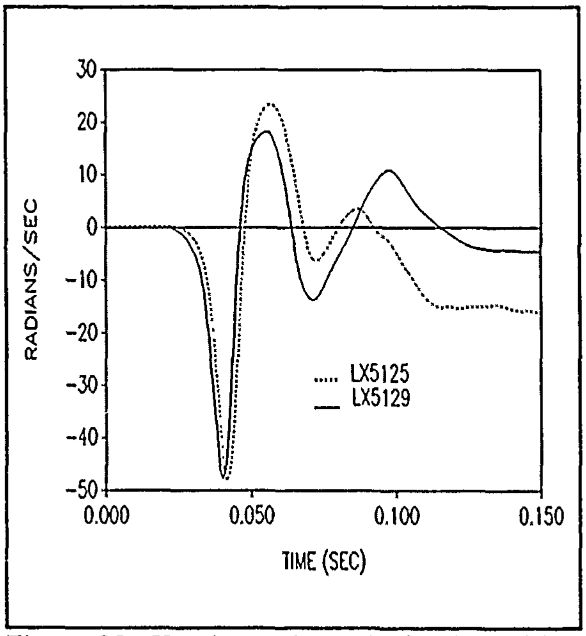

Figure 98. Head angular velocity (Y-axis).

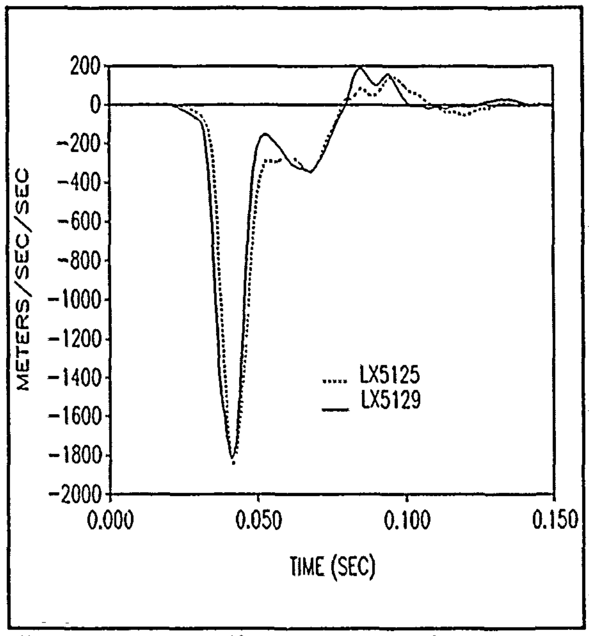

Figure 99. Head linear acceleration (X-component).

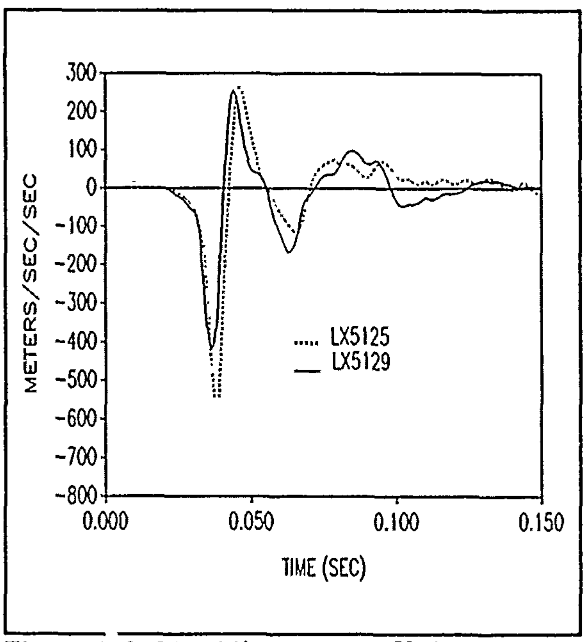

Figure 100. Head linear acceleration (Z-component).

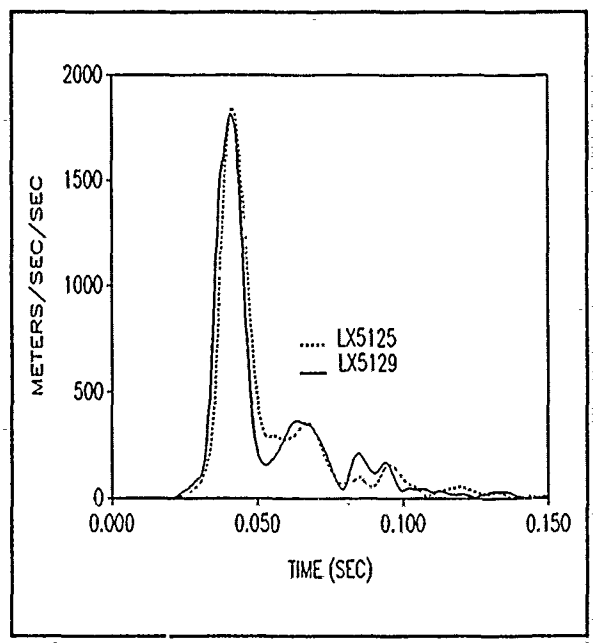

Figure 101. Resultant head linear acceleration (X-Z plane).

Anesthetized vs. Unanesthetized Subjects, 74 g, NFCD.

TABLE B14.						
TEST	**SUBJECT**	**G LEVEL**	**PHA**	**PHB**	**PHC**	**QHB**
LX5151	ARNR16	42	-0.031	0.218	-0.490	3920
LX5152	ANR165	42	-0.052	0.225	-0.455	4480
TEST	**SUBJECT**	**RHB**	**AAX**	**AAZ**	**AAR**	
LX5151	ARNR16	-11	-949	-243	954	
LX5152	ARNR16	-12	-950	-238	953	

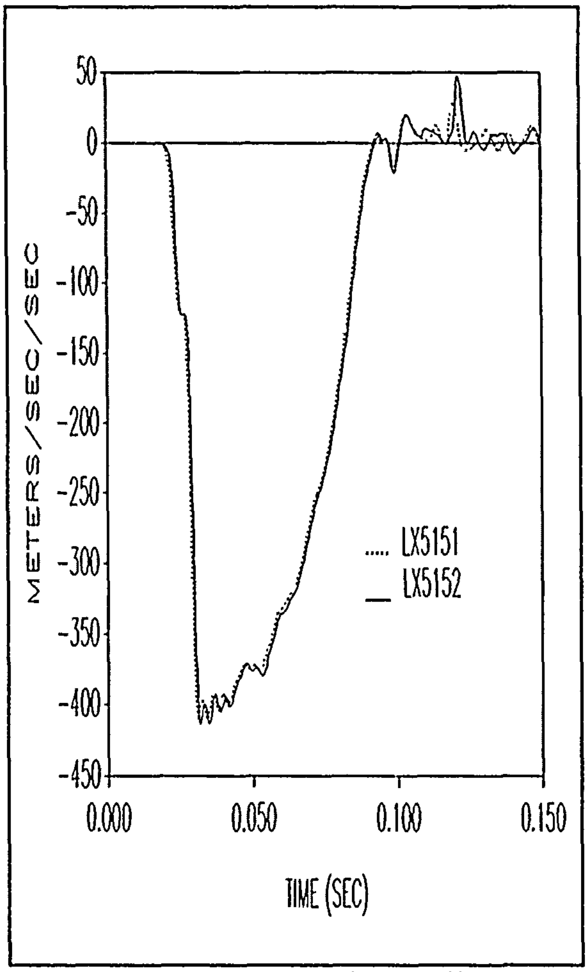

Figure 102. Sled acceleration profile.

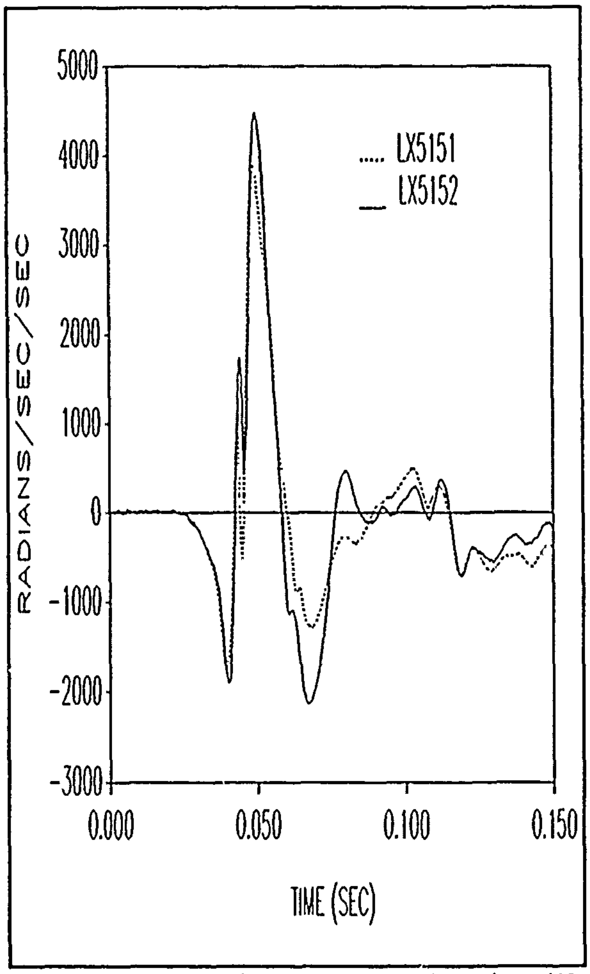

Figure 103. Head angular acceleration (Y-axis).

42 g Anesthetized Subject NFCD Reproducibility (Seven Previous Runs).

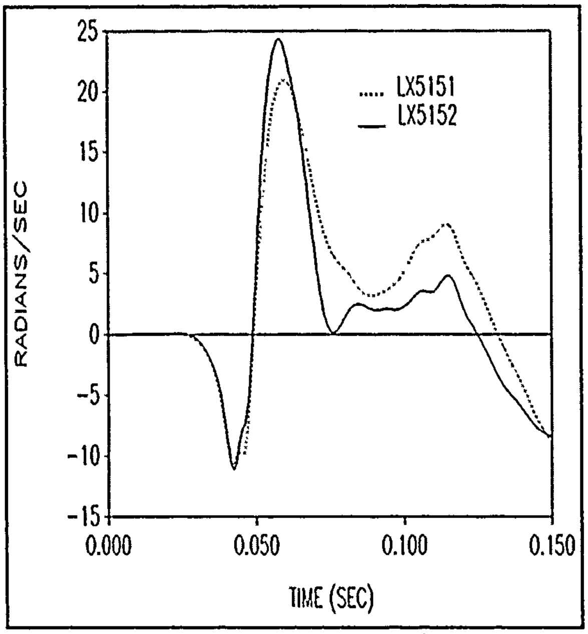

Figure 104. Head angular velocity (Y-axis).

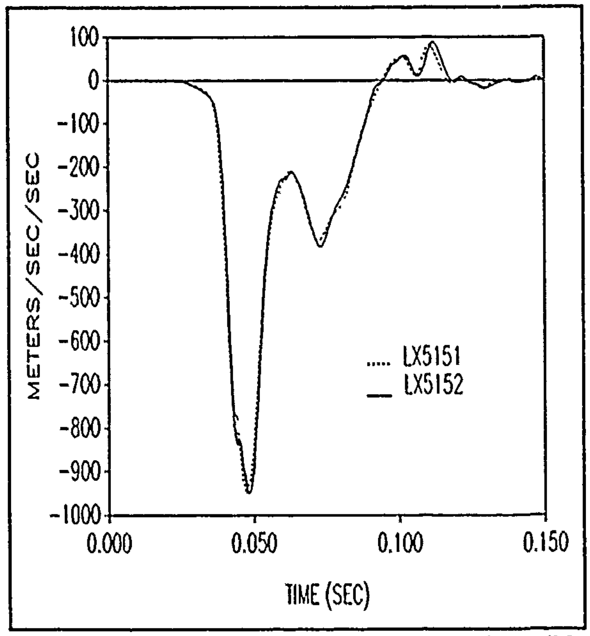

Figure 105. Head linear acceleration (X-component).

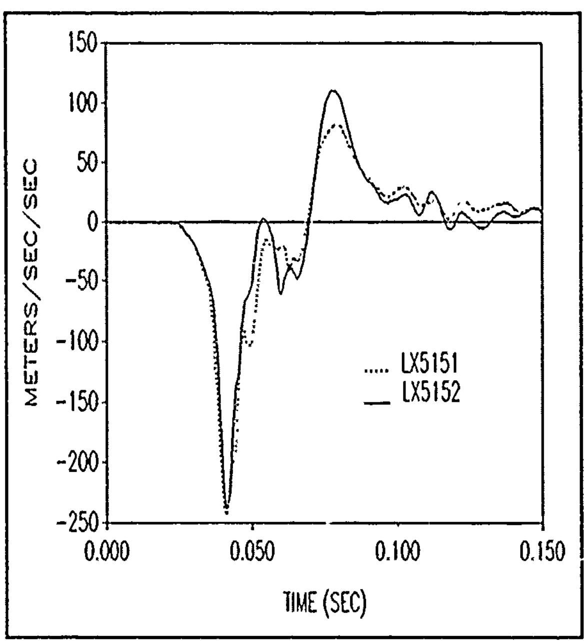

Figure 106. Head linear acceleration (Z-component).

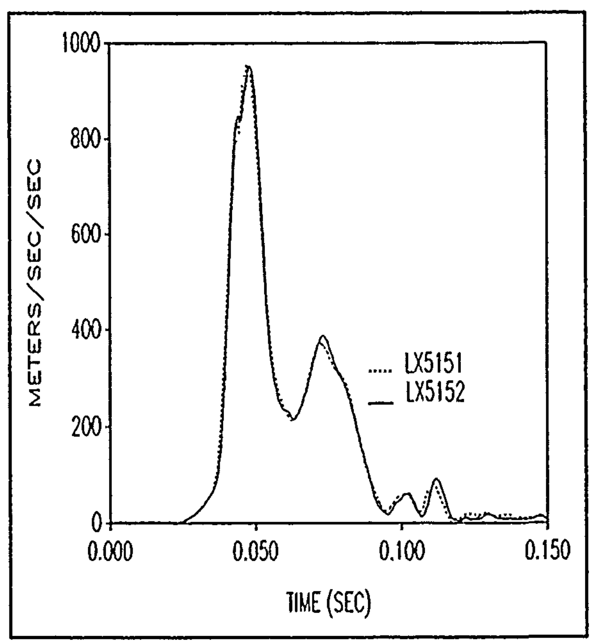

Figure 107. Resultant head linear acceleration (X-Z plane).

42 g Anesthetized Subject NFCD Reproducibility (Seven Previous Runs).

TABLE B15.						
TEST	SUBJECT	G LEVEL	PHA	PHB	PHC	QHB
LX5161	AR0016	74	-0.108	0.505	0.070	-6225
LX5162	AN0065	74	-0.184	0.510	0.068	-7049
TEST	SUBJECT	RHB	AAX	AAZ	AAR	
LX5161	AR0016	-33	-1660	-529	1677	
LX5162	AR0016	-35	-1730	-514	1783	

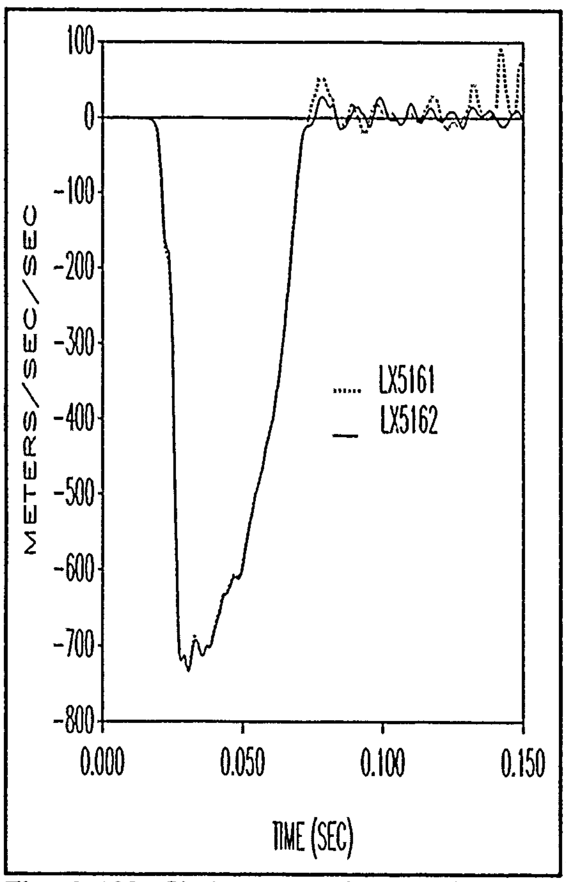

Figure 108. Sled acceleration profile.

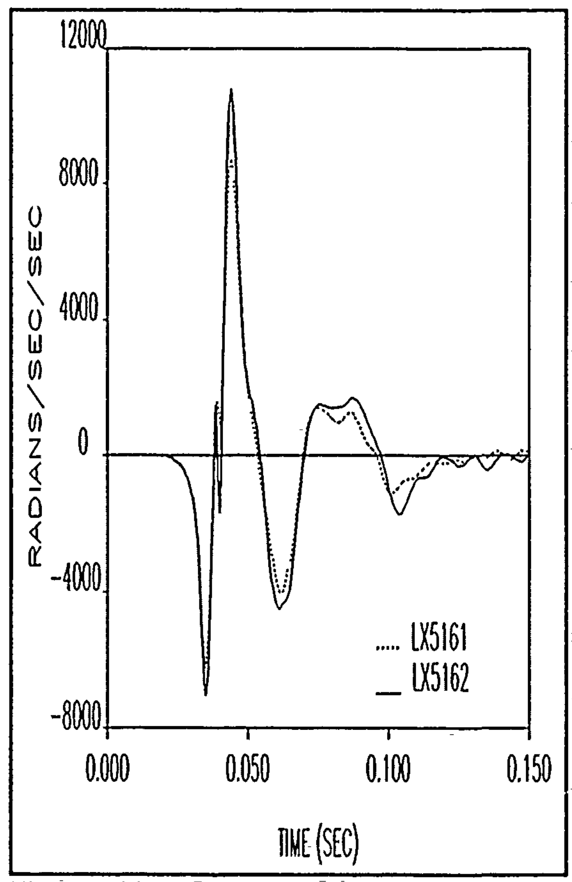

Figure 109. Head angular acceleration (Y-axis).

74 g Anesthetized Subject NFCD Reproducibility (Eight Previous Runs).

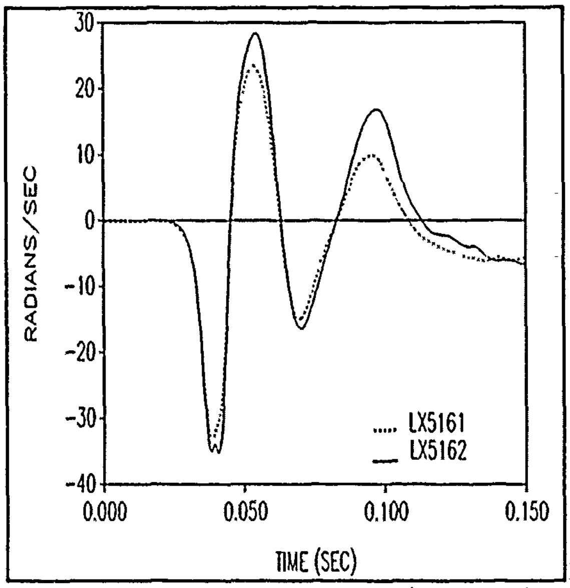

Figure 110. Head angular velocity (Y-axis).

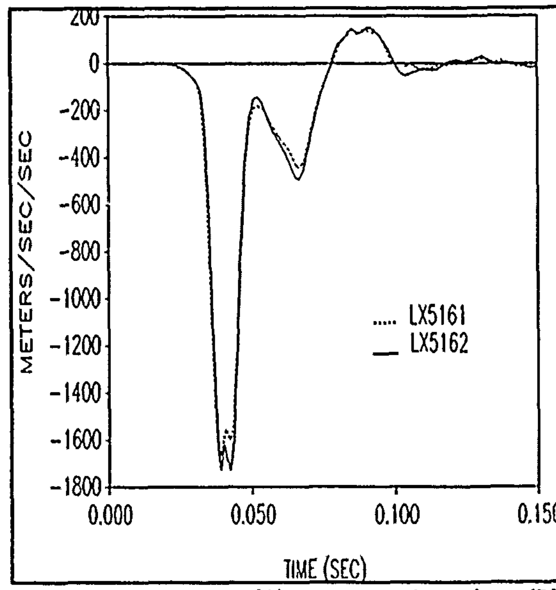

Figure 111. Head linear acceleration (X-component).

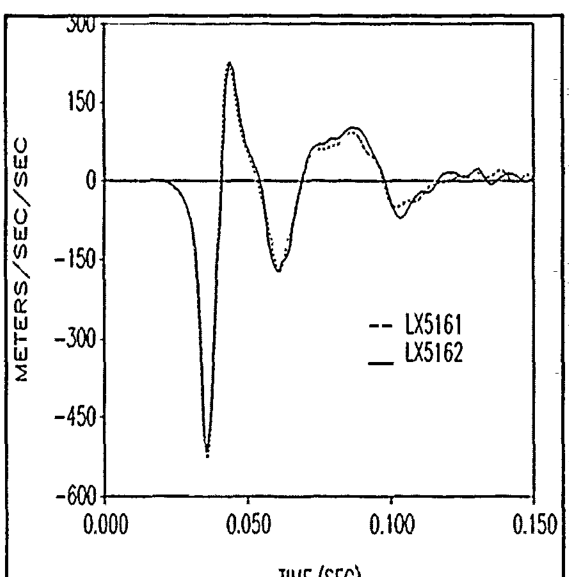

Figure 112. Head linear acceleration (Z-component).

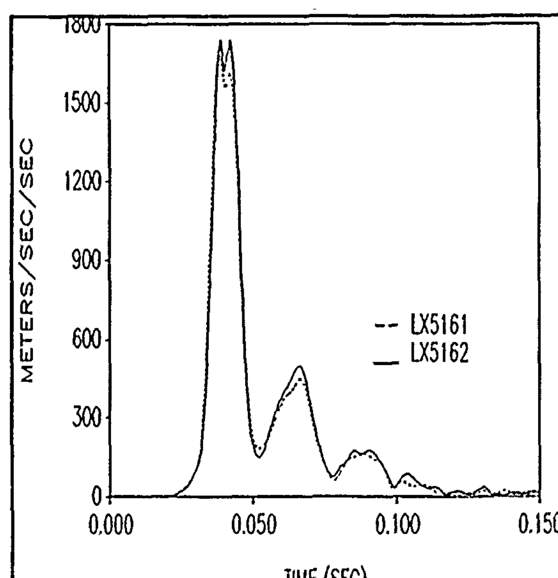

Figure 113. Resultant head linear acceleration (X-Z plane).

74 g Anesthetized Subject NFCD Reproducibility (Eight Previous Runs).

TABLE B16.

TEST	SUBJECT	G LEVEL	PHA	PHB	PHC	QHB
LX5129	ARNR16	74	-0.155	0.632	0.138	-7004
LX5160	ANR165	74	0.013	0.481	0.065	-5388
TEST	**SUBJECT**	**RHB**	**AAX**	**AAZ**	**AAR**	
LX5129	ARNR16	-48	-1813	-416	1813	
LX5160	ARNR16	-36	-1679	-505	1679	

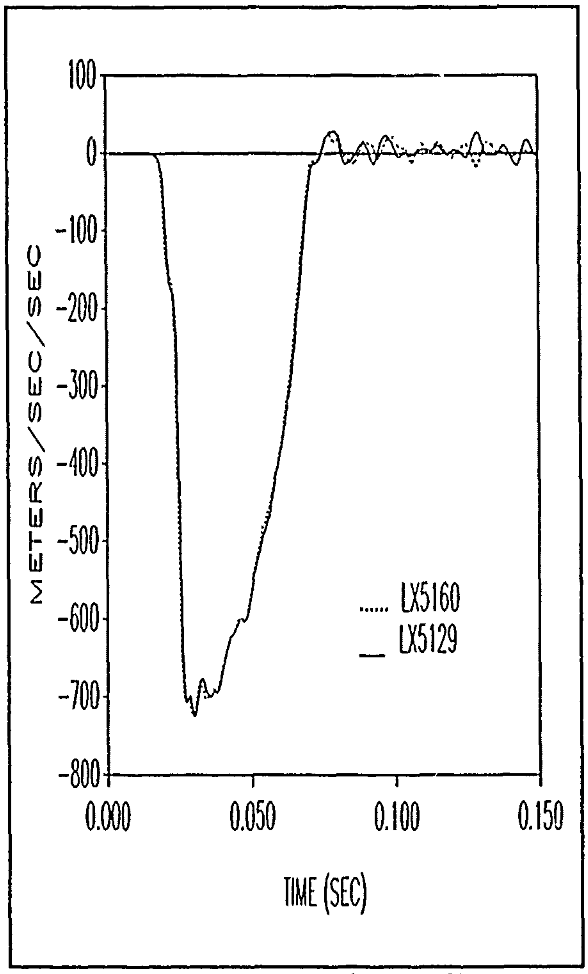

Figure 114. Sled acceleration profile.

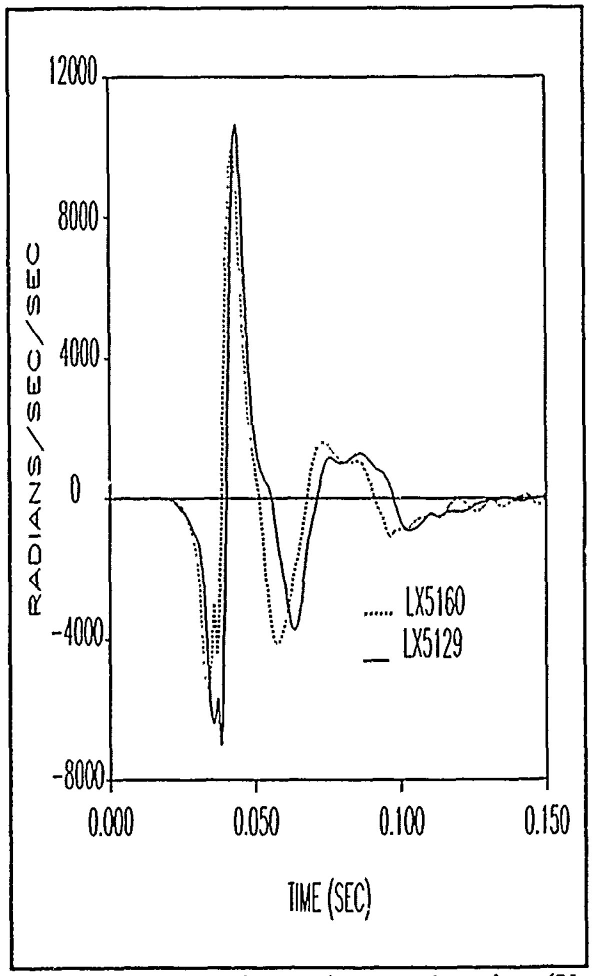

Figure 115. Head angular acceleration (Y-axis).

42 g Anesthetized Subject NFCD Reproducibility
(Three Previous, Three Intervening Runs).

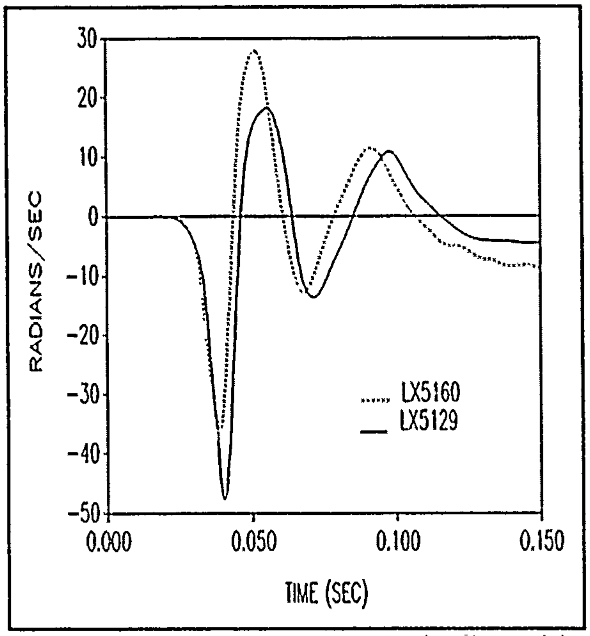

Figure 116. Head angular velocity (Y-axis).

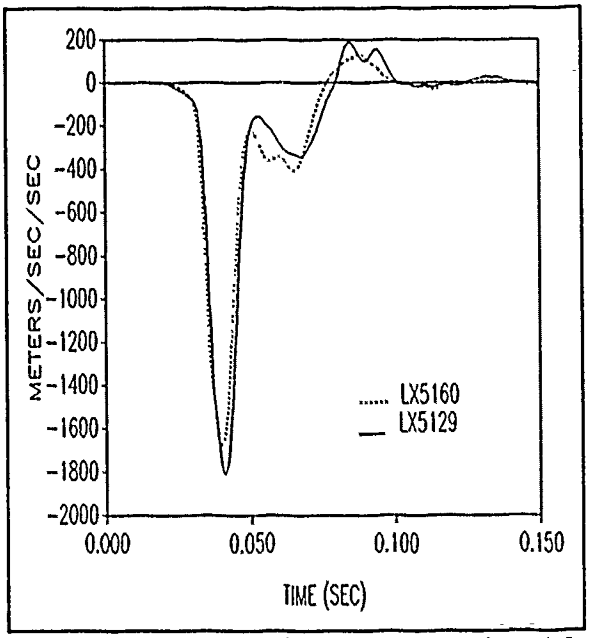

Figure 117. Head linear acceleration (X-component).

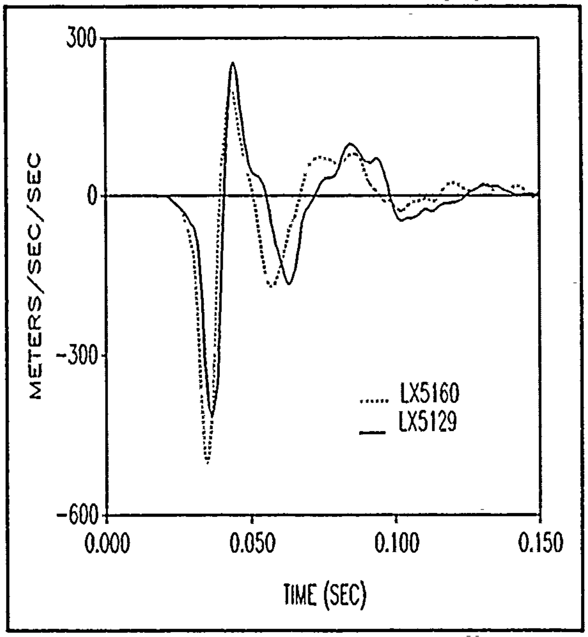

Figure 118. Head linear acceleration (Z-component).

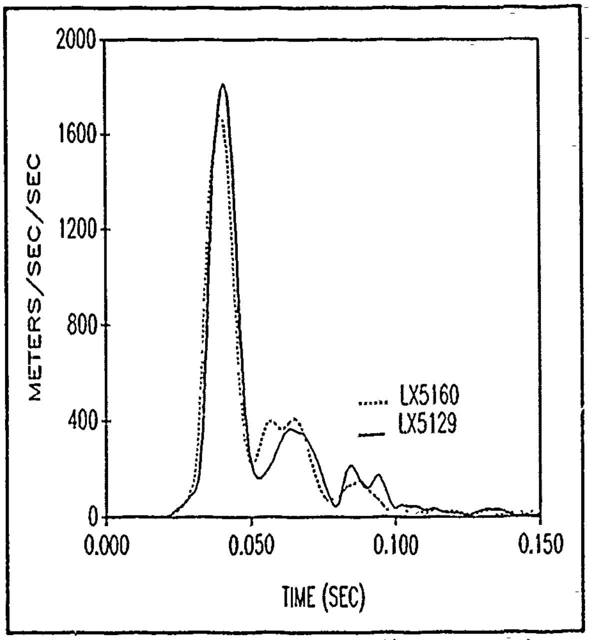

Figure 119. Resultant head linear acceleration (X-Z plane).

42 g Anesthetized Subject NFCD Reproducibility (Three Previous, Three Intervening Runs).

APPENDIX C

DATA BREAKDOWN AND REGRESSION RESULTS

The results for datasets A and B are presented in a packet format consisting of the following elements:

(1) An introductory page giving the name of the dataset, the number of runs in the dataset, the peak choices for each of the five dependent kinematic variables, and the independent sled, head angular orientation, and grouping variables used in the final regressions.

(2) A breakdown of the runs according to animal ID, series, g level, head position, state of consciousness, and evoked potential.

(3) A breakdown of the runs with respect to animal ID, values of the sled parameters and head initial position parameters, together with descriptive statistics.

(4) A breakdown of the runs according to animal ID, state of consciousness, planarity, and peak values of the five dependent kinematic variables, with descriptive statistics.

(5) A table of regression coefficients for each of the five dependent kinematic variables, together with a table of significance of the regression, giving the number of runs used in a particular regression, the R values, the F level of overall regression, the standard error of estimate, and the t level of significance for each regression coefficient.

(6) For each of the five dependent kinematic variables, a table containing the observed and predicted values for each run, and the left- and right-hand endpoints of a simultaneous 95% confidence interval about the mean predicted value for each observation. Descriptive statistics for the various quantities mentioned above are also given. Following the table is an observed- versus predicted-value plot for the kinematic variable.

TABLE C1. Dataset A: Selected peaks for key head kinematic responses. Head Initial Condition: Neck-up, Chin-up (NUCU).

KINEMATIC VARIABLE	SYMBOL	PEAK CHOSEN
Angular Acceleration (Y)	QHB	+
Angular Velocity (Y)	RHB	+
Linear Acceleration (X)	AAX	-
Linear Acceleration (Z)	AAZ	-
Resultant Linear Acceleration (X-Z)	AAR	+

Number of Runs: 29
Independent Variables Chosen:
(1) Peak Sled Acceleration (PSA)
(2) Initial Head Pitch (PHB)
(3) Squared Initial Head Pitch (PHB^2)

TABLE C2. Dataset A: Summary of Experiments.

TEST	ID	SERIES	G LEVEL	CONSCIOUSNESS	EVOKED POTENTIAL
LX4790	ARNR16	1984	85	U	
LX4791	ARNR16	1984	101	U	
LX4799	ARNR18	1984	106	U	YES
LX4801*	ARNR34	1984	102	U	
LX4803*	ARNR24	1984	86	U	YES
LX4810	ARNR23	1984	56	U	YES
LX4814	ARNR36	1984	71	U	
LX4820	AR8739	1984	56	U	YES
LX4822	ARNR39	1984	86	U	
LX5135	AR8845	1985	42	U	
LX5147	AR8845	1985	74	U	
LX5150	ARNR16	1985	42	A	
LX5155	AR0016	1985	42	A	
LX5156	AR0016	1985	42	A	
LX5157	AR0016	1985	42	A	
LX5164	AR0016	1985	75	A	
LX5165	AR0016	1985	76	A	
LX5768	AR5855	1987	58	A	
LX5770	AR5852	1987	57	A	
LX5772	AR986B	1987	57	A	YES
LX5774	AR5855	1987	57	A	
LX5777	AR8776	1987	75	A	YES
LX5779	AR0019	1987	57	A	YES
LX5782	AR5851	1987	75	A	YES
LX5784	AR5852	1987	75	A	
LX5786	AR894C	1987	89	A	YES
LX5793	AR5853	1987	90	A	
LX5795	AR798B	1987	92	A	
LX5797	ARNR20	1987	91	A	

* Fatal run.

Number of tests: 29
Number of anesthetized subjects: 18
Number of unanesthetized subjects: 11
Number of evoked potentials: 9
Number of fatal runs: 2

TABLE C3. Dataset A: Sled Parameters for NUCU Runs.

TEST	ID	PSA	ROO	ESV
LX4790	ARNR16	834	79893	26.1
LX4791	ARNR16	988	112651	28.3
LX4799	ARNR18	1040	133118	29.0
LX4801	ARNR34	995	133798	28.4
LX4803	ARNR24	844	98833	26.4
LX4810	ARNR23	545	42859	21.4
LX4814	ARNR36	692	64523	23.9
LX4820	AR8739	545	42122	21.3
LX4822	ARNR39	843	89519	26.2
LX5135	AR8845	409	21057	18.8
LX5147	AR8845	728	60409	24.8
LX5150	ARNR16	411	20914	18.9
LX5155	AR0016	412	20099	18.9
LX5156	AR0016	415	25639	19.0
LX5157	AR0016	411	20274	18.8
LX5164	AR0016	732	56488	24.8
LX5165	AR0016	744	71209	25.3
LX5768	AR5855	570	33716	22.0
LX5770	AR5852	559	40550	22.0
LX5772	AR986B	556	39671	21.9
LX5774	AR5855	555	52025	22.0
LX5777	AR8776	730	54385	25.1
LX5779	AR0019	554	42724	21.9
LX5782	AR5851	733	55144	25.1
LX5784	AR5852	730	52818	25.0
LX5786	AR894C	870	76079	27.1
LX5793	AR5853	880	78933	27.2
LX5795	AR798B	897	75438	27.5
LX5797	ARNR20	889	82634	27.5

TESTS	29	29	29	29
MAXIMUM VALUE	1040	133798	29.0	31.8
MINIMUM VALUE	409	20099	18.8	19.2
MEAN VALUE	693	61294	24.0	24.4
1 STD DEV	194	31497	3.2	4.0
COEFF VAR	28%	51%	13%	16%

TABLE C4. Dataset A: Initial Head Angular and Linear Position for NUCU Runs.							
TEST	**ID**	**PHA**	**PHB**	**PHC**	**DAX**	**DAY**	**DAZ**
LX4790	ARNR16	.215	-.046	-.443	-1.201	.007	.319
LX4791	ARNR16	.310	-.216	-.263	-1.228	-.008	.322
LX4799	ARNR18	.292	-.019	-.839	-1.164	-.024	.301
LX4801	ARNR34	.371	-1.019	-.041	-1.220	-.009	.303
LX4803	ARNR24	.140	.225	-.111	-1.134	.016	.320
LX4810	ARNR23	.250	.057	-.800	-1.148	-.034	.287
LX4814	ARNR36	-.087	.339	.171	-1.114	.007	.278
LX4820	AR8739	.058	.185	-.222	-1.141	.015	.289
LX4822	ARNR39	-.012	.484	.147	-1.126	.019	.278
LX5135	AR8845	-.098	.094	-.030	-1.154	-.004	.309
LX5147	AR8845	.050	-.396	-.285	-1.184	.011	.328
LX5150	ARNR16	.039	.114	-.523	-1.156	-.015	.311
LX5155	AR0016	.076	.144	.325	-1.157	.001	.308
LX5156	AR0016	.144	.130	.390	-1.155	-.005	.315
LX5157	AR0016	.278	.175	.300	-1.150	-.005	.312
LX5164	AR0016	-.001	-.051	.027	-1.172	-.001	.332
LX5165	AR0016	.013	-.820	-.045	-1.195	-.006	.326
LX5768	AR5855	.076	-.205	.128	-1.174	-.004	.316
LX5770	AR5852	.064	-.042	.056	-1.186	-.010	.314
LX5772	AR986B	.049	-.008	.072	-1.188	.008	.322
LX5774	AR5855	-.027	-.126	.132	-1.168	-.002	.319
LX5777	AR8776	.114	-.433	.117	-1.203	.005	.304
LX5779	AR0019	-.203	-.390	-.010	-1.189	.016	.309
LX5782	AR5851	-.034	-.144	.047	-1.177	.014	.317
LX5784	AR5852	-.269	-.213	-.037	-1.200	.024	.312
LX5786	AR894C	-.024	-.063	.022	-1.165	.018	.307
LX5793	AR5853	-.017	-.294	.174	-1.192	-.012	.323
LX5795	AR798B	-.039	-.086	.157	-1.166	.005	.314
LX5797	ARNR20	-.048	-.129	-.080	-1.162	.014	.328
TESTS		29	29	29	29	29	29
MAXIMUM VALUE		.371	.484	.390	-1.114	.024	.332
MINIMUM VALUE		-.269	-1.019	-.839	-1.228	.034	.278
MEAN VALUE		.058	-.095	-.053	-1.171	.001	.311
1 STD DEV		.150	.314	.296	.027	.014	.014
COEFF VAR					2%		

TABLE C5. Dataset A: Table of Peak Values for Key Head Kinematic Variables, Anesthetic State, and Run Planarity.

TEST	ID	A/U	PLANAR	QHB	RHB	AAX	AAZ	AXZ
LX4790	ARNR16	U		10766	58	-2147	-502	2169
LX4791	ARNR16	U		19243	89	-2374	-619	2423
LX4799	ARNR18	U		16726	74	-2820	-578	2879
LX4801*	ARNR34	U		49800	249	-2635	-2266	
LX4803*	ARNR24	U		18836	71	-2526	-558	2536
LX4810	ARNR23	U		10083	54	-1312	-226	1331
LX4814	ARNR36	U	Yes	11710	42	-2146	-441	2157
LX4820	AR8739	U		10508	42	-1544	-429	1548
LX4822	ARNR39	U			22	-2514	-402	2522
LX5135	AR8845	U	Yes	9546	55	-1120	-214	1120
LX5147	AR8845	U		21238	120	-1373	-860	1613
LX5150	ARNR16	A		4661	22	-1058	-206	1058
LX5155	AR0016	A		2562	21	-958	-288	979
LX5156	AR0016	A		3671	28	-922	-321	930
LX5157	AR0016	A		3415	18	-895	-310	925
LX5164	AR0016	A	Yes	7600	52	-1600	-500	1637
LX5165	AR0016	A	Yes	28123	153	-1500	-1124	
LX5768	AR5855	A	Yes	9044	69	-1097	-342	1121
LX5770	AR5852	A	Yes	10114	63	-1435	-253	1435
LX5772	AR986B	A	Yes	12256	56	-1374	-385	1403
LX5774	AR5855	A		9862	62	-1177	-330	1200
LX5777	AR8776	A	Yes	22637	123	-1522	-808	1613
LX5779	AR0019	A	Yes	15799	86	-1253	-542	1278
LX5782	AR5851	A	Yes	15417	77	-1612	-530	1691
LX5784	AR5852	A	Yes	18868	94	-1827	-552	1838
LX5786	AR894C	A	Yes	17661	89	-2132	-511	2186
LX5793	AR5853	A		14933	85	-1730	-662	1806
LX5795	AR798B	A		20472	93	-1907	-547	1910
LX5797	ARNR20	A	Yes	20052	87	-2347	-748	2388
TESTS				29	29	29	29	27
MAXIMUM VALUE				49800	249	895	-206	2879
MINIMUM VALUE				2562	18	-2820	-2267	925
MEAN				1484	75	-1685	-554	1692
STD DEV				9367	46	564	391	558
COEFF VAR				63%	62%	34%	71%	33%

* Fatal exposures.

TABLE C6. Dataset A: Regression Results.

Table of Regression Coefficients

	CONSTANT	PSA	PHB	PHB^2
QHB	-2,861.0	22.00	-5,839.0	2,169.0
RHB	15.0	0.06	-76.0	108.0
AAX	304.0	-2.89	-1,039.0	-782.0
AAZ	4.2	-0.06	164.0	-1,515.0
AAR	-312.0	2.90	955.0	1,103.0

Significance of Regression

	TESTS	R^2	F LEVEL	SE	T LEVEL PSA	T LEVEL PHB	T LEVEL PHB^2
QHB	28	0.900	0.999	21%	0.999	0.871	0.999
RHB	26	0.840	0.999	18%	0.999	0.999	0.952
AAX	26	0.930	0.999	10%	0.999	0.999	0.740
AAZ	26	0.850	0.999	16%	0.999	0.908	0.999
AAR	26	0.940	0.999	9%	0.999	0.999	0.904

TABLE C7. Dataset A: Table of Observed and Predicted Head Angular Accelerations (QHB) and 95% Confidence Intervals.

TEST	OBSERVED QHB	PREDICTED QHB	95% CONFIDENCE INTERVAL LEFT	RIGHT	LENGTH
LX4790	10770.0	15418.0	8648.0	22188.1	13540.1
LX4791	19240.0	20714.5	13715.7	27713.2	13997.5
LX4799	16730.0	19646.2	12457.5	26835.0	14377.6
LX4801	49800.0	47525.2	38991.7	56058.6	17066.9
LX4803	18840.0	15118.3	7882.5	22354.1	14471.6
LX4810	10080.0	8617.0	1897.5	15336.4	13438.9
LX4814	11710.0	12617.5	5050.1	20184.9	15134.8
LX4820	10510.0	8551.0	1683.2	15418.9	13735.7
LX5135	9546.0	5597.7	-1291.8	12487.2	13778.9
LX5147	21240.0	18601.4	11751.9	25450.9	13698.9
LX5150	4661.0	5611.8	-1284.1	12507.8	13791.9
LX5155	2562.0	5628.8	-1290.5	12548.1	13838.6
LX5156	3671.0	5695.2	-1206.1	12596.5	13802.6
LX5157	3415.0	5647.8	-1313.8	12609.4	13923.2
LX5164	7600.0	13264.8	6578.5	19951.1	13372.6
LX5165	28120.0	32856.8	25402.9	40310.7	14907.8
LX5768	9044.0	11541.0	4703.4	18378.6	13675.2
LX5770	10110.0	9453.0	2729.3	16176.7	13447.3
LX5772	12260.0	9162.9	2450.5	15875.3	13424.7
LX5774	9862.0	10177.8	3392.5	16963.0	13570.5
LX5777	22640.0	19543.2	12673.4	26412.9	13739.5
LX5779	15800.0	14723.5	7698.6	21748.5	14049.9
LX5782	15420.0	14220.4	7506.5	20934.2	13427.7
LX5784	870.0	15111.1	8362.8	21859.3	13496.5
LX5786	17660.0	16333.2	9519.1	23147.3	13628.2
LX5793	14930.0	19721.9	12870.0	26573.8	13703.8
LX5795	20470.0	17118.3	10268.4	23968.2	13699.8
LX5797	20050.0	17392.8	10558.0	24227.6	13669.6
TESTS	28	28	28	28	28
MAXIMUM	49800.0	47525.2	38991.7	56058.6	17066.9
MINIMUM	870.0	5597.7	-1313.8	12487.2	13372.6
MEAN	4200.4	14843.3	7871.6	28814.9	13943.2
STD DEV	9692.1	8879.0	8604.1	9160.7	746.3
COEFF VAR	68%	60%	109%	32%	5%

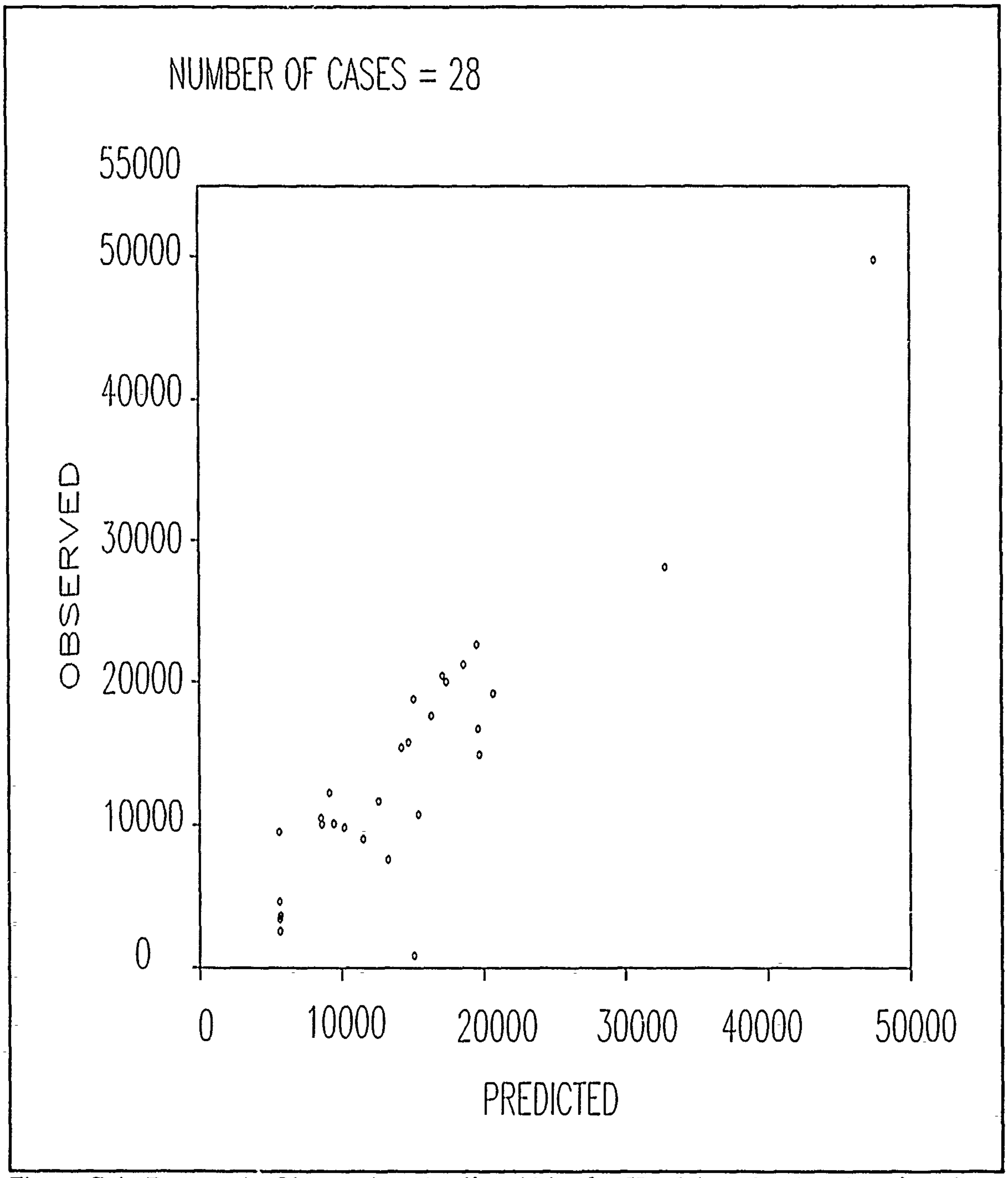

Figure C-1. Dataset A: Observed vs. Predicted Plot for Head Angular Acceleration about Y-Axis (QHB).

TABLE C8. Dataset A: Table of Observed and Predicted Head Angular Velocities (RHB) and 95% Confidence Intervals.

TEST	OBSERVED RHB	PREDICTED RHB	95% CONFIDENCE INTERVAL LEFT	RIGHT	LENGTH
LX4790	58.0	72.4	46.8	97.9	51.1
LX4791	89.0	100.0	73.8	126.3	52.4
LX4799	74.1	83.4	56.3	110.5	54.2
LX4803	71.3	57.6	30.1	85.1	55.0
LX4810	54.2	46.0	20.6	71.4	50.7
LX4814	42.1	46.2	15.7	76.7	61.0
LX4820	48.6	39.6	13.9	65.4	51.5
LX5135	55.0	35.0	9.1	61.0	51.9
LX5147	120.0	108.9	81.6	136.2	54.6
LX5150	22.0	34.1	8.2	60.0	51.8
LX5155	21.0	32.7	6.8	58.6	51.9
LX5156	28.0	33.6	7.7	59.5	51.8
LX5157	18.0	31.4	5.3	57.4	52.2
LX5164	52.0	66.2	40.9	91.5	50.6
LX5768	69.9	71.7	46.0	97.4	51.4
LX5770	63.6	54.2	28.7	79.8	51.0
LX5772	55.7	51.3	25.9	76.8	50.9
LX5774	62.4	61.9	36.3	87.6	51.3
LX5777	123.0	115.1	86.7	143.6	56.8
LX5779	86.3	96.7	69.0	124.4	55.4
LX5782	76.7	75.3	50.0	100.6	50.6
LX5784	94.0	83.0	57.7	108.3	50.6
LX5786	89.4	76.2	50.5	101.9	51.4
LX5793	85.3	103.3	77.4	129.2	51.8
LX5795	92.9	80.0	54.2	105.8	51.6
LX5797	87.3	83.7	58.0	109.4	51.4
TESTS	26	26	26	26	26
MAXIMUM	123.0	115.1	86.7	143.6	61.0
MINIMUM	18.0	31.4	5.3	57.4	50.6
MEAN	66.9	66.9	40.7	93.2	52.5
STD DEV	27.9	25.6	25.4	25.8	2.4
COEFF VAR	42%	38%	62%	28%	5%

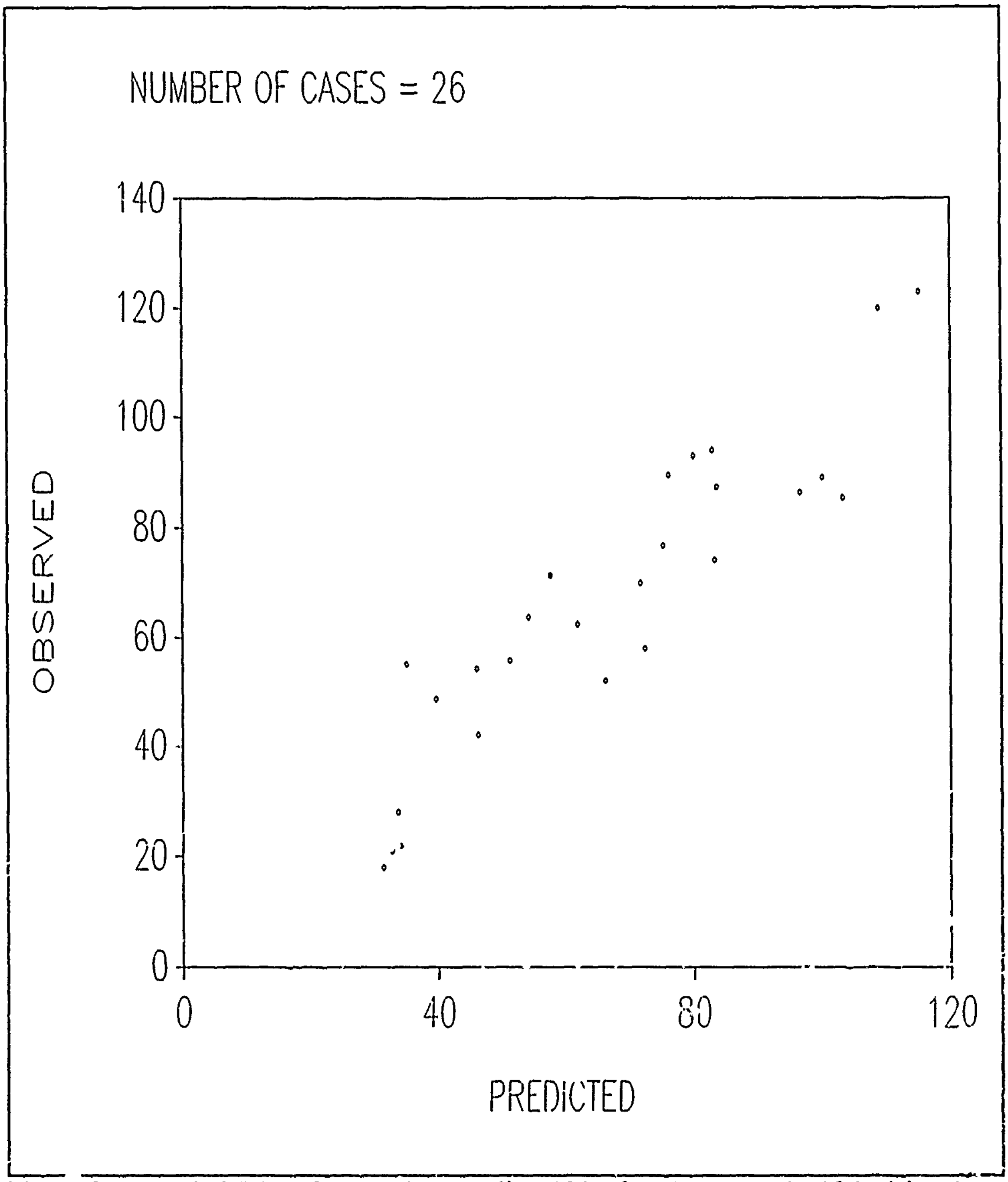

Figure C-2. DATASET A: Observed vs. Predicted Plot for Head Angular Velocities about Y-Axis (RHB).

TABLE C9. Dataset A: Table of Observed and Predicted X- Component of Head Linear Acceleration (AAX) and 95% Confidence.

	OBSERVED	PREDICTED	95% CONFIDENCE INTERVAL		
TEST	AAX	AAX	LEFT	RIGHT	LENGTH
LX4790	-2147.0	-2080.7	-2415.9	-1745.5	670.3
LX4791	-2374.0	-2388.2	-2731.4	-2045.0	686.4
LX4799	-2820.0	-2709.8	-3063.9	-2355.8	708.1
LX4803	-2526.0	-2419.8	-2781.1	-2058.5	722.6
LX4810	-1312.0	-1339.3	-1672.9	-1005.7	667.2
LX4814	-2146.0	-2136.1	-2537.5	-1734.6	802.9
LX4820	-1544.0	-1491.0	-1829.9	-1152.0	677.8
LX5135	-1120.0	-982.4	-1323.8	-641.0	682.8
LX5147	-1373.0	-1514.7	-1874.0	-1155.3	718.6
LX5150	-1058.0	-1011.0	-1352.0	-670.0	681.9
LX5155	-958.0	-1049.9	-1391.2	-708.6	682.5
LX5156	-922.0	-1042.4	-1383.1	-701.6	681.4
LX5157	-895.0	-1085.8	-1428.8	-742.7	686.2
LX5164	-1600.0	-1777.2	-2109.3	-1445.2	664.1
LX5768	-1097.0	-1169.9	-1507.9	-831.9	676.1
LX5770	-1435.0	-1276.4	-1612.0	-940.8	671.2
LX5772	-1374.0	-1302.8	-1637.6	-968.0	669.5
LX5774	-1177.0	-1189.1	-1526.7	-851.6	675.1
LX5777	-1522.0	-1505.4	-1879.3	-1131.4	748.0
LX5779	-1253.0	-1009.1	-1373.4	-644.9	728.5
LX5782	-1612.0	-1695.7	-2027.6	-1363.8	663.8
LX5784	-1827.0	-1633.6	-1966.0	-1301.2	664.8
LX5786	-2132.0	-2170.1	-2507.0	-1833.2	673.8
LX5793	-1730.0	-2018.2	-2358.0	-1678.3	679.7
LX5795	-1907.0	-2227.1	-2565.3	-1889.0	676.3
LX5797	-2347.0	-2164.7	-2501.4	-1827.9	673.5
TESTS	26	26	26	26	26
MAXIMUM	-895.0	-982.4	-1323.8	-641.0	802.9
MINIMUM	-2820.0	-2709.8	-3063.9	-2355.8	663.8
MEAN	1623.4	-1630.4	-1975.3	-1285.5	689.7
STD DEV	536.6	524.3	527.4	521.6	31.7
COEFF VAR	33%	32%	27%	41%	5%

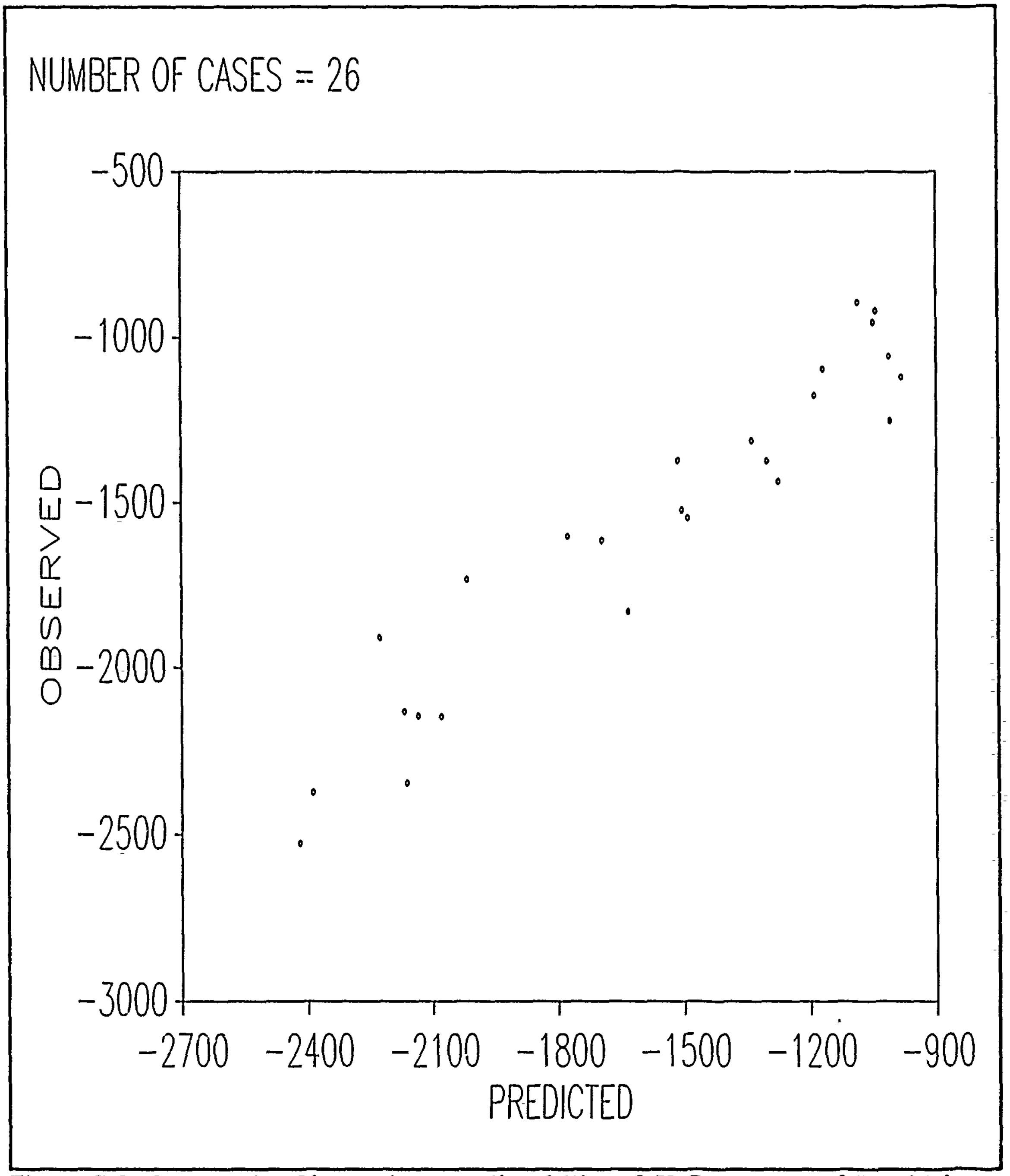

Figure C-3. Dataset A: Observed vs. Predicted Plot of X-Component of Head Linear Acceleration (AAX).

TABLE C10. Dataset A: Table of Observed and Predicted Z-Component of Head Linear Acceleration (AAZ) and 95% Confidence Intervals.

TEST	OBSERVED AAZ	PREDICTED AAZ	95% CONFIDENCE INTERVAL LEFT	RIGHT	LENGTH
LX4790	-502.0	-506.5	-668.5	-344.6	323.9
LX4791	-619.0	-694.3	-860.4	-528.2	332.2
LX4799	-578.5	-622.6	-794.2	-451.0	343.2
LX4803	-558.8	-541.3	-715.3	-367.2	348.2
LX4810	-226.0	-318.0	-478.7	-157.4	321.2
LX4814	-441.4	-529.3	-722.6	-336.0	386.6
LX4820	-428.9	-343.8	-506.9	-180.6	326.3
LX5135	-214.0	-239.0	-403.3	-74.6	328.7
LX5147	-860.0	-735.0	-907.9	-562.0	345.9
LX5150	-206.0	-243.1	-407.2	-78.9	328.3
LX5155	-288.0	-250.4	-414.7	-86.1	328.6
LX5156	-321.0	-248.9	-412.9	-84.8	328.1
LX5157	-310.0	-259.8	-425.0	-94.6	330.4
LX5164	-500.0	-447.0	-607.2	-286.8	320.4
LX5768	-342.4	-434.7	-597.5	-272.0	325.5
LX5770	-253.2	-340.2	-501.8	-178.5	323.3
LX5772	-385.3	-330.5	-491.7	-169.3	322.4
LX5774	-330.5	-373.2	-535.8	-210.6	325.1
LX5777	-808.1	-788.2	-968.2	-608.2	360.1
LX5779	-542.5	-622.5	-797.9	-447.1	350.8
LX5782	-529.6	-490.1	-650.2	-330.0	320.2
LX5784	-552.0	-537.2	-697.4	-376.9	320.5
LX5786	-510.7	-533.7	-696.6	-370.8	325.7
LX5793	-662.1	702.5	-866.5	-538.5	328.0
LX5795	-546.9	-558.7	-722.2	-395.1	327.1
LX5797	-748.0	-574.7	-737.5	-411.8	325.7
TESTS	26	26	26	26	26
MAXIMUM	206.0	-239.0	-403.3	-74.6	386.6
MINIMUM	-860.0	-788.2	-968.2	-608.2	320.2
MEAN	-471.7	-471.7	-638.0	-305.4	332.5
STD DEV	180.6	166.5	169.9	163.3	15.2
COEFF VAR	38%	32%	27%	53%	5%

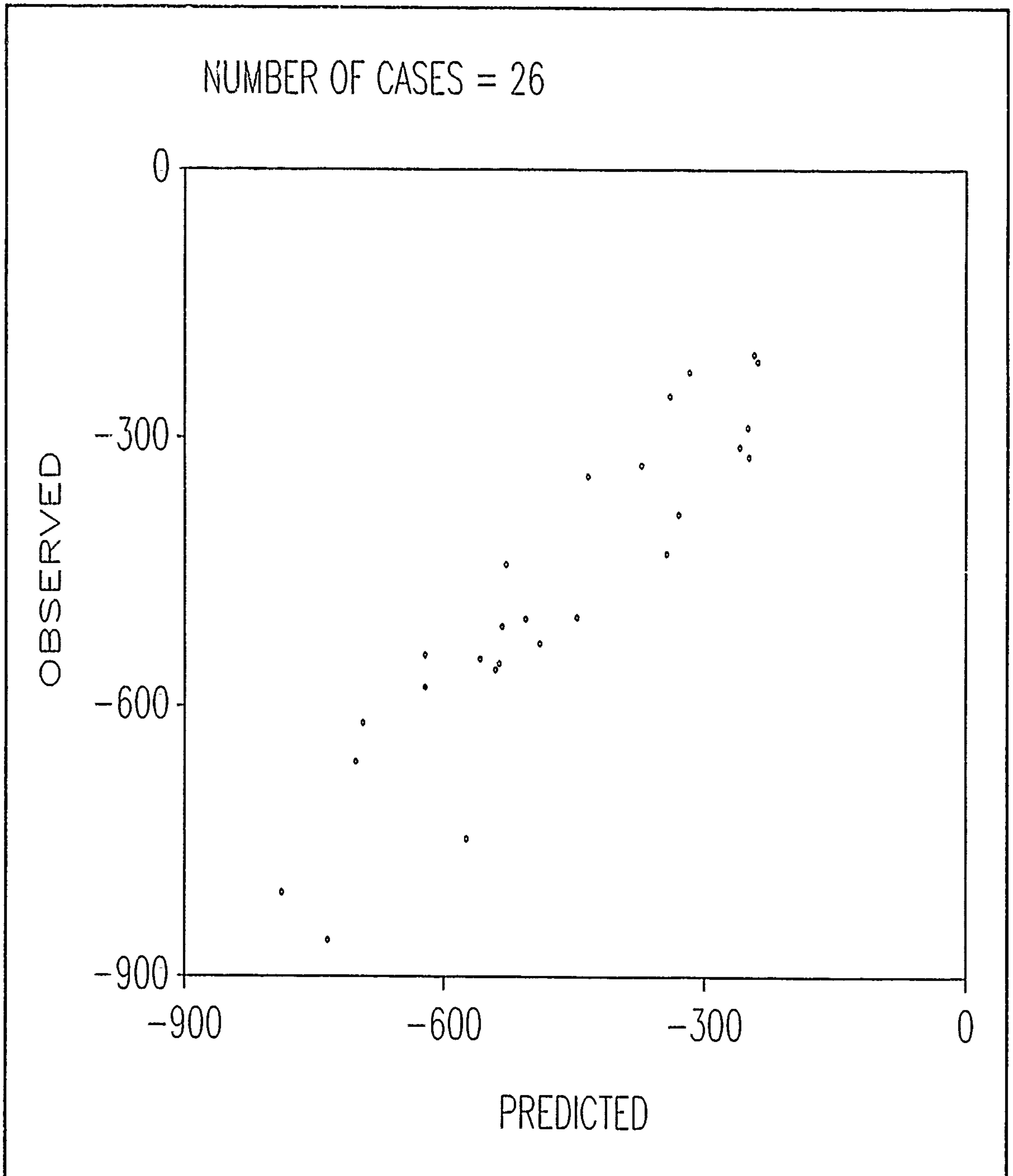

Figure C-4. Dataset A: Observed vs. Predicted Plot of Z - Component of Head Linear Acceleration (AAZ).

TABLE C11. Dataset A: Table of Observed and Predicted Resultant Head Linear Acceleration (X-Z Plane) and 95% Confidence Intervals.

TEST	OBSERVED AAR	PREDICTED AAR	95% CONFIDENCE INTERVAL LEFT	RIGHT	LENGTH
LX4790	2169.0	2094.0	1781.1	2406.8	625.7
LX4791	2423.0	2432.6	2111.8	2753.5	641.7
LX4799	2879.0	2721.0	2389.4	3052.5	663.1
LX4803	2536.0	2434.8	2098.5	2771.0	672.5
LX4810	1331.0	1345.1	1034.9	1655.4	620.6
LX4814	2157.0	2170.0	1796.6	2543.4	746.8
LX4820	1548.0	1501.0	1185.8	1816.1	630.3
LX5135	1120.0	987.7	670.2	1305.2	635.0
LX5147	1613.0	1617.8	1283.7	1952.0	668.3
LX5150	1058.0	1016.6	699.5	1333.8	634.2
LX5155	978.9	1056.7	739.3	1374.2	634.8
LX5156	930.1	1048.6	731.7	1365.4	633.8
LX5157	925.0	1094.6	775.5	1413.8	638.3
LX5164	1637.0	1790.8	1481.3	2100.2	618.9
LX5768	1121.0	1210.5	896.1	1525.0	628.9
LX5770	1435.0	1288.6	976.3	1600.8	624.5
LX5772	1403.0	1311.8	1000.4	1623.3	622.9
LX5774	1200.0	1213.1	899.1	1527.2	628.1
LX5777	1613.0	1623.8	1276.1	1971.6	695.5
LX5779	1278.0	1109.3	770.5	1448.1	677.6
LX5782	1691.0	1723.4	1414.1	2032.7	618.6
LX5784	1838.0	1676.6	1367.0	1986.2	619.2
LX5786	2186.0	2185.4	1870.7	2500.0	629.3
LX5793	1806.0	2084.6	1767.8	2401.4	633.6
LX5795	1910.0	2245.5	1929.6	2561.5	631.9
LX5797	2388.0	2190.0	1875.4	2504.5	629.1
TESTS	26	26	26	26	26
MAXIMUM	2879.0	2721.0	2389.4	3052.5	746.8
MINIMUM	925.0	987.7	670.2	1305.2	618.6
MEAN	1660.5	1660.5	1339.3	1981.8	624.4
STD DEV	542.1	524.9	521.4	528.8	29.3
COEFF VAR	33%	32%	27%	41%	5%

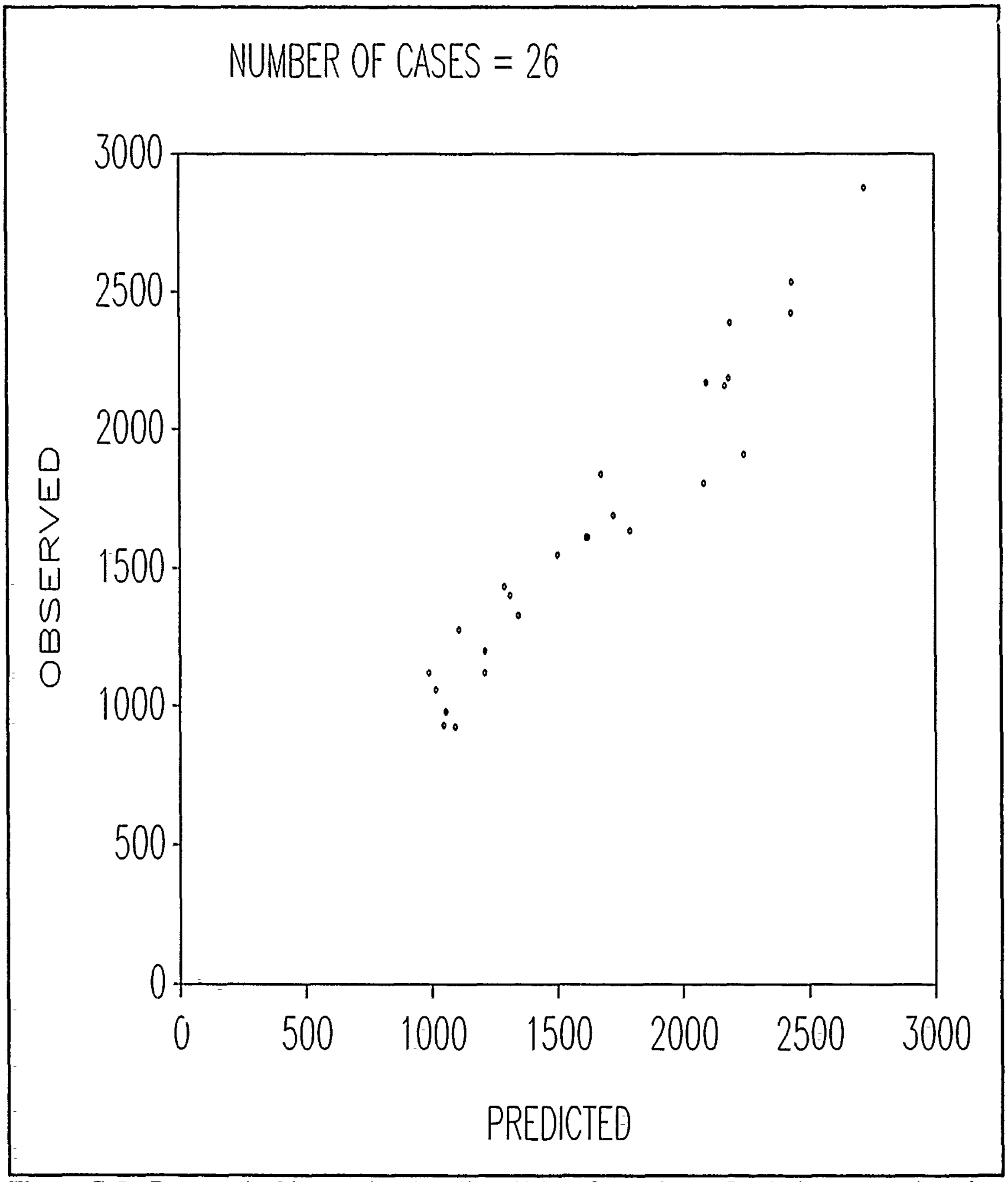

Figure C-5. Dataset A: Observed vs. Predicted Plot of Resultant Head Linear Acceleration (X-Z Plane).

TABLE C12. Dataset B: Selected peaks for key head kinematic responses. Head Initial Condition: Neck-forward, Chin Down (NFCD).

KINEMATIC VARIABLE	SYMBOL	PEAK CHOSEN
Angular Acceleration (Y)	QHB	-
Angular Velocity (Y)	RHB	-
Linear Acceleration (X)	AAX	-
Linear Acceleration (Z)	AAZ	-
Resultant Linear Acceleration (X-Z)	AAR	+

Number of Runs: 24
Independent Variables Chosen:
(1) Peak Sled Acceleration (PSA)
(2) Initial Head Pitch (PHB)
(3) Squared Initial Head Pitch (PHB^2)

TABLE C13. Dataset B: Summary of Experiments.					
TEST	**ID**	**SERIES**	**G LEVEL**	**CONSCIOUSNESS**	**EVOKED POTENTIAL**
LX4783	AR660B	1984	57	U	
LX4784	AR660B	1984	64	U	
LX4785	AR660B	1984	79	U	
LX4786	AR660B	1984	96	U	
LX4788	ARNR16	1984	56	U	
LX4789	ARNR16	1984	71	U	
LX4795	ARNR21	1984	101	U	YES
LX4806	ARNR11	1984	86	U	
LX4808	AR8739	1984	56	U	
LX4812	AR8696	1984	86	U	YES
LX4818	AR8789	1984	71	U	YES
LX5123	AR0016	1985	41	U	
LX5125	AR0016	1985	74	U	
LX5128	AR0016	1985	42	U	
LX5129	AR0016	1985	74	A	
LX5132	AR8858	1985	42	U	
LX5138	ARNR16	1985	42	U	
LX5141	ARNR16	1985	75	U	
LX5144	AR8858	1985	75	U	
LX5151	ARNR16	1985	42	A	
LX5152	ARNR16	1985	42	A	
LX5160	AR0016	1985	74	A	
LX5161	AR0016	1985	75	A	
LX5162	AR0016	1985	75	A	

Number of tests: 24
Number of NUCU: 0
Number of NFCD: 24
Number of anest: 6
Number of unanest: 18
Number of evoked potentials: 3
Number of fatal runs: 0

TABLE C14. Dataset B: Sled Parameters for NFCD runs.

TEST	ID	PSA	ROO	ESV	DOP
LX4783	AR660B	556	45791	21.5	25.2
LX4784	AR660B	625	45328	22.8	23.4
LX4785	AR660B	777	82057	25.2	22.6
LX4786	AR660B	940	119035	27.5	20.4
LX4788	ARNR16	552	40681	21.5	24.1
LX4789	ARNR16	699	59345	24.1	23.4
LX4795	ARNR21	985	123212	28.4	20.4
LX4806	ARNR11	839	103576	26.2	22.9
LX4808	AR8739	544	45641	21.4	26.2
LX4812	AR8696	845	105203	26.3	22.5
LX4818	AR8789	700	66283	24.0	24.1
LX5123	AR0016	404	35669	18.7	34.2
LX5125	AR0016	720	60421	24.5	22.3
LX5128	AR0016	406	20350	18.7	30.7
LX5129	AR0016	725	66334	24.6	22.6
LX5132	AR8858	408	19313	18.8	30.6
LX5138	ARNR16	414	20482	19.0	30.6
LX5141	ARNR16	731	59887	24.9	22.3
LX5144	AR8858	732	61773	24.9	22.6
LX5151	ARNR16	411	22789	18.9	31.9
LX5152	ARNR16	414	20193	18.9	30.6
LX5160	AR0016	724	74318	24.6	23.2
LX5161	AR0016	733	62816	25.0	22.8
LX5162	AR0016	734	58484	25.1	22.3
TESTS		24	24	24	24
MAXIMUM VALUE		985	123212	28.4	34.2
MINIMUM VALUE		404	19313	18.7	20.4
MEAN VALUE		651	59124	23.1	25.1
1 STD DEV		176	30600	3.0	4.0
COEFF VAR		27%	52%	13%	16%

TABLE C15. Dataset B: Initial Head Angular and Linear Position for NFCD Runs.

TEST	ID	PHA	PHB	PHC	DAX	DAY	DAZ
LX4783	AR660B	-.150	.705	-.035	-1.155	-.007	.270
LX4784	AR660B	-.062	.515	.293	-1.167	.018	.290
LX4785	AR660B	-.204	.603	.074	-1.156	.024	.274
LX4786	AR660B	-.143	.657	-.024	-1.151	.006	.262
LX4788	ARNR16	-.287	.850	.304	-1.151	.013	.283
LX4789	ARNR16	-.525	.846	.800	-1.148	.033	.276
LX4795	ARNR21	-.775	1.074	.918	-1.132	.035	.252
LX4806	ARNR11	-.215	1.212	.097	-1.128	.028	.308
LX4808	AR8739	.467	.429	-.461	-1.131	-.033	.283
LX4812	AR8696	.111	.364	-.411	-1.117	.014	.296
LX4818	AR8789	.295	.526	-.637	-1.109	-.032	.301
LX5123	AR0016	.189	.214	.305	-1.158	-.015	.317
LX5125	AR0016	.062	.543	-.075	-1.156	-.031	.318
LX5128	AR0016	.090	.336	.318	-1.151	.005	.315
LX5129	AR0016	-.155	.632	.138	-1.142	-.009	.294
LX5132	AR8858	-.031	.277	.405	-1.160	.004	.332
LX5138	ARNR16	.098	.336	-.476	-1.154	-.004	.309
LX5141	ARNR16	.040	.596	-.149	-1.150	-.012	.305
LX5144	AR8858	.038	.358	-.025	-1.161	.002	.340
LX5151	ARNR16	-.031	.218	-.490	-1.155	-.007	.313
LX5152	ARNR16	-.052	.225	-.455	-1.155	-.008	.316
LX5160	AR0016	.013	.481	.065	-1.150	.001	.294
LX5161	AR0016	-.108	.505	.070	-1.141	-.011	.291
LX5162	AR0016	-.184	.510	.068	-1.144	-.003	.296
TESTS		24	24	24	24	24	24
MAXIMUM VALUE		.467	1.212	.918	-1.109	.035	.340
MINIMUM VALUE		-.775	.214	-.637	-1.167	-.033	.252
MEAN VALUE		-.063	.542	.026	-1.147	.000	.297
1 STD DEV		.251	.258	.392	.014	.019	.022
COEFF VAR					1%		7%

TABLE C16. Dataset B: Table of Peak Values for Key Head Kinematic Variables, Anesthetic State and Run Planarity.

TEST	ID	A/U	PLANAR	QHB	RHB	AAX	AAZ	AXZ
LX4783	AR660B	U	Yes	-6386	-53		-355	1416
LX4784	AR660B	U		-7233	-46	-1773	-651	1774
LX4785	AR660B	U		-8717	-46	-584	-1100	
LX4786	AR660B	U	Yes	-12218	-58	-2405		2411
LX4788	ARNR16	U		-9575	-66	-1226	-354	1226
LX4789	ARNR16	U		-11520	-74	-1588	-369	1599
LX4795	ARNR21	U		-19293	-103	-2314	-347	2403
LX4806	ARNR11	U	Yes	-11085	-68	-2167	-106	2216
LX4808	AR8739	U		-3162	-9	-1514	-159	1525
LX4812	AR8696	U		-8121	-37	-2544	-619	2546
LX4818	AR8789	U		-7515	-34	-2088	-454	2091
LX5123	AR0016	U		-3352	-19	-1194	-376	1201
LX5125	AR0016	U	Yes	-8231	-48	-1844	-553	1850
LX5128	AR0016	U		-2456	-15	-1016	-276	1018
LX5129	AR0016	A	Yes	-7004	-48	-1813	-416	1813
LX5132	AR8858	U		-2650	-16	-1312	-396	1320
LX5138	ARNR16	U		-1901	-13	-1010	-193	1010
LX5141	ARNR16	U	Yes	-6996	-46	-1827	-507	1828
LX5144	AR8858	U	Yes	-4824	-33	-2152	-722	2155
LX5151	ARNR16	A		-1674	-11	-949	-243	955
LX5152	ARNR16	A		-1903	-12	-950	-238	953
LX5160	AR0016	A	Yes	-5388	-36	-1679	-505	1679
LX5161	AR0016	A	Yes	-6225	-33	-1660	-529	1677
LX5162	AR0016	A	Yes	-7049	-35	-1730	-514	1738
TESTS				24	24	23	23	23
MAXIMUM VALUE				-1674	-9	-584	-106	2546
MINIMUM VALUE				-19293	-103	-2544	1100	953
MEAN VALUE				-6853	-40	-1623	-434	1670
1 STD DEV				4085	23	526	215	485
COEFF VAR				60%	58%	32%	50%	29%

TABLE C17. Dataset B: Regression Results.

Table of Regression Coefficients

	CONSTANT	**PSA**	**PHB**	**PHB²**
QHB	1,233.0	-14.00	14,990.0	22,236.00
RHB	-2.5	-0.05	65.0	132.0
AAX	-136.0	-3.0	1,120.0	-494.0
AAZ	114.0	-0.76	-557.0	737.0
AAR	139.0	3.00	-1054.0	507.0

Significance of Regression

	RUNS	**R^2**	**F LEVEL**	**SE**	**T LEVEL PSA**	**T LEVEL PHB**	**T LEVEL PHB²**
QHB	22	0.930	0.999	15%	0.999	0.944	0.997
RHB	22	0.920	0.999	16%	0.999	0.808	0.994
AAX	22	0.890	0.999	10%	0.999	0.855	0.673
AAZ	22	0.650	0.999	26%	0.999	0.809	0.983
AAR	22	0.900	0.999	10%	0.999	0.872	0.726

Number of runs: 24

TABLE C18. Dataset B: Table of Observed and Predicted Head Angular Accelerations (QHB) and 95% Confidence Intervals.

TEST	OBSERVED QHB	PREDICTED QHB	95% CONFIDENCE INTERVAL LEFT	RIGHT	LENGTH
LX4783	-6386.0	-6828.0	-8913.8	-4742.3	4171.5
LX4784	-7233.0	-5464.2	-7456.7	-3471.7	3985.0
LX4785	-8717.0	-8421.9	-10390.5	-6453.4	3937.1
LX4786	-12220.0	-11350.0	-13470.3	-9229.6	4240.7
LX4788	-9575.0	-9628.5	-11900.6	-7356.3	4544.3
LX4789	-11520.0	-11538.8	-13800.7	-9276.9	4523.8
LX4808	-3162.0	-3851.8	-5853.6	-1850.1	4003.5
LX4812	-8122.0	-7785.4	-9958.3	-5612.6	4345.7
LX4818	-7515.0	-6589.4	-8552.4	-4626.4	3926.0
LX5123	-3288.0	-2088.3	-4195.6	19.0	4214.6
LX5125	-8231.0	-7007.8	-8970.4	-5045.1	3925.3
LX5128	-1858.0	-1784.8	-3829.6	260.0	4089.6
LX5129	-7004.0	-8046.3	-10011.9	-6080.6	3931.3
LX5132	-2053.0	-1889.3	-3904.2	125.7	4029.8
LX5138	-1901.0	-1887.3	-3923.9	149.3	4073.2
LX5141	-6996.0	-7691.4	-9655.0	-5727.8	3927.1
LX5144	-4748.0	-6231.6	-8258.5	-4204.7	4053.8
LX5151	-1674.0	-2162.9	-4260.6	-65.3	4195.3
LX5152	-1903.0	-2163.4	-4243.8	-83.1	4160.7
LX5160	-5388.0	-6568.8	-8531.1	-4606.5	3924.5
LX5161	-6225.0	-6866.5	-8829.6	-4903.3	3926.3
LX5162	-7049.0	-6921.7	-8885.1	-4958.3	3926.8
TESTS	22	22	22	22	22
MAXIMUM	-1674.0	-1784.8	-3829.6	260.6	4544.3
MINIMUM	-12222.0	-11538.8	-13800.7	-9276.9	3924.5
MEAN	-6034.9	-6034.9	-8081.6	-3988.2	4093.4
STD DEV	3149.3	3037.8	3063.8	3014.5	189.5
COEFF VAR	52%	50%	38%	76%	5%

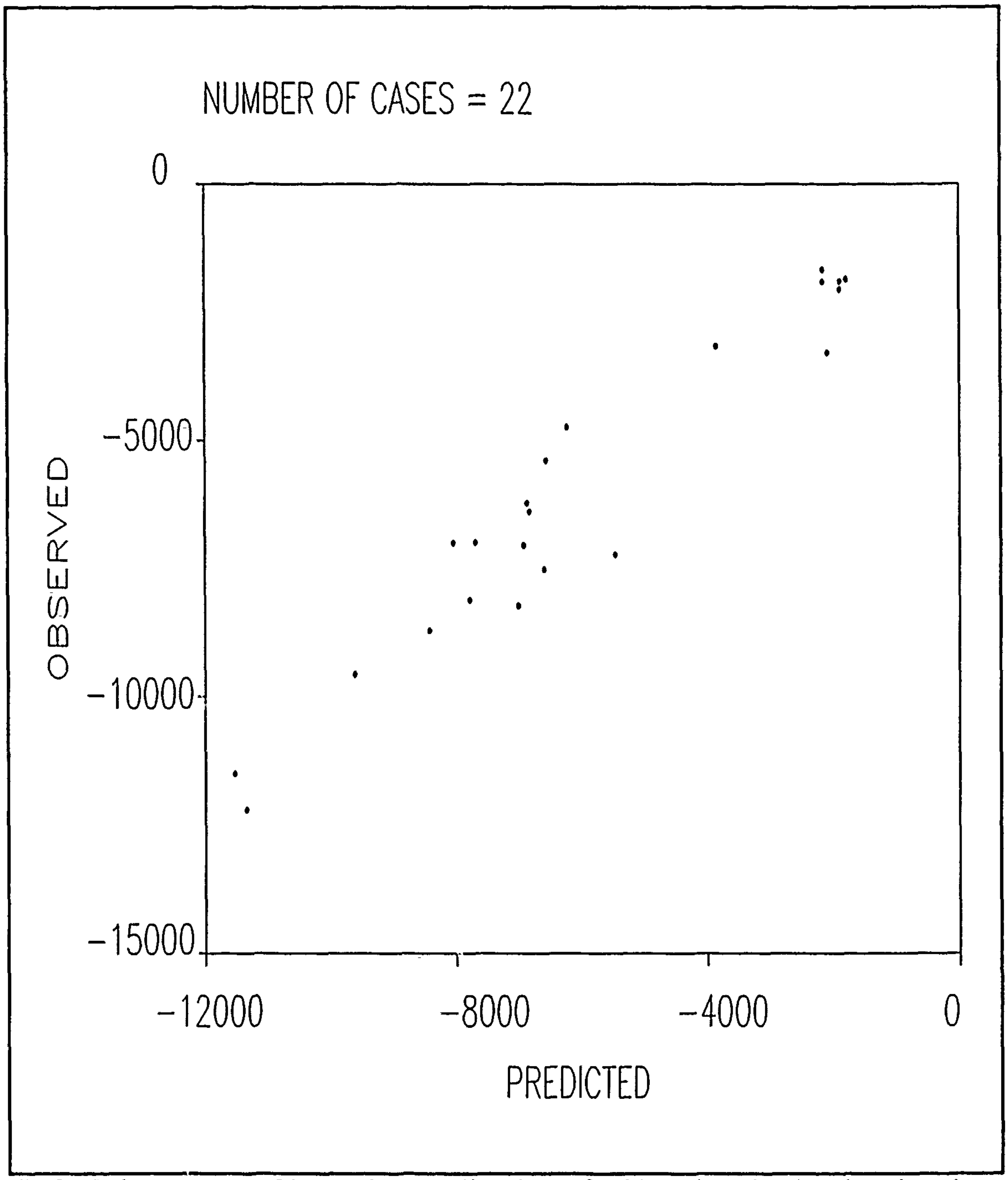

Figure C-6. Dataset B: Observed vs. Predicted Plot for Head Angular Acceleration about Y-Axis (QHB).

TABLE C19. DATASET B: Table of Observed and Predicted Head Angular Velocities (RHB) and 95% Confidence Intervals.

TEST	OBSERVED RHB	PREDICTED RHB	95% CONFIDENCE INTERVAL LEFT	RIGHT	LENGTH
LX4783	-53.0	-48.1	-61.7	-34.5	27.2
LX4784	-46.0	-33.1	-46.2	-20.1	26.0
LX4785	-46.0	-47.5	-60.4	-34.7	25.7
LX4786	-58.0	-60.6	-74.4	-46.7	27.7
LX4788	-66.0	-68.2	-83.1	-53.4	29.7
LX4789	-74.0	-74.4	-89.2	-59.6	29.5
LX4808	-9.0	-24.3	-37.4	-11.2	26.1
LX4812	-37.0	-35.7	-49.9	-21.5	28.4
LX4818	-33.0	-37.5	-50.3	-24.7	25.6
LX5123	-19.0	-13.5	-27.2	.3	27.5
LX5125	-48.0	-39.7	-52.5	-26.9	25.6
LX5128	-15.0	-14.6	-27.9	-1.2	26.7
LX5129	-48.0	-47.8	-60.6	-35.0	25.7
LX5132	-16.0	-13.7	-26.8	-.5	26.3
LX5138	-13.0	-14.9	-28.2	-1.6	26.6
LX5141	-46.0	-44.6	-57.5	-31.8	25.6
LX5144	-33.0	-30.2	-43.5	-17.0	26.5
LX5151	-11.0	-13.8	-27.5	-.1	27.4
LX5152	-12.0	-13.9	-27.4	-.3	27.2
LX5160	-36.0	-35.5	-48.3	-22.7	25.6
LX5161	-33.0	-37.5	-50.3	-24.7	25.6
LX5162	-35.0	-37.9	50.7	-25.1	25.6
TESTS	22	22	22	22	22
MAXIMUM	-9.0	-13.5	-26.0	0.3	29.7
MINIMUM	-74.0	-74.4	-89.2	-59.6	25.6
MEAN	-35.8	-35.8	-49.1	-22.4	26.7
STD DEV	18.7	17.9	18.1	17.7	1.2
COEFF VAR	52%	50%	37%	79%	4%

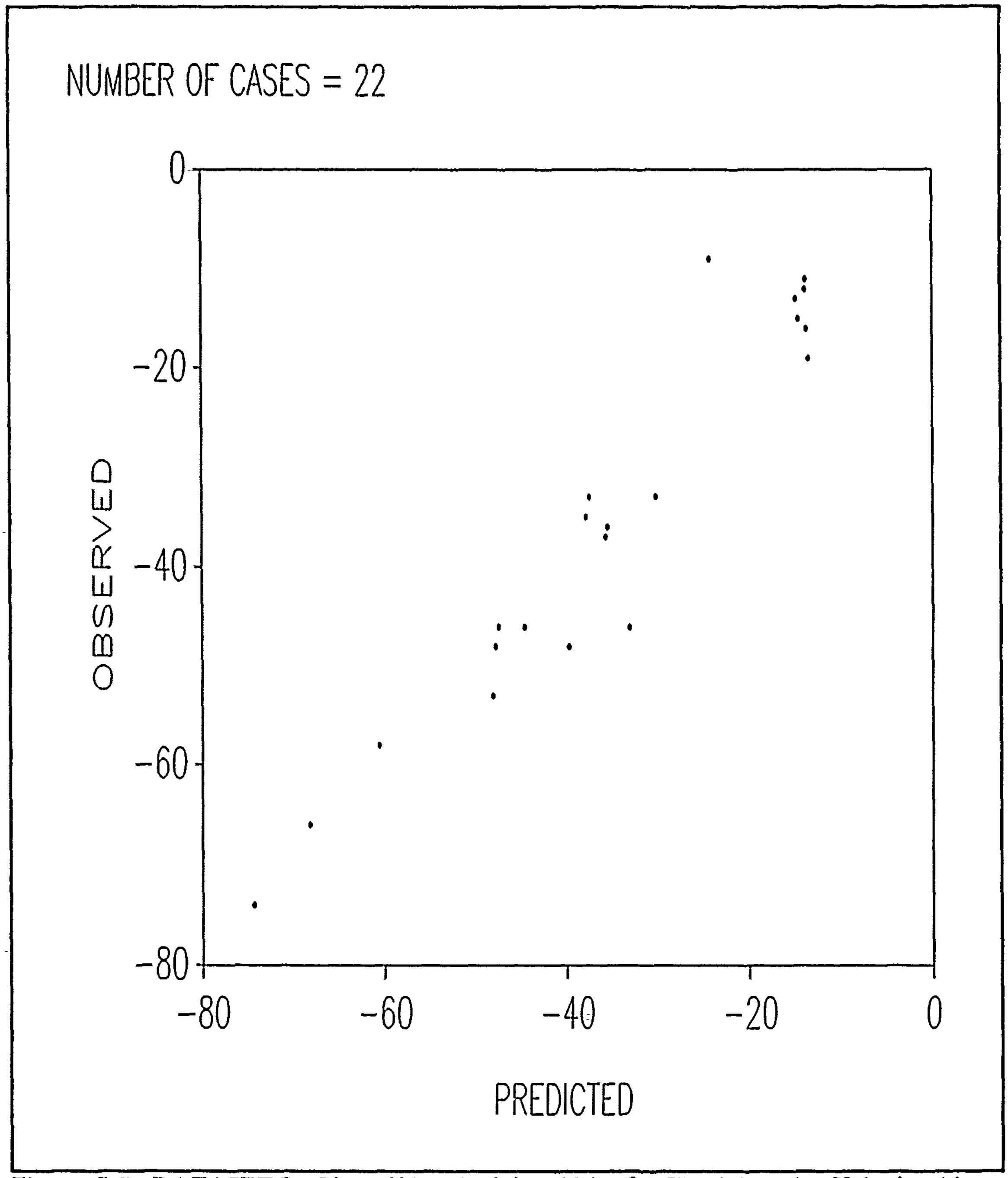

Figure C-7. DATASET B: Observed vs. Predicted Plot for Head Angular Velocity About the Y-axis for NFCD.

TABLE C20. Dataset B: Table of Observed and Predicted X Component of Head Linear Acceleration (AAX) and 95% Confidence Intervals.

TEST	OBSERVED AAX	PREDICTED AAX	95% CONFIDENCE INTERVAL LEFT	RIGHT	LENGTH
LX4784	-1773.0	-1574.4	-1949.8	-1198.9	751.0
LX4786	-2405.0	-2447.1	-2843.4	-2050.8	792.6
LX4788	-1226.0	-1205.4	-1628.4	-782.4	846.0
LX4789	-1588.0	-1649.0	-2041.6	-1256.5	785.1
LX4795	-2314.0	-2472.0	-2890.5	-2053.4	837.1
LX4806	-2167.0	-2031.5	-2495.7	-1567.2	928.6
LX4808	-1514.0	-1387.4	-1761.9	-1013.0	748.9
LX4812	-2544.0	-2342.1	-2754.6	-1929.6	825.0
LX4818	-2088.0	-1793.8	-2167.9	-1419.7	748.2
LX5123	-1194.0	-1135.9	-1533.0	-738.8	794.2
LX5125	-1844.0	-1843.9	-2218.9	-1468.9	750.0
LX5128	-1016.0	-1040.5	-1425.0	-656.1	768.9
LX5129	-1813.0	-1809.1	-2188.1	-1430.1	758.1
LX5132	-1312.0	-1094.2	-1479.3	-709.0	770.3
LX5138	-1010.0	-1063.1	-1446.5	-679.8	766.7
LX5141	-1827.0	-1846.1	-2223.3	-1468.9	754.4
LX5144	-2152.0	-2003.7	-2391.6	-1615.9	775.7
LX5151	-949.0	-1153.7	-1549.5	-757.9	791.6
LX5152	-950.0	-1155.5	-1549.4	-761.7	787.7
LX5160	-1679.0	-1893.5	-2268.2	-1518.9	749.3
LX5161	-1660.0	-1905.9	-2281.0	-1530.9	750.0
LX5162	-1730.0	-1907.0	-2282.1	-1531.9	750.2
TESTS	22	22	22	22	22
MAXIMUM	-949.0	-1040.5	-1425.0	-656.1	928.6
MINIMUM	-2544.0	-2472.0	-2890.5	-2053.4	748.2
MEAN	1670.7	-1670.7	-2062.3	-1279.1	783.2
STD DEV	485.4	458.6	463.4	454.7	43.7
COEFF VAR	29%	27%	22%	36%	6%

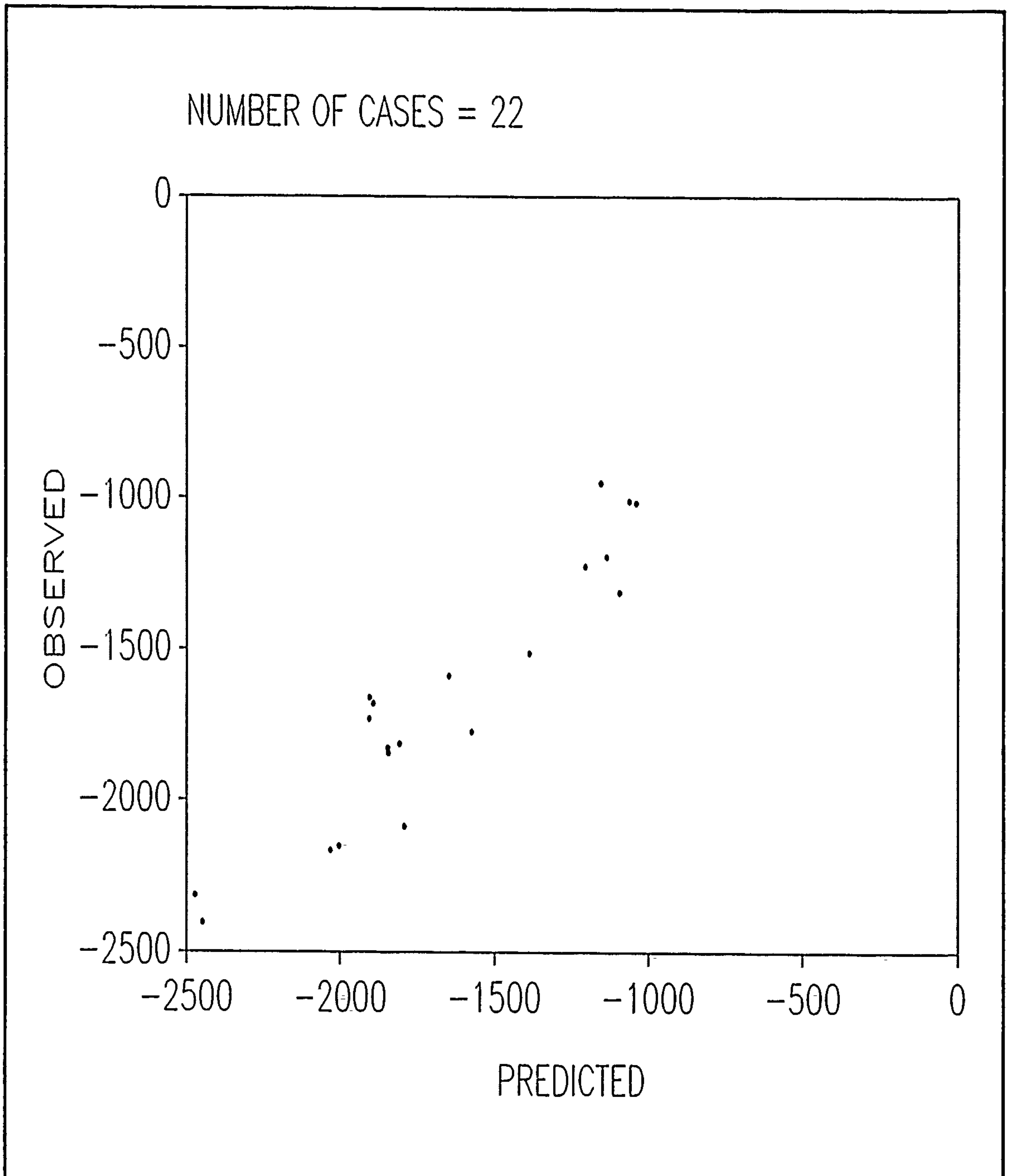

Figure C-8. Dataset B: Observed vs. Predicted Plot of X - Component of Head Linear Acceleration (AAX).

TABLE C21. Dataset B: Table of Observed and Predicted Z-Component of Head Linear Acceleration (AAZ) and 95% Confidence Intervals.

TEST	OBSERVED AAZ	PREDICTED AAZ	95% CONFIDENCE INTERVAL LEFT	RIGHT	LENGTH
LX4783	-355.0	-335.7	-575.2	-96.2	479.0
LX4784	-651.0	-453.5	-678.4	-228.5	449.9
LX4788	-354.0	-247.0	-494.5	.5	495.0
LX4789	-369.0	-361.7	-594.5	-128.8	465.8
LX4795	-347.4	-384.3	-637.7	-130.9	506.8
LX4806	-106.0	-116.7	-395.9	162.6	558.5
LX4808	-159.0	-403.8	-628.1	-179.6	448.6
LX4812	-619.1	-635.0	-884.7	-385.3	499.4
LX4818	-453.8	-507.7	-733.3	-282.1	451.2
LX5123	-376.0	-278.9	-518.1	-39.7	478.4
LX5 25	-553.0	-519.2	-745.6	-292.7	452.8
LX5128	-276.0	-299.3	-530.1	-68.6	461.5
LX5129	-416.0	-495.5	-723.3	-267.7	455.5
LX5132	-396.0	-294.6	-526.6	-62.6	464.0
LX5138	-193.0	-305.1	-535.2	-74.9	460.2
LX5141	-507.0	-512.5	-739.8	-285.2	454.6
LX5144	-722.0	-548.0	-782.3	-313.8	468.5
LX5151	-243.0	-285.2	-523.6	-46.9	476.7
LX5152	-238.0	-288.9	-526.1	-51.7	474.4
LX5160	-505.0	-534.8	-761.6	-308.0	453.6
LX5161	-529.0	-537.4	-764.4	-310.3	454.1
LX5162	-514.0	-537.5	-764.6	-310.4	454.2
TESTS	22	22	22	22	22
MAXIMUM	-106.0	-116.7	-395.9	162.6	558.5
MINIMUM	-722.0	-635.0	-884.7	-385.7	448.6
MEAN	-403.7	-403.7	-639.3	-168.2	471.0
STD DEV	162.6	131.5	125.1	138.8	25.7
COEFF VAR	40%	33%	20%	83%	5%

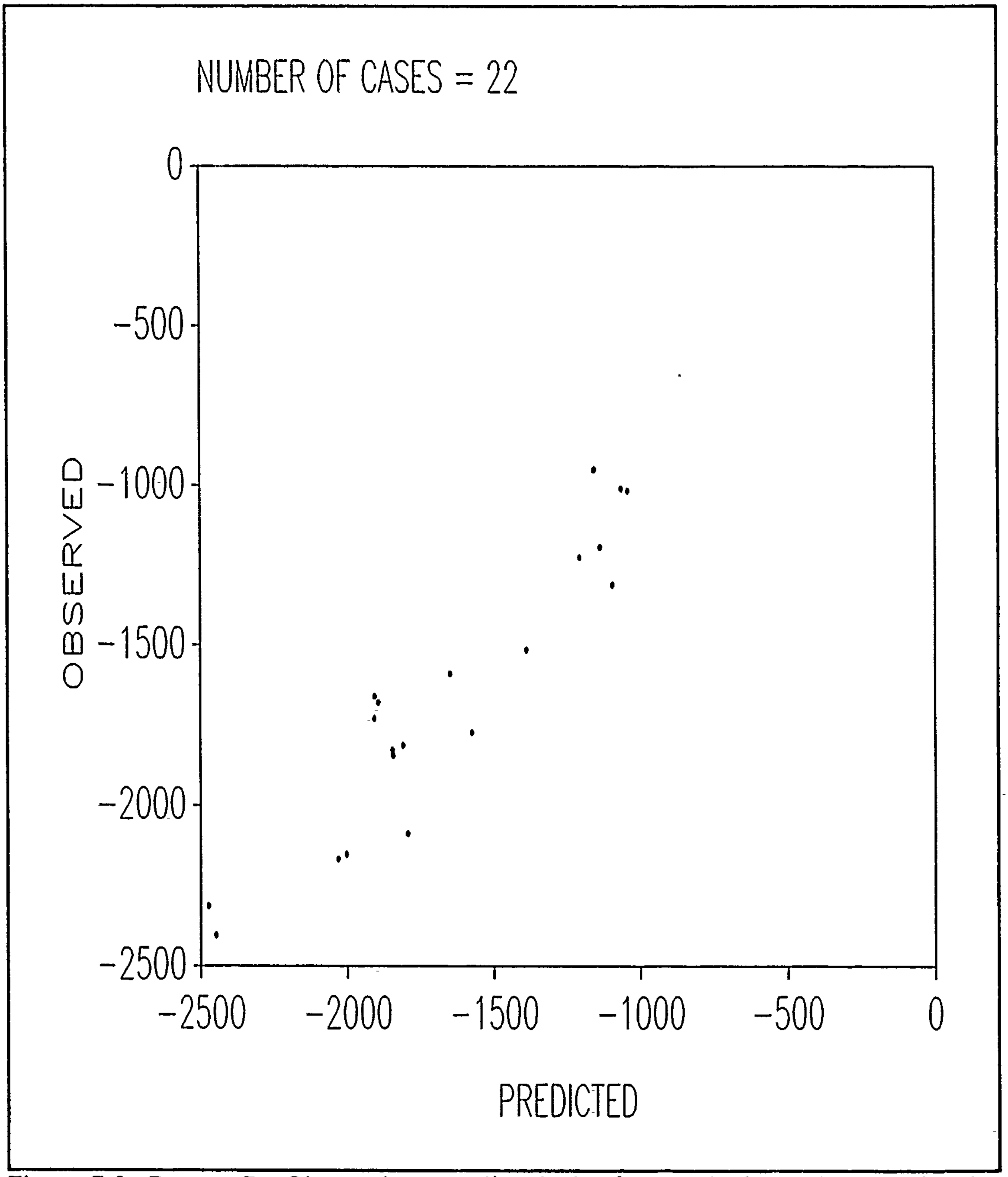

Figure C-9. Dataset B: Observed vs. Predicted Plot for Head Linear Acceleration (Z-component) for NFCD.

TABLE C22. Dataset B: Table of Observed and Predicted Resultant Head Linear Acceleration (X-Z Plane) and 95% Confidence Intervals.

RUNID	OBSERVED AAR	PREDICTED AAR	95% CONFIDENCE INTERVAL LEFT	RIGHT	LENGTH
LX4783	1416.0	1300.5	914.6	1686.4	771.8
LX4784	1774.0	1588.8	1226.8	1950.8	723.9
LX4786	2411.0	2460.1	2076.0	2844.1	768.1
LX4788	1226.0	1250.9	852.5	1649.3	796.8
LX4789	1599.0	1688.1	1313.0	2063.1	750.1
LX4795	2403.0	2520.1	2114.6	2925.6	810.9
LX4806	2216.0	2099.0	1649.1	2549.0	900.0
LX4808	1525.0	1398.5	1037.1	1759.9	722.8
LX4812	2546.0	2335.9	1939.9	2731.9	792.0
LX4818	2091.0	1806.0	1444.2	2167.8	723.6
LX5123	1201.0	1137.1	752.5	1521.8	769.3
LX5125	1850.0	1856.7	1493.9	2219.4	725.5
LX5128	1018.0	1050.4	679.3	1421.4	742.1
LX5129	1813.0	1828.9	1463.6	2194.2	730.6
LX5132	1320.0	1099.6	726.5	1472.7	746.3
LX5138	1010.0	1072.7	702.5	1442.8	740.3
LX5141	1828.0	1862.7	1498.4	2226.9	728.5
LX5144	2155.0	2001.8	1627.2	2376.4	749.2
LX5151	953.9	1154.9	771.5	1538.3	766.8
LX5152	952.6	1157.1	775.5	1538.6	763.1
LX5160	1679.0	1901.3	1538.2	2264.3	726.1
LX5161	1677.0	1915.2	1551.9	2278.4	726.6
LX5162	1738.0	1916.6	1553.2	2279.9	726.7
TESTS	23	23	23	23	23
MAXIMUM	2546.0	2520.1	2114.6	2925.6	900.0
MINIMUM	952.6	1050.4	679.3	1421.4	722.8
MEAN	1669.7	1669.7	1291.4	2048.0	756.6
STD DEV	485.1	459.5	55.3	464.6	40.6
COEFF VAR	29%	28%	35%	23%	5%

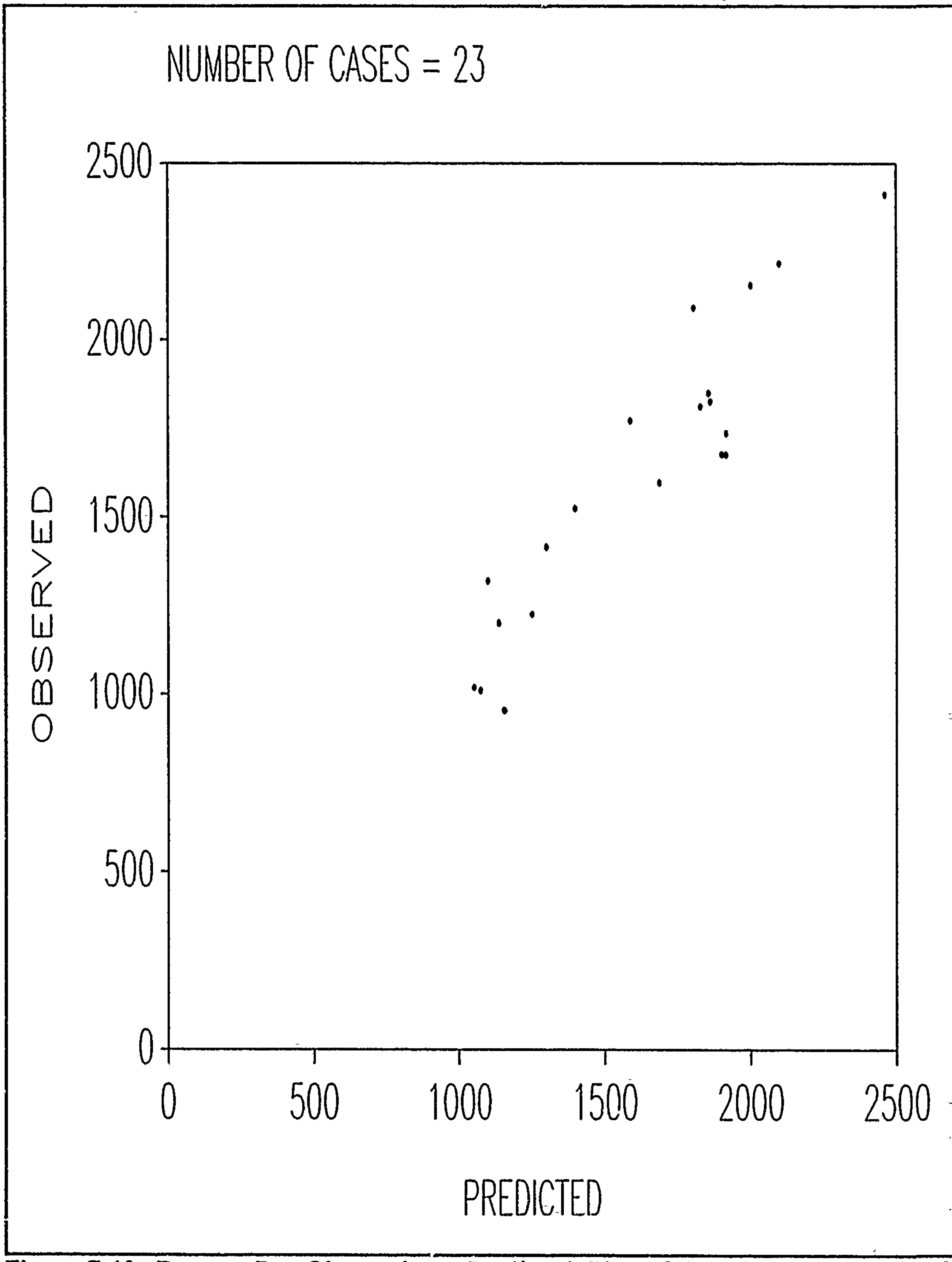

Figure C-10. Dataset B: Observed vs. Predicted Plot of Resultant Head Linear Acceleration (X-Z Plane).